Plant Natriuretic Peptides - Elucidation of the Mechanisms of Action

by

Oziniel Ruzvidzo

Submitted in partial fulfilment of the requirements for the degree of Doctor of Philosophy (PhD) in Biotechnology in the Department of Biotechnology, University of the Western Cape, South Africa

Supervisor: Professor Chris Gehring

May 2009

Declaration

I, Oziniel Ruzvidzo, declare that the thesis entitled "Plant Natriuretic Peptides – Elucidation of the Mechanisms of Action" is my work and has not been submitted for any degree or examination at any other university and that all sources of my information have been quoted as indicated in the text and/or list of references.

Name: Oziniel Ruzvidzo Date: May 2009

Signature: …… Date: ……

Dedicated to Mai Panashe, Beaular, Bibie, Nady, VaMuchembu and Mdara Nedza.

You are all special!!

Table of Contents

Acknowledgements

I would like to express my sincere gratitudes and appreciation to **Professor Chris Gehring** for his excellent, wonderful and overwhelming supervision during my studies.

I also would like to thank **my entire family** in Zimbabwe for their long-standing support and long-lasting love during this challenging period during which I was pursuing my highest academic and intellectual excellences.

Tatenda (*my sweetie*), I thank you a lot for being there for me all the time and even during those instances when 'science' seemed to overtake 'love'. You were just patient, understanding, sincere and very supportive. I really thank you very very much for that my dear.

My three beautiful girls: **Makanakaishe**, **Kudzaishe** and **Panaishe**. I know that you missed your dad so many times when you deeply needed him but deservingly, this really was for a great and wonderful cause. This is what I have done *my three sisters*!! Setting a special example for you to aspire, challenge and even do better than your old man.

I sincerely thank all the previous and current **members** of Plant Biotechnology Laboratory: **Suhail**, for integrating me into Science; **Ndiko**, for intellectual advice and motivation; **Monique Morse**, for academic guidance and encouragement; **Rene**, for moral support; **Lara**, for experimental facilitation; **Monique Maqungo**, for being you; **Kwezi**, for your gravitas company and brotherhood; **Lyndon**, **Tony**, **Takalani**, **Siya**, **Seipati** and **Grace**, for giving me wings to fly out of the fridge!!!

I wish to thank the **National Research Foundation** for its financial support of my entire studies.

Cloning and preparation of the AtPNP-A and AtWAKL10 clones used in this study was made possible with assistance of **Dr. Monique Morse**, Department of Biotechnology, University of the Western Cape, Bellville, South Africa.

All physiological assays with the recombinant AtPNP-A were done with the technical support and academic guidance of **Dr. Alex Valentine**, Department of Biodiversity and Conservation Biology, University of the Western Cape, Bellville, South Africa.

Microarray data on the role of AtWAKL10 in pathogen responses and plant defense mechanisms was generated with the help of **Dr. Stuart Meier**, South African National Bioinformatics Institute, University of the Western Cape, Bellville, South Africa.

Collaborative work on sugar metabolism due to recombinant AtPNP-A treatments were carried out by **Mr. Gavin George**, Institute for Plant Biotechnology, University of Stellenbosch, Stellenbosch, South Africa.

I finally give all my **Praise, Glory and Honour** to **The Almighty** for everything that I have acquired during this long but hopeful journey. [Mai **Olivia Charamba's** latest album "**The Gospel**" was just *instrumental*, *melodious*, *blessing* and *inspirational* during my entire research period and particularly the writing quota].

Abbreviations

ABA: Abscisic acid

ACC: 1-aminocyclopropane-1-carboxylic acid

AMP: Adenosine 5′-monophosphate

ANF: Atrial natriuretic factor

ANOVA: A one-way analysis of variance

ANP: Atrial natriuretic peptide

AtBRI1: *Arabidopsis thaliana* brassinosteroid receptor 1

AtCNG2: *Arabidopsis thaliana* cyclic nucleotide-gated 2

AtGC1: *Arabidopsis thaliana* guanylate cyclase 1

ATP: Adenosine 5′-triphosphate

AtPNP-A: *Arabidopsis thaliana* plant natriuretic peptide-A

AtPNP-B: *Arabidopsis thaliana* plant natriuretic peptide-B

AtWAKL10: *Arabidopsis thaliana* wall associated kinase-like 10

BHT: Benzothiadiazole S-methylester

BNP: Brain natriuretic peptide

bp: base pair

cADPR: Cyclic adenosine diphosphate ribose

cAMP: Cyclic 3′,5′-adenosine monophosphate

cGMP: Cyclic 3′,5′-guanosine monophosphate

CjBAp12: *Citrus jambhiri* blight associated protein 12

CLV: Clavata

CNG: Cyclic nucleotide-gated

CNGC: Cyclic nucleotide-gated channel

CNP: C-type natriuretic peptide

cv: column volume

ECGG: Expression correlated gene group

ECM: Extracellular matrix

EGF: Epidermal growth factor

EIA Enzyme immunoassay

ENOD40: Early nodulin 40

EST: Expressed sequence tag

ET: Ethylene

FPLC: Fast protein liquid chromatography

G3P: Glyceraldehydes-3-phosphate

GA: Gibberellic acid

GC: Guanylate cyclase

GO: Gene ontology

GTP: Guanosine 5′-triphosphate

hANP: Human atrial natriuretic peptide

HR: Hypersensitive response

IAA: Indole-3-acetic acid

IBMX: 3-isobutyl-1-methyl xanthine

IPT: Adenosine 5′-monophosphate (AMP)-isopentenyl transferase

IPTG: isopropyl-β-D-thiogalactopyranoside

IRGA: Infra-red gas analyzer

irPNP: Immunoreactant plant natriuretic peptide

JA: Jasmonic acid

kDa: KiloDalton

LRR: Leucine-rich repeat

MCP: Mesophyll cell protoplast

MSMO: Murashige and Skoog basal salt with minimum organics

NADPH: Reduced nicotinamide adenine dinucleotide phosphate

NCAPs: Non-cell-autonomous proteins

Ni-NTA: Nickel-nitrilotriacetic acid

NP: Natriuretic peptide

NPR: Natriuretic peptide receptor

NSCC: Non-selective cation channel

NMR: Nuclear magnetic resonance

PCR: Polymerase chain reaction

PM: Plasma membrane

PNP: Plant natriuretic peptide

PR: Pathogenesis-related

PR-1: Pathogenesis-related protein 1

PSK: Phytosulfokine

R: Resistance

RALF: Rapid alkalinisation factor

rANP: Rat atrial natriuretic peptide

RLK: Receptor-like kinase

RlpA: Rare lipoprotein A

RFU: Relative fluorescent unit

RT-PCR: Reverse transcriptase polymerase chain reaction

Rubisco: Ribulose-1,5-biphosphate carboxylase

SA: Salicylic acid

SAR: Systemic acquired resistance

SCR: S-locus cysteine rich

SDS-PAGE: Sodium dodecyl sulphate polyacrylamide gel electrophoresis

SE: Standard error

SNK: Student Newman Kuehls

SP: Signal peptide

StPNP: *Solanum tuberosum* plant natriuretic peptide

TF: Transcription factor

TMV: Tobacco mosaic virus

UV: Ultraviolet

VIC: Voltage independent channels

WAK: Wall-associated kinase

WAKL: Wall associated kinase-like

WAKL10: Wall associated kinase-like 10

XWP: Xylem water potential

List of Figures and Tables

Summary

Several lines of cellular and physiological evidence have suggested the presence of a novel class of systemically mobile plant molecules that are recognized by antibodies generated against vertebrate atrial natriuretic peptides (ANPs). Functional characterization of these immunoanalogues, referred to as immunoreactive plant natriuretic peptides (irPNPs) or plant natriuretic peptides (PNPs), has shown that they play important roles in a number of cellular processes crucial for plant growth and maintenance of cellular homeostasis. Although the various biological roles of PNPs in plants are known, their exact mode of action remains elusive. To elucidate the mechanisms of action for these immunoanalogues, we have prepared a biologically active recombinant PNP from *Arabidopsis thaliana* (AtPNP-A) and the biological activity was demonstrated by showing its ability to induce water uptake into *Arabidopsis thaliana* protoplasts. In addition, the molecule was shown to down-regulate photosynthesis while at the same time up-regulating respiration, transpiration as well as net water uptake and retention capacities in the sage *Plectranthus ecklonii*. Further analysis of the recombinant AtPNP-A indicated that the peptide can induce systemic response signalling though the phloem.

A recombinant Arabidopsis wall associated kinase-like protein (AtWAKL10) that has a domain organization resembling that of vertebrate natriuretic peptide (NP) receptors was also partially characterized as a possible receptor for the recombinant AtPNP-A. Vertebrate NP receptors contain an extracellular ligand-binding domain and an intracellular guanylate cyclase (GC)/kinase domain and signal through the activity of their GC domain that is capable of generating intracellular cGMP from GTP. The structural resemblance of AtWAKL10 to vertebrate NP receptors could suggest a

functional homology with receptor molecules and it is conceivable that such a receptor may recognize PNPs as ligands. The characterization of the recombinant AtWAKL10 showed that the molecule functions as both a GC and a kinase *in vitro*. This strengthened the suggestion that AtWAKL10 could be a possible AtPNP-A receptor especially considering the fact that AtPNP-A applications to plant cells also trigger cGMP transients. Furthermore, a bioinformatic analysis of the functions of AtPNP-A and AtWAKL10 has inferred both molecules in plant pathogen responses and defense mechanisms, thus indirectly functionally linking the two proteins.

Chapter 1

Literature Review

1.1 Introduction

Maintenance of growth, development and physiological processes in general are a key requirement for survival of multicellular organisms such as plants and animals. Enzymes and hormones produced by these organisms play important roles in such processes. In plants, the action of a hormone involves its perception and the initiation of a specific response pathway, which is independent of transcriptional or translational control and a sustained response under the new steady-state growth conditions, which requires the hormone-dependant regulation of transcription (Johri and Mitra, 2001; Vogler and Kuhlemeier, 2003). In many cases, the early responses evoked within a few minutes are at the level of ion fluxes and generation of second messengers such as Ca^{2+}, cyclic adenosine diphosphate ribose (cADPR) or cyclic guanosine-3′,5′-monophosphate (cGMP) (Johri and Mitra, 2001; Vogler and Kuhlemeier, 2003). Besides mediating the response, these second messengers also amplify the signal and thus sustaining the generated response (Johri and Mitra, 2001; Vogler and Kuhlemeier, 2003).

Since this thesis will be examining the roles and mechanisms of action of vertebrate natriuretic peptide analogues in plant growth and homeostasis, this literature review will begin by providing some brief descriptions and functions of the five classical plant hormones and other plant peptidic signalling molecules. This will be followed by a focus on the structure and functions of natriuretic peptides (NPs) in vertebrates as

well as the general modulation of various responses in plants by these peptides. The literature review will then go on to focus on early reports on the existence of a vertebrate natriuretic peptide analogue in plants as well as the general physiological roles of these analogues in plant growth and homeostasis. The modulation of the second messenger cyclic 3′,5′-guanosine monophosphate (cGMP) levels by vertebrate natriuretic peptide analogues in plants will be briefly covered followed by a comprehensive focus on the general roles of this second messenger in plants and particularly the modulation of plant natriuretic peptide-dependent effects via this second messenger. The enzymes, guanylate cyclases (GCs) that catalyse the conversion reaction of the substrate guanosine-5′-triphosphate (GTP) to the second messenger cGMP will also be briefly discussed in the final part of this literature review and such discussions including a brief summary on the identification of the first GC candidate molecules in higher plants.

1.2 The Five Classical Hormones

The five classical hormones, often referred to as the classical five, represent five distinct groups of signalling molecules (Johri and Mitra, 2001). These classical plant hormones are small, non-protein molecules that have specific effects on a large number of developmental and physiological processes (Vogler and Kuhlemeier, 2003).

Auxin was the first plant hormone to be isolated and characterized and its primary form is indole-3-acetic acid (IAA) (Basra, 2000). Other compounds with auxin activity, such as indole-3-butyric acid, phenyl acetic acid and 4-chloro-IAA (Normanly *et al*., 1995), have not yet been well-characterized. For many years, it has

been assumed that tryptophan is the precursor of IAA until this was finally confirmed in seedlings of *Phaseolus vulgaris* with stable isotope labeling studies (Bialek *et al*., 1992). IAA is synthesized from tryptophan through three proposed routes namely, via indole-3-pyruvic acid, tryptamine or indole-3-acetonitrile (Kende and Zeevaart, 1997). Indole-3-acetonitrile is found primarily in the Cruciferae and may be derived from indoleglucosinolates (Normanly *et al*., 1995). Four genes encoding nitrilase, which converts indole-3-acetonitrile to IAA, have been cloned in Arabidopsis and have all been shown to be differentially regulated (Bartel and Fink, 1994).

Work with tryptophan auxotrophic mutants has established that IAA biosynthesis can also take place via a tryptophan-independent route. For example, the orange pericarp mutant in maize does not produce tryptophan yet it accumulates IAA to levels of 50-fold higher than in the wild type (Wright *et al*., 1991). Tryptophan auxotrophs in Arabidopsis also accumulate more IAA than the wild-type plants (Kende and Zeevaart, 1997). On the basis of these data, it was proposed that IAA can be synthesized through a branch point of the tryptophan biosynthetic pathway at indole or indole-glycerol phosphate (Normanly *et al*., 1995). Supporting this idea is the finding that in a cell-free system from immature maize endosperm, radioactive indole is converted to IAA (Rekoslavskaya and Bandurski, 1994). In addition to findings from the tryptophan auxotrophic mutants, certain bacteria and plant cells transformed with *Agrobacterium tumefaciens* do synthesize IAA via a unique pathway in which tryptophan is converted to IAA in two steps. The first enzyme, tryptophan monooxygenase, converts tryptophan to indole-3-acetamide, which in turn is converted to IAA by indole-3-acetamide hydrolase. The genes encoding these two

enzymes have since been used to alter IAA levels in transgenic plants (Klee and Romano, 1994).

IAA occurs not only in the free form but also conjugated to amino acids, peptides, or carbohydrates. These IAA conjugates are biologically inactive and appear to serve functions as IAA storage forms in seeds and hormonal homeostasis. The *iaglu* gene in maize, which encodes an enzyme that esterifies IAA to glucose, has been cloned (Szerszen *et al*., 1994). In Arabidopsis, a gene family that encodes IAA conjugate hydrolases has been identified (Bartel, 1997). Until the late 90s, IAA catabolism was thought to occur via oxidative decarboxylation (*i.e*., through the action of an IAA oxidase). However, the major catabolic route of IAA *in vivo* later appeared to be its oxidation to oxindole-3-acetic acid and subsequent glycosylation through an added 7-hydroxyl (Normanly *et al*., 1995). Another catabolic pathway is via IAA-acetylaspartate to dioxindole-3-acetylaspartate-3-O-glucoside (Kende and Zeevaart, 1997).

Auxins have been shown to promote plant growth by stimulating formation of lateral root primordia as well as through the promotion of cell elongation (Kende and Zeevaart, 1997). The hormone has also been shown to act synergistically with cytokinins in the regulation of cell division (John *et al*., 1993).

Cytokinins can exist naturally and are N^6-substituted adenine derivatives. Besides their availability in higher organisms like plants, several bacterial genera, including Agrobacterium, produce them (Gaudin *et al*., 1994). The key biosynthetic step of cytokinins in Agrobacterium is the addition of an isopentenyl group from isopentenyl

diphosphate to the N^6 of AMP, which is catalyzed by an AMP-isopentenyl transferase (IPT). A similar enzyme activity has also been observed in extracts from plant sources (Blackwell and Horgan, 1994; Chen and Ertl, 1994), but because of its instability, the enzyme has only been partially purified (Chen and Ertl, 1994). The *IPT* gene from Agrobacterium has been cloned and expressed in transgenic plants (Klee and Romano, 1994). However, there are no reports of plant DNA sequences with similarity to the bacterial *IPT* genes (Binns, 1994).

lsopentenyladenosine 5′-monophosphate is the precursor of all other forms of cytokinins (Martin *et al*., 1993). Through hydroxylation of the isopentenyl side-chain and reduction of the double bond, the ribotides of zeatin and dihydrozeatin are formed. It is generally thought that the free bases, such as isopentenyl adenine, zeatin, and dihydrozeatin, are the active forms of cytokinins. Cytokinins with a hydroxylated side chain can be glycosylated to form the O-glucoside or O-xyloside, and these reactions are reversible, because O-glycosylated cytokinins have biological activity. Zeatin O-xylosyl transferase has been isolated from bean embryos, and antibodies against it have been prepared. The enzyme is predominantly localized in the endosperm (Martin *et al*., 1993).

Cytokinins are inactivated irreversibly by two different reactions: formation of N-conjugates with glucose at the 7- or 9-positions or with alanine at the 9-position and the oxidative cleavage of the N^6 side chain of the cytokinin substrate by cytokinin oxidase (Martin *et al*., 1993). The substrates for cytokinin oxidase are isopentenyladenine, zeatin, and their ribosides. By contrast, dihydrozeatin is resistant to cytokinin oxidase. Tobacco plants transformed with the *IPT* gene, which had

elevated cytokinin levels, exhibited increased cytokinin oxidase activities in both leaves and roots (Motyka *et al*., 1996). These results therefore indicated that cytokinin oxidase is induced by its own substrate and thus the substrate plays a role in regulating cytokinin levels in plants. Hence possible genetic manipulation of the cytokinin oxidase may provide a strategy through which cytokinin levels can be modified (Martin *et al*., 1993).

Cytokinins are involved in cell division (John *et al*., 1993) and also play an important role in cell differentiation as well as in organogenesis of plant tissue cultures (Goodwin and Mercer, 1983).

Gibberellic acids (GAs) are a large family of tetracyclic compounds whose several members (over 112 members) have been identified (Hisamatsu *et al*., 1997). Efforts to determine their physiological roles and to elucidate their biosynthetic pathways have been greatly facilitated by the availability of GA-deficient (*i.e*., dwarf) mutants (Kende and Zeevaart, 1997). Metabolic studies have been conducted with systems that are rich sources of GAs, such as the fungus *Gibberella fujikuroi* and immature seeds of pumpkin, pea, and bean. However, maize is the only higher plant in which the entire biosynthetic pathway of GAs has been demonstrated in vegetative tissues by feeding various intermediates (Suzuki *et al*., 1992; Kobayashi *et al*., 1996). These and other studies have shown that the GA biosynthetic pathway can be divided into three different stages as is outlined by MacMillan *et al*., (1997), Hedden and Kamiya (1997), and Graebe (1988).

Gibbererellic acids regulate the mobilization of soluble sugars from starch in cereal grains and co-regulate germination and growth (Kende and Zeevaart, 1997). They have also been shown to induce stem growth in many rosette plants and dwarf mutants and such a growth response was due to a combined result of enhanced cell division and increased cell elongation activities in the sub-apical meristems (Kende and Zeevaart, 1997).

Abscisic acids (ABAs) are synthesized from carotenoids with xanthoxin acting as a sole intermediate (Davies and Jones, 1991). Work on ABA biosynthesis was a good example of how a combination of genetic, molecular, and biochemical approaches could lead to the elucidation of a complex biosynthetic pathway (Kende and Zeevaart, 1997). Earlier on, the similarity in structure between ABA and the end groups of certain carotenoids led to the proposal that ABA may be a breakdown product of carotenoids, with xanthoxin as an intermediate. This idea was supported by the finding that plants that do not accumulate carotenoids (either because of mutation or treatment with inhibitors) also lack ABA (Kende and Zeevaart, 1997). Furthermore, labeling studies with $^{18}O_2$ established that one $^{18}O_2$ atom is rapidly incorporated into the carboxyl group of ABA, indicating that there is a large precursor pool (*i.e.*, carotenoids) that already contains the oxygens on the ring of the ABA molecule (Zeevaart *et al.*, 1991). Finally, in etiolated leaves and roots, which have low levels of carotenoids, a 1:l stoichiometry was found between the disappearance of violaxanthin and neoxanthin and the appearance of ABA and its catabolites (Li and Walton, 1990; Parry *et al.*, 1992).

The ABA-deficient *aba1* mutant of Arabidopsis is blocked in the epoxidation of zeaxanthin to antheraxanthin and violaxanthin, indicating that the epoxycarotenoids violaxanthin and neoxanthin are essential for ABA production (Rock and Zeevaart, 1991). The *aba2* mutant of *Nicotiana plumbaginifolia* is orthologous with *aba1* of Arabidopsis and has been cloned. The corresponding fusion protein has zeaxanthin epoxidase activity (Marin *et al*., 1996).

The last two steps in the pathway, from xanthoxin to ABA-aldehyde to ABA, are catalyzed by constitutively expressed enzymes (Sindhu and Walton, 1988; Schwartz *et al*., 1997), with the result that the level of xanthoxin in leaves is always very low relative to ABA (Parry *et al*., 1990). The *aba2* mutant in Arabidopsis is the only known mutant for the conversion of xanthoxin to ABA-aldehyde. By contrast, mutants for the final step, ABA-aldehyde to ABA, have been found in a number of species (Taylor, 1991). In some cases (*e.g*., *nar2a* in barley, *flacca* in tomato, and *aba3* in Arabidopsis), the lesion is not in the aldehyde oxidase apoprotein but in the molybdenum cofactor that is required by the enzyme (Taylor, 1991).

The biosynthesis of ABA increases when plant cells lose turgidity (Zeevaart and Creelman, 1988; Creelman and Mullet, 1991), which is an indication that there is a step in the biosynthetic pathway that is activated by water stress. Considering that the immediate epoxycarotenoid precursors are always present in large excess relative to ABA (Norman *et al*., 1990) and that the enzyme activities of the final two steps from xanthoxin to ABA are not affected by dehydration, it follows that the cleavage reaction from epoxycarotenoids to xanthoxin is the most likely regulatory step in the water stress activated pathway.

ABAs are growth inhibitors and are involved in the regulation of stomatal closures, adaptation to various stresses, induction of dormancy and formation of seeds (Walton, 1980). They are also involved in the promotion of abscission as well as induction of bud and seed dormancy (Walton, 1980). ABAs also control seed formation and maturation as well as synthesis of storage proteins (Walton, 1980).

Ethylene is biosynthesized via a 1-aminocyclopropane-1-carboxylic acid (ACC) as its immediate precursor (Peiser *et al*., 1984; Yang and Hoffmann, 1984). The breakthrough in its biosynthetic pathway was unravelled in 1979, where the first committed step in its biosynthesis is the conversion of S-adenosyl-L-methionine to 5'-methylthioadenosine and ACC (Yang and Hoffmann, 1984). This commited initial step is also the key regulatory step in ethylene biosynthesis (Yang and Hoffmann, 1984) and the enzyme that catalyzes this step, ACC synthase, was partially purified before its corresponding gene was cloned (Kende, 1993; Zarembinski and Theologis, 1994). ACC synthase is encoded by a multigene family whose members are differentially expressed in response to developmental, environmental, and hormonal factors. For example, by using gene-specific probes, the differential expression of tomato ACC synthase family members has been investigated (Olson *et al*., 1991; Yip *et al*., 1992). Transcripts of one isoform increased during fruit ripening, those of another increased in response to wounding, and those of a third form increased in response to treatment with auxin (Olson *et al*., 1991; Yip *et al*., 1992). ACC synthase genes expressed in response to a particular stimulus (*e.g*., the application of auxin) are more similar to genes controlled by the same stimulus in other species than they are to other ACC genes in the same species (Liang *et al*., 1992; Trebitsh *et al*., 1997).

The final step in ethylene biosynthesis, the conversion of ACC to ethylene, is catalyzed by ACC oxidase. ACC oxidase was first identified by expressing the tomato cDNA pTOM13 in an antisense orientation, which then resulted in greatly reduced ethylene production in tomato (Hamilton *et al*., 1990). The deduced amino acid sequence of pTOM13 is similar to that of dioxygenases that require Fe^{2+} and ascorbate as cofactors. When these cofactors were added to assays for ACC oxidase, enzyme activity was completely recovered (Ververidis and John, 1991). Later, it was found that CO_2 is also an essential activator of ACC oxidase (Fernández-Maculet *et al*., 1993).

Numerous cDNAs for ACC oxidase have been isolated from different species (Barry *et al*., 1996). As is the case with ACC synthase, ACC oxidase is encoded by small multigene families. Although the initial evidence indicated that ethylene synthesis is controlled at the level of ACC synthase, there is now considerable evidence that ACC oxidase also plays a significant role in regulating ethylene biosynthesis (Barry *et al*., 1996). By using gene-specific probes for three ACC oxidase genes of tomato, distinct patterns of expression in various organs and at different stages of development have been observed (Barry *et al*., 1996). Moreover, the positive feedback loop in which treatment of tissue with ethylene often stimulates ethylene production by that tissue appears to take place through enhanced expression of ACC synthase and ACC oxidase (Kende, 1993).

Besides being converted to ethylene, ACC can also be irreversibly conjugated to form N-malonyl-ACC (Kionka and Amrhein, 1984). Malonylation of ACC regulates the

level of ACC and thus the production of ethylene. Ethylene can be metabolized by plant tissues to ethylene oxide and ethylene glycol (Sanders *et al*., 1989; Bleeker, 2001), but the physiological significance of this metabolism remains to be established. As a gas (Bleecker and Kende, 2000), ethylene can readily diffuse from plant tissues and therefore, its catabolism is not essential for its removal (Kende and Zeevaart, 1997).

Ethylene has profound effects on plant growth and development (Chang and Shockey, 1999). It is involved in promotion or inhibition of flowering, evokes the classical triple response in Arabidopsis seedlings grown in the dark (these responses are characterized by an exaggerated curvature of the apical hook, a radial swelling of the hypocotyl and an inhibition of hypocotyl and root elongation) and is critically associated with ripening of fruits (Johri and Mitra, 2001). Furthermore, several environmental stresses such as wounding, pathogen attack, and flooding can induce ethylene production and this in turn can lead to defense responses such as accelerated senescence, apoptosis and abscission of infected organs as well as the induction of specific defense proteins (Chang and Shockey, 1999).

1.3 Regulatory Peptides

In higher plants, herbivores and pathogens cause wounding that triggers the expression of serine protease inhibitors (Kende and Zeevaart, 1997). These proteins were found to accumulate in undamaged parts of wounded leaves at fentomolar concentrations (Green and Ryan, 1972; Ryals *et al*., 1996). The observation suggested the presence of a mobile factor operating as a hormone in plant wound-defense response system. This factor was later purified biochemically leading to the

identification of an 18 amino acid residue peptide (Ryals *et al*., 1996) now commonly known as systemin. This molecule is a proteolytically-processed form of a 200 amino acid residue precursor called pro-systemin (Pearce *et al*., 1991). In addition to systemin, two more prosystemin isoforms produced by an alternative splicing mechanism were also shown to be active as signals in the wound response system (McGurl and Ryan, 1992).

The production and perception of systemin involve the post-translational processing of a precursor molecule (prosystemin) and the recognition of the peptide by a presumed 160 kiloDalton (kDa) membrane receptor that then induces the activation of defense genes (Takayama and Sakagami, 2002). The systemin-activated signalling cascades are lipid-based that are initiated by a release of a linoleic acid from membranes feeding into the pathway (Scheer and Ryan, 1999). Oxylipin is one of the components and is a structural analogue of prostaglandins (Bergey *et al*., 1996). Some similarities between the defence-signalling pathways in tomato leaves and macrophages (and mast cells) have led to some speculations about a common ancestral origin between plant and animal defence pathways (Bergey *et al*., 1996).

Early nodulin 40 (ENOD40) is a plant-encoded peptide expressed in response to Nod factors and classical hormones such as auxin and cytokinins in legumes and non-legumes (Hirsch and Fang, 1994; van de Sande *et al*., 1996; Fang and Hirsch, 1998). Unlike systemin, ENOD40 is not synthesized via a precursor and as a signal peptide, it has a role in root nodulation (Rohring *et al*., 2002).

Phytosulfokine (PSK) is a signaling peptide that has been purified from dispersed asparagus mesophyll suspension cell culture medium (Fang and Hirsch, 1998) and to date, it is the only peptide produced from post-translational sulfation of tyrosine residues in plants (Takayama and Sakagami, 2002). PSK is widely distributed in higher plants and is present in both monocotyledon and dicotyledon cell lines (Fang and Hirsch, 1998). The peptide can induce dedifferentiation and callus growth at very low concentrations ($\geq 10^{-8}$ M) and at low cell density (~300 cells/ml) (Matsubayashi and Sakagami, 1996). At this concentration level, it can be suggested that PSK alone can not induce cellular dedifferentiation and re-differentiation, perhaps and in addition, it may require certain ratios and concentrations of auxins and cytokinins (Basra, 2000). The production and perception of PSKs involve the post-translational processing of a precursor molecule (pre-proPSK) and the recognition of the peptide by a 120 kDa membrane receptor which would then induce genes responsible for cell proliferation (Takayama and Sakagami, 2002).

The *Arabidopsis thaliana* genes *CLAVATA1* (*CLV1*) and *CLAVATA3* (*CLV3*) are the main important members of the *CLAVATA* gene family. They appear to play important roles in the regulation of shoot meristem development (Clark *et al*., 1997; Meyerowitz, 1997). CLAVATA1 and CLAVATA3 cause a progressive enlargement of shoot and floral meristems (Clark *et al*., 1997; Meyerowitz, 1997). *CLAVATA1* encodes a predicted 105 kDa receptor-like kinase (RLK) that has 21 extracellular leucine-rich repeats (LRRs), a single transmembrane domain and an extracellular Ser/Thr kinase (Clark *et al*., 1997). On the other hand, *CLAVATA3* encodes a 96 residue peptide containing an N-terminal secretion signal (Fletcher *et al*., 1999).

Both CLAVATA1 and CLAVATA3 are expressed in shoot apical meristems and there is a strong possibility that CLAVATA3 is a ligand for the CLAVATA1 receptor-like kinase (Clark *et al*., 1997; Meyerowitz, 1997). It has been shown by biochemical studies that CLAVATA1 can exist in two different complexes of 185 and 450 kDa (Trotochaud *et al*., 1999). Also, the mRNA of both complexes accumulates in deeper cell layers (Clark *et al*., 1997; Meyerowitz, 1997). CLAVATA3 is localized to the extracellular space (Rojo *et al*., 2002) and is expressed specifically in the central zone of the outermost meristem. It then, travels through the extracellular space to the shoot meristems.

Several other peptidic molecules that have also been identified include S-locus cysteine rich (SCR) proteins that act in self-incompatibility (Schofer *et al*., 1999), rapid alkalinization factor (RALF) which arrests root growth and development (Pearce *et al*., 2001), POLARIS that influences cell expansion and plant growth (Casson *et al*., 2002; Lindsey *et al*., 2002), and those other molecules that are involved in antimicrobial activities (Garcia-Olmedo *et al*., 2001). Most of these regulatory peptides function in cell-cell communication and signalling through an interaction with their specific receptors as is outlined in Table 1.1 below.

Table 1.1: Peptide growth factors and their specific receptors in higher plant

Peptide	Sequence[a]	Biological activity	Receptor(s)
Systemin	AVQSKPPSKRDPPKMQTD (Tomato) RGANLPPPSPASSPPSKE (Tobacco) NRKPLSPPSPKPADGQRP (Tobacco)	Defense signaling	160 kDa membrane protein
Phytosulfokine	Y(SO_3H)IY(SO_3H)TQ	Cell proliferation	120 kDa and 160 kDa membrane proteins
CLAVATA3	MDSKSFVLLLLLFCFLFLHDASD LTQAHAHVQGLSNRKMMMMKMES EWVGANGEAEKAKTKGLGLHEEL RTVPSGPDPLHHHVNPPRQPRNN FQLP (Deduced sequence from cDNA)	Growth regulation of meristem	CLV1 and CLV2 (185 kDa receptor kinase complex)
SCR (SP11)	MKSAVYALLCFIFIVSGHIQELE ANLMKRCTRGFRKLGKCTTLEEE KCKTLYPRGQCTCSDSKMNTHSC DCKSC (Deduced sequence from SCR_8 cDNA)	Self incompatibility SRK	(110 kDa receptor kinase)

[a]Predicted signal sequence is underlined.

The table represents the receptor sequences and sizes as well as the biological activities into which the four different signal peptides are involved. (Table adapted from Matsubayashi *et al*., 2001).

1.4 Natriuretic Peptides

1.4.1 Natriuretic Peptides in Animal Systems

Natriuretic peptides (NPs) are a family of bioactive polypeptides that have been identified in vertebrate species ranging from elasmobranches to mammals. The NPs exist in the brain and various segments of the kidney (Goetz, 1991), and are strongly implicated in the regulation of salt and water homeostasis as well as blood pressure in vertebrates (Kourie and Rive, 1999; Kone, 2001). In mammals, four types of NPs have been isolated namely; atrial NP (ANP) (deBold *et al*., 1981), brain NP (BNP) (Sudoh *et al*., 1988), C-type NP (CNP) (Sudoh *et al*., 1990), and urodilatin (Feller *et al*., 1989). ANP, also referred to as atrial natriuretic factor (ANF) or atriopeptin, was first discovered in extracts of rat atria (deBold *et al*., 1981). It is encoded by a gene

with three exons that encodes a PrePro-ANP containing a signal peptide (SP). The 24 amino acid SP at the N-terminal and the two C-terminal arginine residues found in some vertebrate molecules are cleaved off to yield Pro-ANP (1-126). Subsequent proteolytic steps yield the ANP (1-98) and ANP (99-126). The main biologically active ANP is believed to be the C-terminal 28-mer ANP (99-126) which forms a circular structure due to the formation of disulphide bonds (Fig. 1.1 from Gehring, 1999).

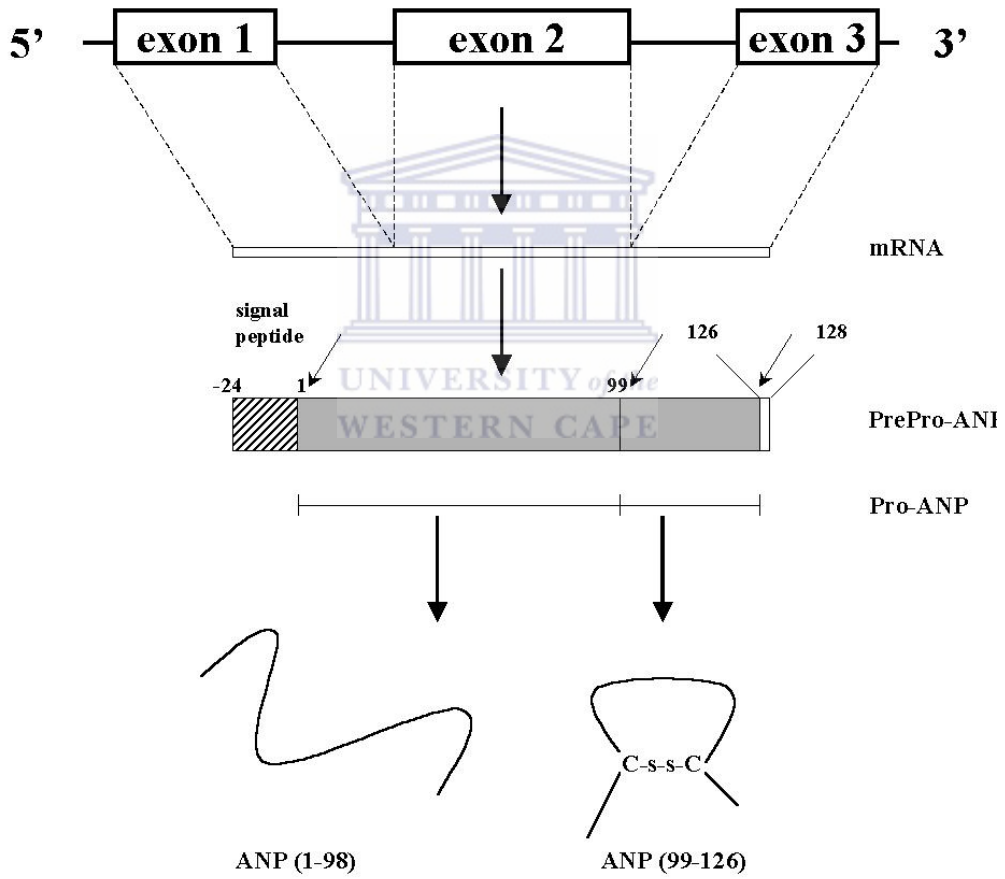

Figure 1.1: Representation of the gene structure and major processing steps of ANP. Small arrows mark the major cleavage sites. ANP (99-126) is the main and best established biologically active compound. ANP (1-98) has also been reported to be cleaved further into ANP (1-30), ANP (31-67), ANP (68-77) and ANP (78-98). The mode of action and function of these cleavage products is still debated. (Figure from Gehring, 1999).

1.4.2 Natriuretic Peptides and their Receptor Systems in Animals

The functions of NPs in animals are mediated by two types of receptor systems; natriuretic receptor A (NPR-A) and natriuretic receptor B (NPR-B) system, and natriuretic receptor C (NPR-C) system (Garbers and Lowe, 1994). The NPR-A and NPR-B receptor system consists of an amino terminal extracellular ligand binding domain, a single membrane spanning region, an intracellular kinase homology domain and a carboxy-terminal guanylate cyclase (GC) catalytic domain (Garbers and Lowe, 1994). Binding of a ligand to the extracellular part of this domain stimulates intracellular production of cyclic 3′,5′-guanosine monophosphate (cGMP) (Garbers and Lowe, 1994), which will act as a second messenger for a number of physiological processes. NPR-C receptor system lacks a GC domain, and is suggested to be linked to cyclic 3′,5′-adenosine monophosphate (cAMP) pathways although it is known to function as a clearance receptor that metabolises and internalises NPs (Koller and Goeddel, 1992; Maack, 1992; Anand-Srivastava and Trachte, 1993).

All the three NP receptors have been cloned in prokaryotic systems (Nankervis *et al*., 2007; Powell *et al*., 2008), and the NPR-A and NPR-B system constitutes a classic family of receptor-guanylate cyclases (Chinkers *et al*., 1989). The three NP receptors appear as single transmembrane proteins with extracellular domains of approximately 440 amino acids (Chinkers *et al*., 1989). However, while both NPR-A and NPR-B have bipartite intracellular domains of roughly 280 and 250 amino acids respectively, the NPR-C has an intracellular domain of only 37 amino acids (Chinkers *et al*., 1989). It has been found that particular NPs show distinctive affinities for different receptors. For instances, CNP has its highest affinity for NPR-B, while ANP shows the highest affinity to NPR-A and NPR-C (Chinkers *et al*., 1989).

1.4.3 Plant Responses to Animal Natriuretic Peptides

The NPs isolated from animals have been demonstrated to have some biological effects in plants. They rapidly and significantly increase the rate of transpiration, solute flow and uptake in *Dianthus caryophillus* and *Chrysanthemum mosifolium* (Vesely *et al*., 1993). It was also established that rat atrial natriuretic peptide (rANP) induces stomatal opening in *Tradescantia multiflora* in a concentration-dependant manner (Gehring *et al*., 1996). Rat ANP was also shown to rapidly and transiently induce elevation of cGMP levels in maize (*Zea mays*) root stele tissue (Pharmawati *et al*., 1998a) as well as increasing some radial water movements in *Tradescantia multiflora* (Suwastika and Gehring, 1998).

1.4.4 The Discovery of Natriuretic Peptides in Plant Systems

With reference to the functions of NPs in animals, Vesely *et al*., (1993) proposed that an ANP-like molecules and system might also be present in the plant kingdom. They later provided some evidence for such an idea by showing that NP-like molecules were present in roots, stems, and leaves of a wide variety of embryophyta. Their radioimmunoassay experiment on tissue extracts from Florida beauty (*Dracena godseffiana*) was an initial indication to show that NP immunoanalogues are present in plants (Vesely and Giordano, 1991). They prepared and used antibodies against the N-terminus (ANP, 1-98), the mid-portion (ANP, 31-67) and the C-terminus (ANP, 99-126) of a vertebrate ANP to detect some peptides in plant leaves and stems. They also presented some more evidence that NP-like transcripts existed in plants through Southern and Northern blotting of English ivy (*Hedra helix*) DNA and RNA

respectively using the ANP gene sequence as a probe (Vesely *et al*., 1993), although there was some debate about the validity of the data and the conclusions. However, immunoaffinity purification using rabbit anti-human ANP (1-28, human canine) antiserum, successfully isolated immunoreactive PNPs from *Hedra helix* (Billington *et al*., 1997).

1.4.5 Characterization of Immunoreactant Plant Natriuretic Peptides

Partial protein sequencing of immunoaffinity purified PNPs eventually led to the identification of a homologous molecule in *Arabidopsis thaliana* (accession number: AAD 08935). This PNP was termed *Arabidopsis thaliana* plant natriuretic peptide-A (AtPNP-A) and a second related molecule was named AtPNP-B (accession number: CAB 79756). AtPNP-A and -B share 37% of sequence identity (Ludidi *et al*., 2002). Another peptide from *Citrus jambhiri*, the blight associated protein 12 (CjBAp12) (accession number: AAD 03398) (Ceccardi *et al*., 1998) was also noted to be similar to PNPs. AtPNP-A is a small protein of 126 amino acids in length (MW: 14016; pI: 9.22) (Fig. 1.2) that is encoded for by a 478 base pair (bp) gene with a single intron of 100 bp. The protein contains a 24 amino acid signal peptide (MW: 2249) that is necessary for its secretion into the extracellular space but not required for its biological function (Fig. 1.2). The part most conserved between PNPs from different plant species (between amino acids 33 and 66) has also been shown to be a key to its biological function (Morse *et al*., 2004; Wang *et al*., 2007) and is the one that shares some similarity to animal NPs and in particular human atrial natriuretic peptide (hANP) (99-126) (Fig. 1) (Meier *et al*., 2008a).

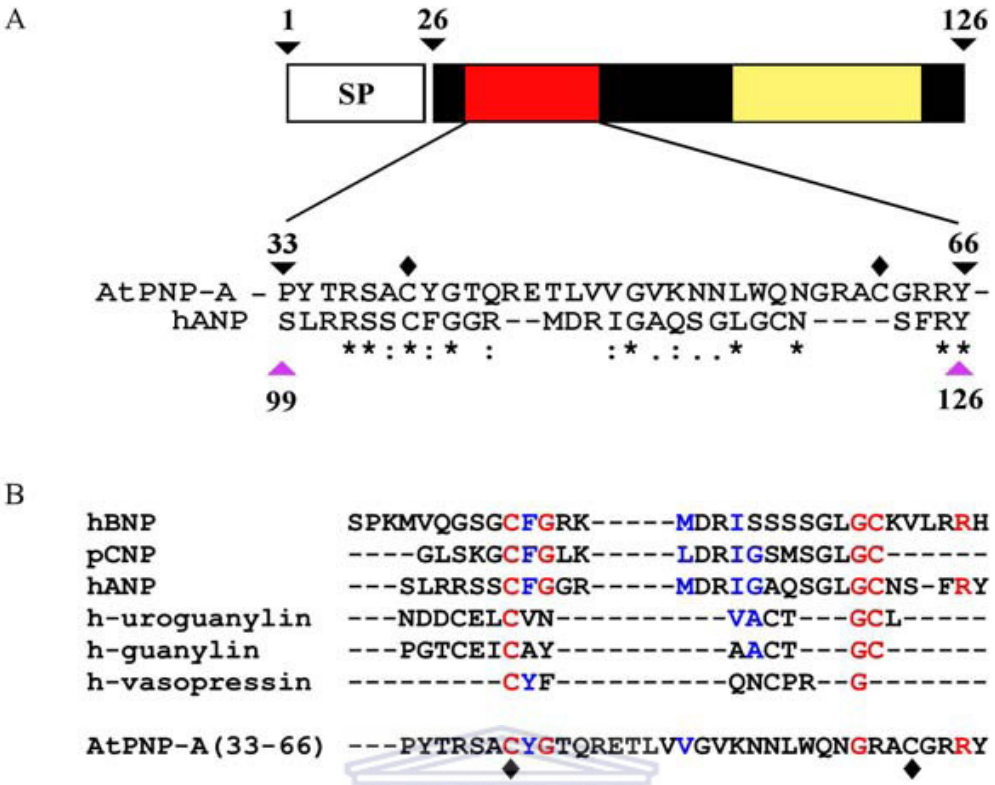

Figure 1.2: Amino acid sequence comparison of AtPNP-A and its analogues. (**A**) *Arabidopsis thaliana* PNP-A. The first 25 N-terminal amino acids are the signal peptide (SP) that directs the protein into the extracellular space. Amino acids 33 to 66 convey the homeostasis regulating biological activity (in red). The C-terminus also contains a rare lipoprotein A (RlpA) domain (DPBB_1; e value = 0.002) marked in yellow. The amino acid sequence of AtPNP-A (33-66) is compared to human ANP [hANP (99-126) delineated by purple triangles] and asterisks (*) signify identical amino acids, colons (**:**) are conservative replacements, full stops (**.**) are semi-conservative replacements and the lozenges (♦) indicate cysteine residues in AtPNP-A that can form disulfide bridges. (**B**) Alignment of amino acid sequences of NP-like molecules. Identical amino acids are in red, conservative substitutions are in blue and the lozenges (♦) indicate cysteine residues in AtPNP-A that can form disulfide bridges. (Figure from Meier *et al*., 2008a).

The AtPNP-A, its related sequences AtPNP-B and orthologues in other higher plant species (CjBAp12) share domains with the cell wall-loosening expansins (Fig. 1.3 from Ludidi *et al*., 2002) and therefore can be classified as expansin-related on the basis of such homology. Interestingly, the C-terminus domain of α- and β-expansins (Cosgrove, 2000) is encoded by an entire exon that is absent in immunoreactant PNP-like molecules (Ludidi *et al*., 2002). Expansins are distantly related to glucanases and cellulases where in the latter, the C-termini have been proven to be cell wall-binding (Linder and Teeri, 1997; Barre and Rouge, 2002; Ludidi *et al*., 2002) and the same

function has been suggested for α- and β-expansins C-terminus (Cosgrove, 2000). Since expansins, which are the closest relatives of immunoreactant PNPs, and the more distantly related glucanases and cellulases, all contain the C-terminus, it may be reasonable to argue that the immunoreactant PNP-like molecules have lost this domain (Ludidi *et al*., 2002). This is in keeping with the fact that the domain is delineated by an intron-exon border (Ludidi *et al*., 2002). Therefore, loss of the wall-binding domain in immunoreactant PNP-like molecules could result in their increased mobility (Ludidi *et al*., 2002). It also follows from phylogenetic data that similarities between AtPNP-A and ANP are the result of convergent evolution (Ludidi *et al*., 2002; Gehring and Irving, 2003).

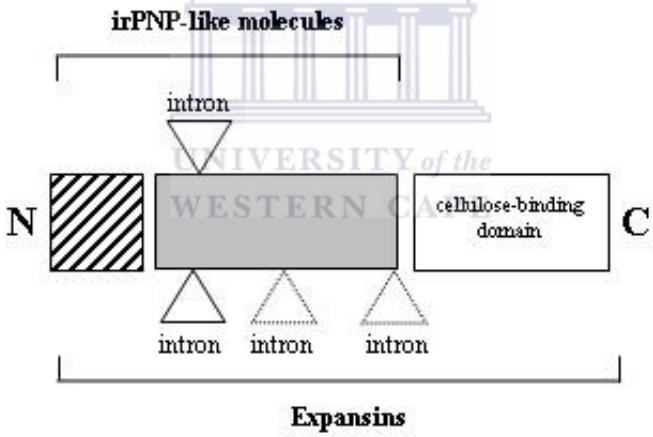

Figure 1.3: Domain comparison of expansins and immunoreactant PNP-like molecules. The open triangles represent the intronic sites while their major structural difference is borne on the cellulose-binding domain. (Figure from Ludidi *et al*., 2002).

A model (Fig. 1.4 from Ludidi *et al*., 2002) of AtPNP-A (amino acids 27 to 126) based on the crystal structure of the N-terminal domain of Phl P 1 Timothy Grass Pollen Allergen (Accession No: P43213) determined to 2.9Å (pdb code = 1n10) using the structure prediction program MODELLER (Sali and Blundell, 1993) revealed (Z score: >5) that this molecule has the same fold as the N-terminal domain of a Phl P 1 (Ludidi *et al*., 2004). The basic common fold for these molecules is a double-psi (ψ) β barrel structure where a six-stranded β barrel assumes a pseudo-two-fold axis in which the parallel strands form two psi structures (Castillo *et al*., 1999). Such a psi structure comprises a loop and a strand that resembles the Greek letter psi (ψ). The first psi loop connects strands β1 and β2, whereas the second psi loop connects strands β4 and β5. In the currently known structures, the protein active sites cluster around the psi loops indicating that its rigidity, protrusion and free main chain functional groups might be well suited to providing a framework for catalysis (Castillo *et al*., 1999). In AtPNP-A, the first psi loop connects strands β1 and β2, whereas the second psi loop connects strands β4 and β5.

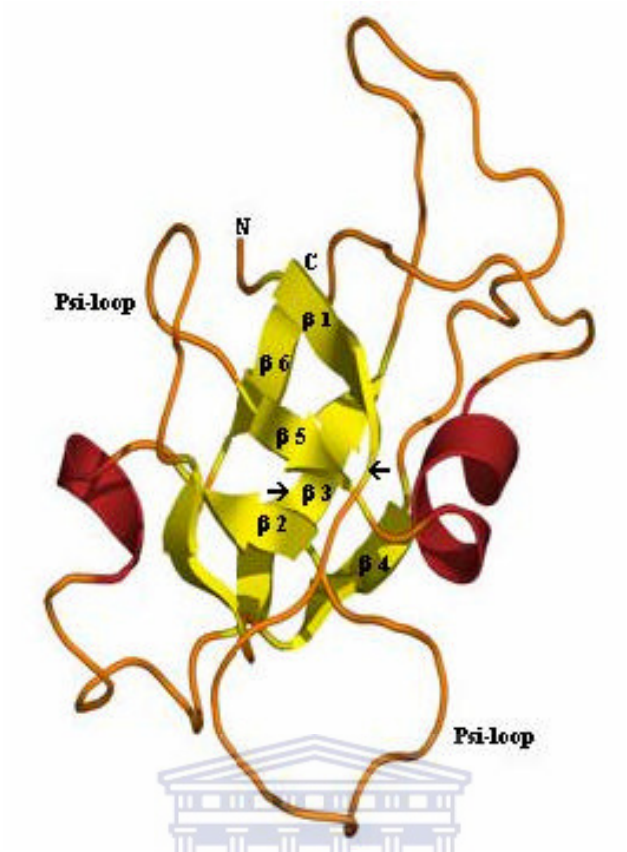

Figure 1.4: A fold model of AtPNP-A (amino acids 27 to 126). The model shows the six stranded double-psi β barrel structure that assumes a pseudo-two-fold axis with parallel strands forming two *psi* structures. The α-helices are in red, the 6 β-strands are in yellow. The signal peptide was not included in the model and the domain conferring activity is between arrows. The model was generated using the software MOLSCRIPT (Kraulis, 1991). (Figure from Ludidi *et al*., 2004).

1.4.6 Biological Roles of Immunoreactant Plant Natriuretic Peptides in Plants

1.4.6.1 Promotion of radial water movements from the xylem tissue

In vascular plants, water and solutes are taken up from the soil mainly via the root system and are transported either actively or passively to different plant organs and cells. The bulk of water is lost via the stomatal pores, whereas ions generally remain in the system and fulfil specific structural, metabolic or signalling roles and/or are sequestered into specific organelles (Davies, 1995). Suwastika and Gehring (1998) demonstrated that both ANP and immunoreactant PNP significantly increased radial water movements out of the xylem of shoots of *Tradescantia multiflora.* They

presented indirect evidence for a systemic role of a natriuretic peptide system operating in plants and this suggestion was compatible with previously reported ANP- and immunoreactant PNP-dependant stomatal opening (Gehring *et al*., 1996; Pharmawati *et al*., 1998b).

1.4.6.2 Promotion of leaf stomatal opening

Plants normally regulate their water movements primarily by controlling the rate of transpiration through stomatal pores whose aperture width is controlled by guard cells. Therefore, any changes in guard cell volumes will alter the stomatal aperture. Stomatal guard cell volume is in turn regulated mainly by movement of K^+ and counter ions such as Cl^- (or malate) into the guard cells during opening, and their movement out of the guard cells during closure (Assmann and Shimazaki, 1999). The mechanism for stomatal opening involves the active transport of potassium ions into the guard cells. This can be initiated by the sensing of blue light wavelengths of daylight by carotenoids, which then activates a H^+-ATPase in the plasma membrane of the guard cell (Assmann and Shimazaki, 1999). The H^+-ATPase then hydrolyses adenosine 5′-triphosphate (ATP) generated from the light reactions of photosynthesis to produce enough energy that then drives the ion pumping. Protons are pumped out of the cytoplasm thereby creating a "proton motive force" which results in the opening of some voltage-operated channels in the membrane, thus allowing potassium ions to flow into the cell from surrounding cells. Chloride ions also enter the cell (their movement is coupled to the re-entry of some of the extruded protons) to act as counter ions to the potassium ions (Assmann and Shimazaki, 1999). As potassium ions enter the cell, water molecules also follow, resulting in an increase in turgidity

and subsequent stomatal opening. In contrast, under conditions of turgor loss, the pore closes.

The influx and efflux of K^+, with either Cl^- or malate, across the plasma and vacuolar membranes largely, but not exclusively, drive changes in guard cell turgor (Hetherington, 2001). Billington *et al*., (1997) showed that immunoreactant PNP isolated from *Hedera helix* can induce stomatal opening in a concentration dependent manner and that the effect of this peptide was observed at concentrations significantly smaller than those required to elicit a similar response with ANP (Billington *et al*., 1997).

1.4.6.3 Induction of protoplast cell volume changes

Since stomatal opening requires guard cell swelling caused by water uptake, and both ANP and immunoreactant PNP have been shown to cause stomatal opening, Maryani *et al*. (2001) tested whether immunoreactant PNP could effect cell volume changes. They treated mesophyll cell protoplasts (MCPs) suspended in 200 mM sorbitol with immunoaffinity purified potato PNP and found that the peptide could cause significant increases in swelling of the cells (Maryani *et al*., 2001). The swelling response effect was established to be both time-dependent and dose-dependent (Maryani *et al*., 2001). A similar response was also observed in *Arabidopsis thaliana* MCPs when they were treated at nanomolar concentration with three different forms of recombinant AtPNP-A (Morse *et al*., 2004). In an attempt to delineated the active domain of the AtPNP-A, Morse *et al*., (2004) used the full length size of AtPNP-A (1-126), a fragment that lacked the signal peptide (26-126) and a short peptide with some sequence homology to vertebrate peptide (33-66) and demonstrated that all three

forms of the molecule could show significant biological function (Morse *et al*., 2004). Furthermore, in an attempt to identify the biologically active domains of AtPNP-A, Wang *et al*. (2007) used the native recombinant AtPNP-A fragment lacking the signal peptide (26-126) and smaller synthetic peptides; peptide A (33-66), peptide B (33-44), peptide C (45-56), and peptide D (55-66) and demonstrated that all molecules except peptide B could induce cell swelling in *Arabidopsis thaliana* MCPs (Wang *et al*., 2007). Peptide B failed to demonstrate biological activity because it has the least amount of secondary structure, while the other peptides have at least the secondary structures required for biological activity (Wang *et al*., 2007).

1.4.6.4 Modulation of plasma membrane H^+-ATPase

A key function for the plasma membrane (PM) H^+-ATPase is to generate a proton electrochemical gradient that provides a driving force for the uptake and efflux of ions and metabolites (sugars,) across the plasma membrane and against osmotic and ionic gradients. Essential nutrients such as nitrates and sulphates are taken into cells against concentration and electrical gradients by H^+-coupled anion symporters. The electrical gradient across the PM also determines the direction and extent of passive ion flow through ion-specific channels (Sze *et al*., 1999).

Since guard cell and radial water movements are at least in part dependent on PM H^+-ATPase activity (Maryani *et al*., 2000), the question arose; 'Can NPs and in particular PNPs exert a direct effects on this key enzyme and consequently on the H^+ gradients?' Immunoreative PNP was demonstrated to rapidly and significantly modulate ATP-dependent proton gradients in PM vesicles from *Solanum tuberosum* leaf cells (Maryani *et al*., 2000). It was further observed that the immunoreactant PNP

molecule did not reduce ATP-dependent generation of inorganic phosphate, concluding that it modulated the transmembrane proton gradient by activating H^+/Cl^- symporters rather than by inhibiting the ATPase (Maryani *et al*., 2000). On the other hand, Pharmawati *et al*., (2001) further found that immunoreative PNP stimulated the PM H^+-ATPase in guard cells but did not lead to increased H^+ gradients (Pharmawati *et al*., 2001), and this can be explained in two ways. Either immunoreactant PNP affects H^+ permeability or it simply modulated those symporters that carry H^+ back into the cell, which may in turn further stimulate the ATPase.

1.4.6.5 Modulation of K^+, Na^+ and H^+ ion fluxes

Using non-invasive ion-selective vibrating microelectrodes to measure the net fluxes of K^+, Na^+ and H^+ in maize conductive tissue, immunoreactive PNP was shown to cause an immediate net H^+ influx and delayed net K^+ and Na^+ uptake (Pharmawati *et al*., 1999). It was further demonstrated that a recombinant AtPNP-A could also causes some rapid H^+ influxes in the elongation zone of *Arabidopsis thaliana* roots, but not in the mature zone (Ludidi *et al*., 2002). The recombinant protein also induced some significant K^+ and Na^+ effluxes in the mature zone only. The qualitatively similar characteristic of Na^+ and K^+ flux changes and a relatively constant stoichiometry between Na^+ and K^+ flux changes was interpreted as an effect on non-selective cation channels (NSCC) in response to immunoreactive PNP (Ludidi *et al*., 2002).

1.4.6.6 Modulation of cyclic 3´,5´-guanosine monophosphate levels

While it was shown that guard cell responses to kinetin and natriuretic peptides are cGMP-dependent (Pharmawati *et al*., 1998b), immunoreactant PNPs (from *Hedera helix*) were shown to modulate cGMP levels in conductive tissue of *Zea mays* root stele (Pharmawati *et al*., 1998a). The levels of cGMP in control samples were recorded as 0.29 pmol/g fresh weight compared to levels of cGMP in treated samples which were recorded as 1.38 pmol/g fresh weight. This elevation in cGMP levels occurred within 30 seconds and was maintained for 10 minutes before reverting to basal levels. The immunoreactant PNPs were found to induce cytosolic elevations of cGMP to levels that were almost identical to those induced by ANP in erythrocytes (Pharmawati *et al*., 1998a).

Cyclic GMP levels have also been shown to be modulated by salt and osmotic stresses. Donaldson *et al*., (2004) measured cGMP levels in *Arabidopsis thaliana* seedlings in response to NaCl and osmotic stress and found that the cGMP content of the seedlings increased rapidly after the NaCl or osmotic stress (Donaldson *et al*., 2004). The increase in cGMP levels were detectable within 5 seconds and were significantly higher compared to untreated control seedlings after 15 minutes. For the osmotic stress induction, they used sorbitol concentrations that were osmotically equivalent to the NaCl treatments and reported that the initial rate of increase of cGMP levels was significantly higher after osmotic stress than NaCl stress (Donaldson *et al*., 2004).

In addition, PNP expressions have been shown to be affected by both salt and osmotic stresses. Using the brassicaseus weed *Erucastrum strigosum*, Rafudeen *et al*., (2003)

have identified an immunoreactant PNP and further demonstrated that when plants were exposed to 300 mM NaCl, the amount of immunoreactant PNP expressed was increased (Rafudeen *et al*., 2003). In *Arabidopsis thaliana* suspension culture cells, exposure to 100 mM NaCl did not lead to an increase in immunoreactant PNP levels, but did cause a reduction in growth of cells. However, in response to 150 mM NaCl, immunoreactant PNP was significantly up-regulated in suspension culture cells, and at this concentration, cell division of the suspension culture cells was somewhat inhibited (Rafudeen *et al*., 2003). An increase in immunoreactant PNP levels in response to 150 mM NaCl may thus suggest an immunoreactant PNP response to counteract increasing osmotic stress rather than to modulate NaCl transport, an interpretation supported by the observation that immunoreactant PNP was also up-regulated in response to 300 mM sorbitol (which is iso-osmotic to 150 mM NaCl). It is also noteworthy that this up-regulation of immunoreactant PNP was even more pronounced in response to 300 mM sorbitol than the one in response to the 150 mM NaCl (Rafudeen *et al*., 2003). These observations served as evidence for the important role of PNP-like molecules in salinity and osmolarity/drought stress responses in plants.

Taken together, all findings described here suggest for an important role of PNP-like molecules in salinity and osmolarity/drought stress responses in plants that might be mediated by the second messenger cGMP (Maathuis and Sanders, 2001; Rafudeen *et al*., 2003; Donaldson *et al*., 2004).

1.4.7 Plant Natriuretic Peptide-dependent Signal Transduction Mechanisms

Information gathered on the physiological roles of immunoreactant PNPs in plants provided some strong basis to suggest for the existence of a membrane-bound PNP receptor system containing an intrinsic guanylate cyclase activity analogous to that of vertebrate ANPs. Firstly, unlabelled rat ANPs and immunoreactant PNPs were shown to competitively displace I^{125}-rANP bound to leaf and stem plasma membranes of *Tradescantia multiflora,* which indicated that there should be an NP system in plants that signals through a specific receptor system (Gehring *et al*., 1996; Suwastika *et al*., 2000). Secondly, immunoreactant PNPs isolated from *Hedera helix* could induce stomatal opening in a concentration dependent manner and that the effect of this peptide was observed at concentrations significantly smaller than those required to elicit a similar response with ANP (Billington *et al*., 1997), suggesting for an interaction between immunoreactant PNP and its receptor that was highly specific. Thirdly, since cGMP is known to act as a second messenger for ANP in vertebrates yet it was shown to be produced both during ANP- and immunoreactant PNP-dependent stomatal opening in *Zea mays* root stele (Pharmawati *et al*., 1998a), it can be inferred that cGMP may have a similar role in plant signal transduction pathways that operates via a membrane-bound receptor system. Lastly, when both the ANP and PNP molecules were reduced and irreversibly linearized through S-carboxymethylation, they displayed no biological activity in stomatal opening assays (Pharmawati *et al*., 1998b; Wang *et al*., 2007). This suggested that the activities of both molecules were not just encoded in their primary amino acid sequences but were indeed dependent on their secondary and tertiary structures, and such a requirement was fully compatible with a specific receptor-ligand interaction (Pharmawati *et al*., 1998b; Wang *et al*., 2007).

1.4.8 Plant Cell Membrane is the Target for Natriuretic Peptides

The following facts suggest that if PNP receptors do exist in plants, then their location should be in plasma membranes. Firstly, radiolabeled rANP binding to *Tradescantia multiflora* leaf and stem microsomes *in vitro* could be competitively displaced by unlabeled rat ANP (Gehring *et al*., 1996) and immunoreactant PNP (Suwastika *et al*., 2000). Secondly, immunoreactant PNPs could rapidly and significantly modulate ATP-dependent proton gradients in plasmalemma vesicles as well as promoting Cl^- net uptake into membrane vesicles of *Solanum tuberosum* (Maryani *et al*., 2000; Pharmawati *et al*., 2001). Thirdly, immunoreactant PNP (Maryani *et al*., 2001) and AtPNP-A recombinants and synthetic peptides (Morse *et al*., 2004; Wang *et al*., 2007) could induce osmoticum-dependent water uptake in mesophyl cell protoplasts of *Solanum tuberosum* and *Arabidopsis thaliana* respectively. Lastly, immunofluorescence assays in embedded *Hedera helix* tissue sections labelled with anti-potato PNP antibodies, indicated strong fluorescence in the stomatal ledge wall, with distinct fluorescence in guard cells restricted to the vacuolar membrane and not in the cytoplasm or cell walls (Maryani *et al*., 2003).

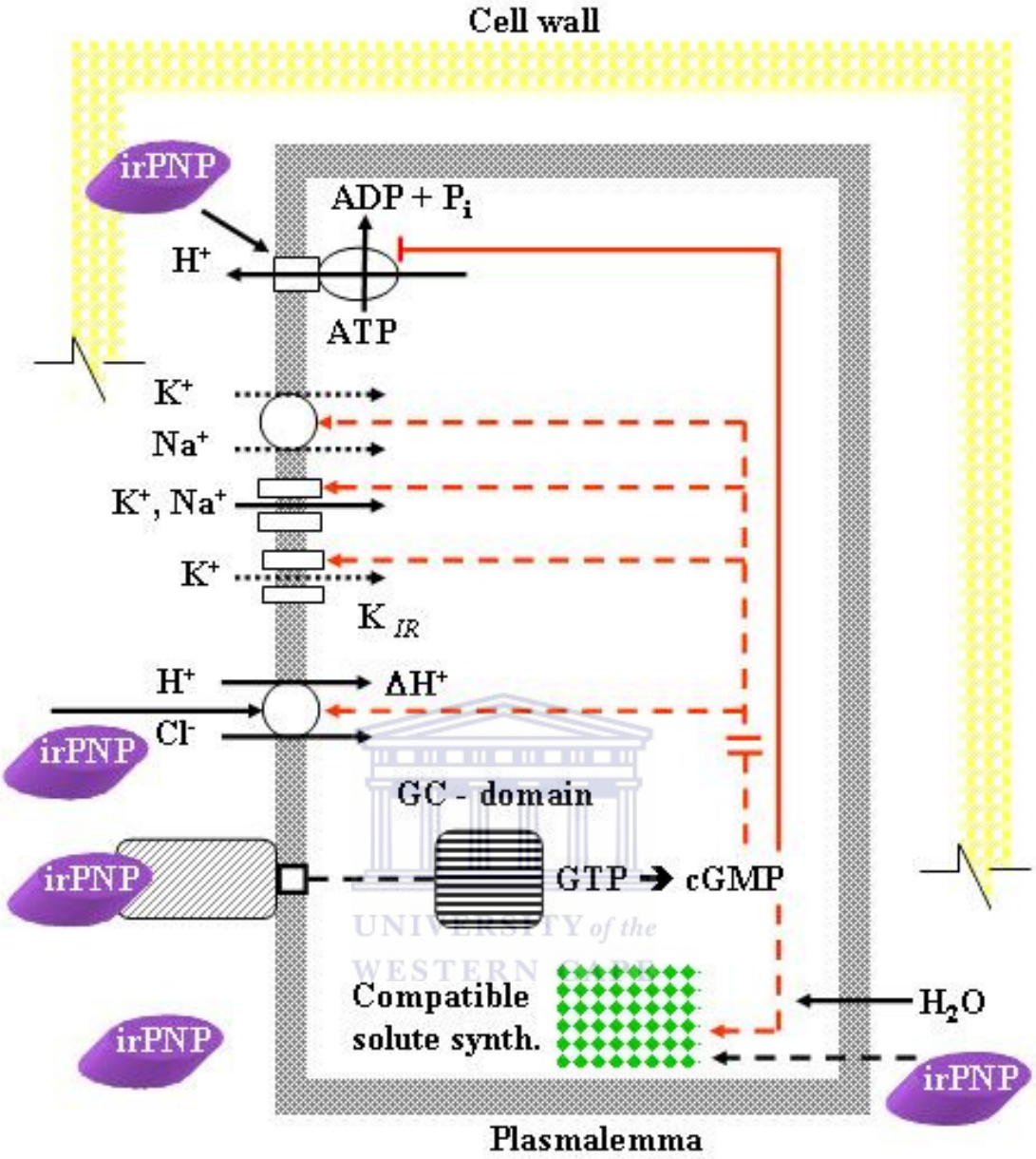

Figure 1.5: **Model of immunoreactant PNP action at cellular level.** The model proposes that immunoreactant PNP can interact with guanylyl cyclases resulting in generation of cGMP. Subsequently, cGMP operates as a second messenger that affects the modulation of ion channels, regulating ion fluxes as well as triggering water uptake into the intracellular space via aquaporins. (Figure from Gehring and Irving, 2003).

1.5 The Role of Cyclic 3′,5′-guanosine Monophosphate (cGMP) in Plants

The role of cyclic nucleotides as second messengers in animals has been well-established where cAMP and cGMP have, as main targets, specific kinases whose activity is modulated by binding of ligands to particular regulatory subunits (Newton and Smith, 2004). Cellular responsiveness of natriuretic peptides in animals is achieved through its interaction with three sub-types of receptors (A and B and C) whose linkage to some kinase systems would always result in the production of the second messenger cGMP (Garbers, 1991b, a; Koller and Goeddel, 1992; Garbers and Lowe, 1994). In plants, reports over the last decade have implicated cGMP in a variety of plant physiological processes including the thigmotropic responses of *Portulaca grandiflora* stamens, pollen germination in *Pinus densiflora*, tumorigenesis in *Nicotiana tabacum*, the autophosphorylation of elongation factor 1 from *Triticum aestivum* embryo and the flowering and circadian rhythmicity of *Lemna paucicostata* (Ames *et al*., 1980; Ejiri and Honda, 1985; Hasunuma *et al*., 1988). These findings helped establishing cGMP as a second messenger in plants.

1.5.1 Mediation of Phototransduction in Plants by cGMP

Cyclic GMP has been shown to mediate a number of phototransduction pathways that are normally regulated by light receptors commonly known as phytochromes (Bowler and Chua, 1994; Bowler *et al*., 1994; Bowler *et al*., 1997). Amongst these processes are the regulation of the expression of a chalcone synthase gene involved in anthocyanin biosynthesis and the regulation of the expression of genes encoding components of the photosystem I and cytochrome b6-f complexes (Bowler and Chua, 1994; Bowler *et al*., 1994; Bowler *et al*., 1997). Phototransduction studies have

shown that anthocyanin production is regulated by cGMP and reciprocally controlled by Ca^{2+} since a high cytosolic free Ca^{2+} level resulted in repression of anthocyanin accumulation (Wu *et al*., 1996). This suggested that cGMP could stimulate the release of Ca^{2+} from intracellular stores (probably via stimulation of a cyclic adenosine diphosphate ribose biosynthesis), which then functions in the regulation of cellular processes including gene expression. It would be expected that once the Ca^{2+} levels exceed a threshold level in the cell, the repression of anthocyanins expression would follow.

Phytochrome A is known to regulate the expression of an asparagine synthase gene, a gene that is normally expressed in the dark and repressed in light (Tsai and Coruzzi, 1990; Neuhaus *et al*., 1997). On the other hand, Phytochrome PfrA was shown to down-regulate the expression of the asparagine synthase gene via a signal transduction pathway that requires G proteins, calcium ions and low concentrations of cGMP (Neuhaus *et al*., 1997). Interestingly, a high concentration of cGMP inhibited the down-regulation of the asparagine synthase gene expression by PfrA (Neuhaus *et al*., 1997). A 17 bp *cis*-acting element, known as RE3 in the asparagine synthase gene promoter has been identified as a binding site for a repressor (Neuhaus *et al*., 1997). The RE3 element contains a motif with the sequence motif (TGGG) found in promoters of most light-down-regulated genes (Neuhaus *et al*., 1997). It is likely that light triggers cGMP synthesis by activating guanylate cyclases, which in turn cause the elevation of cytosolic free Ca^{2+}, thus stimulating PfrA to activate a repressor that then binds to RE3 in the asparagine synthase promoter. Binding of the repressor to the RE3 would then result in the down-regulation of the asparagine synthase gene expression in the light (Neuhaus *et al*., 1997).

1.5.2 Regulation of the Release of Cytosolic-free Ca^{2+} ions by cGMP

Cyclic GMP has been shown to trigger an increase in the release of cytosolic free Ca^{2+} in plants. This was demonstrated in protoplasts of *Nicotiana tabacum* plants that were expressing a Ca^{2+}-activated chemiluminescent protein, aequorin, where addition of a membrane-permeable analogue of cGMP, 8-bromoguanosine 3′,5′-cyclic monophosphate (8-Br-cGMP) resulted in large transient elevation of the cytosolic free Ca^{2+} (Volotovski *et al*., 1998). This free ion increase occurred in the absence of external Ca^{2+} in the cell medium (Volotovski *et al*., 1998) suggesting that the cGMP could invoke some intracellular release of Ca^{2+} from ion stores within the cell. Additionally, the transient cytosolic free Ca^{2+} elevation seen in cGMP-treated protoplasts in the presence of external Ca^{2+} were higher than those observed in the absence of external Ca^{2+} (Volotovski *et al*., 1998). This indicates that cGMP also signals promotion of Ca^{2+} influx, possibly by promoting opening of Ca^{2+} inward channels, leading to Ca^{2+} uptake.

Furthermore, the presence of a cyclic nucleotide monophosphate diesterase inhibitor, 3-isobutyl-1-methyl-2,6-(1H,3H)-purinedione that inhibits conversion of cGMP to GMP also leads to large transient increases in levels of cytosolic free Ca^{2+} (Volotovski *et al*., 1998). However, inclusion of a Ca^{2+}-channel inhibitor, verapamil, strongly blocked this process (Volotovski *et al*., 1998). This therefore confirmed that cGMP, in addition to promoting Ca^{2+} release from intracellular stores, also activates their influx channels. The physiological role of this function in plants seems to include the promotion of water uptake by the cells since cGMP-induced elevation of

cytosolic free Ca^{2+} levels was shown to be followed by an increase in protoplast cell volume swellings (Volotovski *et al*., 1998).

1.5.3 Regulation of Na^+ Uptake in Roots by cGMP

Na^+ and K^+ ions are the major causes of salinity stress in plants and they also play an important role in controlling water flow across plant cells (Rao *et al*., 2002). Ion channels spanning the plant cell membranes are responsible for the regulation of ion flow across cells in plants (Demidchik *et al*., 2002; Demidchik and Tester, 2002). In *Arabidopsis thaliana*, a separate class of non-selective (Na^+ and K^+ permeable) channels called cyclic nucleotide-gated (CNG) is known and is comprised of 20 members (Demidchik *et al*., 2002). However, there are also some inward- and outward-rectifying voltage-dependent channels that are very specific in their ion transport in the sense that they are highly selective for K^+ with very limited permeability to Na^+ (Amtmann *et al*., 1999). Voltage-independent cation channels are thus believed to be the major transport system for Na^+ transport across plant cells (Amtmann *et al*., 1999; Tyerman and Skerrett, 1999; Essah *et al*., 2003). Comparison of K^+:Na^+ current ratios in root protoplasts maintained in media containing either K^+ or Na^+ have been used to confirm that the major pathway for Na^+ uptake by roots is most likely not via voltage-dependent channels (Maathuis and Sanders, 2001). Non-selective monovalent cation channels have been found to have very little or no dependence on voltage across the cell membrane and it has been shown that they are the major transport channels for Na^+ (Maathuis and Sanders, 2001).

It has since been shown that the addition of micromolar concentrations of cGMP to the cytosol could lead to reduced activities of the voltage-independent channels and

that such an inactivation of the voltage-independent channels occurred immediately after the addition of cGMP, thus indicating that the cGMP was possibly binding directly to the channels (Maathuis and Sanders, 2001). However, it appeared that only a subset of the cells was sensitive to cGMP (Maathuis and Sanders, 2001). Furthermore, *Arabidopsis thaliana* plants that normally used to die within 7 days when grown in the presence of 100 mM NaCl were shown to be rescued by the addition of micromolar concentrations of cGMP (Maathuis and Sanders, 2001). This therefore, suggested that the cGMP played an important physiological role of enhancing plant tolerance to NaCl toxicity possibly by inhibiting the voltage-independent cation channels, resulting in the inhibition of Na^+ uptake by roots (Maathuis and Sanders, 2001).

On the other hand, plant growth or survival upon exposure to an equimolar concentration of sorbitol (200 mM) was not improved by addition of cGMP (Maathuis and Sanders, 2001), thus suggesting that the effects of NaCl on plants are most likely due to salinity-induced toxicity rather than an osmolarity-induced toxicity and that, at low concentrations, cGMP functions to enhance salinity tolerance but not osmotic stress/drought tolerance (Maathuis and Sanders, 2001). Reduction in Na^+ uptake, achieved through inactivation of voltage-independent cation channels by cGMP, and/or enhanced Na^+ efflux could be responsible for the prevention of intracellular Na^+ accumulation in plants (Maathuis and Sanders, 2001). Measurements of unidirectional Na^+ uptake by plant cells have been performed using the $^{22}Na^+$ radioisotope and it was demonstrated that micromolar concentrations of cGMP inhibit Na^+ uptake by roots (Maathuis and Sanders, 2001), further confirming that cGMP

enhances salinity tolerance by preventing Na^+ uptake in roots (Maathuis and Sanders, 2001).

1.5.4 Regulation of Cation Channel Activities by cGMP

Cyclic GMP and cAMP have been shown to regulate the flow of K^+ through the α-sub-units of voltage-gated ion channels like KAT1 in *Arabidopsis thaliana* by directly binding to them (Anderson *et al*., 1992). These channels have a structural fold that results in the formation of a pore-like structure through which cations flow (Anderson *et al*., 1992). This pore is selective for K^+ and it was demonstrated that K^+ flow through these channels is triggered and driven by changes in voltage across the cell membrane in a process modulated by direct binding of cGMP or Cyclic 3′,5′-adenosine monophosphate (cAMP) to the channels (Hoshi, 1995).

Cyclic nucleotide gated channels (CNGC) co-regulate cation flow across the cell membrane in a cation non-selective manner with an activity triggered and regulated by cyclic nucleotides like cGMP and cAMP (Zagotta and Siegelbaum, 1996). The Arabidopsis cDNA *AtCNGC2* (an *Arabidopsis thaliana* cyclic nucleotide gated ion channel) was reported to encode a polypeptide that was homologous to the subunit of several animal cyclic nucleotide gated channels. Upon expression in three different heterologous systems, AtCNGC2 facilitated cyclic nucleotide-dependent cation currents (Leng *et al*., 1999) in voltage clamp studies. Leng *et al*., (1999) provided evidence that both cGMP and cAMP trigger K^+ uptake through regulation of AtCNG2 activity. They used a yeast mutant strain deficient in K^+ uptake which expressed AtCNGC2. This mutant strain grows poorly or not at all in low external K^+

concentrations (Ko and Gaber, 1991) but displays an increase in growth in the presence of cGMP or cAMP (Leng *et al*., 1999).

In media containing low external K^+ concentrations, *Saccharomyces cerevisiae* CY162 expressing the AtCNG2 showed increased growth in the presence of cGMP or cAMP compared to *Saccharomyces cerevisiae* CY162 expressing the same protein in the absence of cGMP or cAMP (Leng *et al*., 1999). This therefore served as an indication that cGMP and cAMP could trigger K^+ uptake by the mutant yeast through stimulation and regulation of the AtCNG2 activity. Furthermore, *Xenopus laevis* oocytes transfected to express the AtCNG2 also showed cGMP- and cAMP-dependent K^+ currents in some voltage clamp studies (Leng *et al*., 1999). This was additional evidence to demonstrate that cGMP and cAMP could modulate the activity of AtCNG2. More so, AtCNG2 was also shown to promote Ca^{2+} influx into the cell in a cGMP- and cAMP-triggered and dependent manner (Leng *et al*., 1999).

The AtCNG2 was also found to be involved in the exclusion of Na^+ even in the presence of cGMP or cAMP (Leng *et al*., 1999) demonstrating that it was not directly involved in the regulation of Na^+ fluxes in or out of the cell. Furthermore, a depolarizing voltage on the current in the *Xenopus laevis* oocytes (Leng *et al*., 1999) had no effect on the activity of the AtCNG2 suggesting that its activity was not driven by voltage.

Cyclic GMP has also been implicated in the modulation of non-selective cation channels (NSCC) (Maathuis and Sanders, 2001). Plant inward- and outward-rectifying voltage dependent channels are specific in their ion transport properties

(Amtmann and Sanders, 1999). They are highly selective for K^+ and have limited permeability to Na^+ and so are unlikely to be the mode of transport for Na^+ across plant cells. Voltage independent cation channels are thus believed to be the major transport system for Na^+ across plant cells (Amtmann and Sanders, 1999) with the major pathway for Na^+ uptake in roots being most likely via the NSCC since these channels have very little or no dependence on voltage across the cell membrane (Maathuis and Sanders, 2001).

Maathuis and Sanders (2001) characterized voltage independent channels (VICs) in *Arabidopsis thaliana* roots and found that the opening probabilities of these VICs were dramatically decreased by the presence of micromolar concentrations of cAMP or cGMP (Maathuis and Sanders, 2001). Patch clamp, flux and growth experiments all showed that cyclic nucleotides did down-regulate Na^+ influx. The flux and growth experiments could not conclude whether cyclic nucleotides act directly on channel proteins or whether they are part of a cyclic nucleotide based signaling cascade, or both. The patch clamp experiments strongly suggested a direct interaction between cyclic nucleotides and NSCC. The down-regulation of Na^+ influx via cGMP-sensitive voltage-independent channels can only occur if cGMP is synthesized in response to salt. Consistent with those findings, Donaldson *et al*. (2004) reported the first direct measurement of increased cGMP levels in response to abiotic stress in plants, showing that cGMP is produced in response to salt and osmotic stress.

Furthermore and in line with those findings, the exogenous application of cyclic nucleotide monophosphates (cAMP and cGMP) to *Arabidopsis thaliana* roots has been shown to increase salt tolerance and at the same time, down-regulating Na^+

influx (Maathuis and Sanders, 2001). This was probably achieved through a direct interaction of the nucleotide monophosphates with the NSCCs (Maathuis and Sanders 2001) and once again being consistent with the report that NaCl and osmotic stress could cause rapid cGMP increases in *Arabidopsis thaliana* (Donaldson *et al*., 2004).

1.5.5 Mediation of Gibberellic Acid-regulated gene Expression by cGMP

Gibberellic acid is a plant hormone that functions via its receptor system situated on plasma membranes, and it usually alters the levels of various signalling molecules that include cGMP (Hoffmann-Benning and Kende, 1992; Kende and Zeevaart, 1997; Zentella *et al*., 2002). Many of the processes affected by gibberellic acid are antagonistically regulated by abscisic acid (Hoffmann-Benning and Kende, 1992; Kende and Zeevaart, 1997; Gomez-Cadenas *et al*., 2001). One of the prominent events occurring as a result of gibberellic acid action is a change in the level of expression of a number of genes (Hoffmann-Benning and Kende, 1992; Kende and Zeevaart, 1997; Fridborg *et al*., 2001). The hormone was shown to regulate the expression levels of the enzyme D-amylase in barley aleurone layers (Penson *et al*., 1996).

The regulation was tested by measuring mRNA levels of the D-amylase in barley aleurone layers upon their pre-treatment with a guanylate cyclase inhibitor, 6-(phenylamino)-5,8-quinolinedione, followed by the addition of either gibberellic acid or abscisic acid (Penson *et al*., 1996) in the presence of Ca^{2+}. Northern blots showed that the gibberellic acid in controls, where the inhibitor was absent, significantly increased the D-amylase transcript levels (Penson *et al*., 1996). On the other hand, the 6-(phenylamino)-5,8-quinolinedione treatment resulted in a strong dose-dependent

decrease in D-amylase mRNA levels despite the addition of the gibberellic acid (Penson *et al*., 1996). Notably, the abscisic acid-induced gene expression was not significantly affected by the inhibitor (Penson *et al*., 1996) suggesting that the abscisic acid-mediated signalling system in aleurone layers is not regulated by guanylate cyclases activity.

1.5.6 Mediation of Auxin-induced Root Formation by cGMP

Cyclic GMP was shown to play an important role in auxin-induced root formation when a combination of 2,4-dichlorophenoxyacetic acid, a cell impermeant auxin, and the cell membrane permeable cGMP analogue, 8-Br-cGMP were found to increase the number of roots formed from *Commelina communis* calli in the absence of the active auxin 1-naphthaleneacetic acid (Cousson, 2004). The outcome implied that 1-naphthaleneacetic acid could be replaced with cGMP in combination with 2,4-dichlorophenoxyacetic acid to achieve the same root-generating effect seen when both auxins were used. At the same time, the result served to explain that an interaction between cGMP and auxin is required for the promotion of root formation in plants or in other words, cGMP can mediate the auxin-iduced root formation (Cousson and Vavasseur, 1998).

However, 8-Br-cGMP failed to induce root formation in the absence of 2,4-dichlorophenoxyacetic acid (Cousson, 2004) implying that the cGMP alone could not be sufficient enough to trigger root formation without the auxin. Inclusion of a guanylate cyclase inhibitor, 6-(phenylamino)-5,8-quinolinedione resulted in the inhibition of a 2,4-dichlorophenoxyacetic acid-induced root formation yet this inhibition could be reversed by the addition of the 8-Br-cGMP, although fewer roots

were formed when compared to those formed from calli treated with a combination of 2,4-dichlorophenoxyacetic acid and 8-Br-cGMP (Cousson, 2004). This therefore showed that the inhibition of root formation by 6-(phenylamino)-5,8-quinolinedione was indeed a result of its inhibition of the guanylate cyclase activity and not the calli, since the callus growth was shown not to be affected by the 6-(phenylamino)-5,8-quinolinedione (Cousson, 2004).

A highly selective Ca^{2+} chelator, [1,2-bis(2-aminophenoxy)ethane-N,N,N′,N′-tetraacetic acid], the inhibitor of intracellular Ca^{2+} release, ruthenium red and the antagonist of the synthesis of the cytosolic free Ca^{2+} releasing, cyclic adenosine diphosphate ribose (nicotinamide) all completely inhibited root formation (Cousson, 2004). However, the addition of 8-Br-cGMP to such treated calli resulted in the restoration of normal root formation (Cousson, 2004). The finding therefore, indicated that the cGMP was acting via the stimulation of cyclic adenosine diphosphate ribose (cADPR) biosynthesis that in turn promoted the release of intracellular Ca^{2+}. Alternatively, cGMP may directly promote Ca^{2+} influx into the cell, resulting in the elevation of cytosolic free Ca^{2+} that consequently acts as a signal for the auxin-induced root formation.

1.5.7 Mediation of Kinetin- and NP-induced Stomatal Opening by cGMP

Pharmawati *et al*., (1998) showed that rANP and the synthetic plant hormone kinetin induced the opening of stomata in *Tradescantia albiflora* (Pharmawati *et al*., 1998b). They also showed that the stomatal guard cell response to rANP and kinetin are cGMP-dependent (Pharmawati *et al*., 1998b) since the guanylate cyclase (GC) inhibitors Methylene Blue and LY 83583 were shown to completely prevent the

effects of kinetin and rANP, thus providing evidence that the promotion of opening of stomata by hormones requires a functional GC. Furthermore, the cell-permeant cGMP analogue 8-Br-cGMP has been shown to induce the opening of stomata of *Commelina communis* (Cousson and Vavasseur, 1998) and *Vicia faba* (Pharmawati *et al*., 2001) in a concentration dependent manner.

1.5.8 Modulation of Plasma Membrane H^+-ATPase by cGMP

Since the plasma membrane H^+-ATPase provides the charge gradient required for stomatal opening, where it hyperpolarizes the guard cells and enabling them to take up K^+ ions (Pharmawati *et al*., 2001), stomatal opening is likely to be associated with a stimulation of a proton pump. Since cGMP has been shown to induce stomatal opening and kinetin, ANP and irPNP have been shown to elevate cytosolic levels of cGMP (Pharmawati *et al*., 2001), it seemed important to determine the effect of cGMP on the PM H^+-ATPase and the membrane H^+ gradient. Suwastika and Gehring (1999) showed that in stem and leaf cells of Tradescantia, cGMP modulated PM H^+-ATPase activity and that, depending on the type of experimental protocol, concentrations of ≤ 10 μM or ≤ 1 μM cGMP induced inhibitions *in vitro* (Suwastika and Gehring, 1999). Pharmawati *et al*., (2001) also showed that the activity of the *Solanum tuberosum* guard cell H^+-ATPase was reduced by 8-Br-cGMP (Pharmawati *et al*., 2001).

1.5.9 Regulation of Protein Kinase Activity by cGMP

Although it was well-known that the level of cGMP could be modulated in response to a number of stimuli in plant cells, the presence of intracellular events distal to cGMP metabolism were not as clear in plants as they were in animals (Szmidt-Jaworska *et al*., 2003). Therefore, in an attempt to identify cGMP-dependent kinases in plants, a soluble protein kinase was isolated from *Pharbitis nil* seedlings and assessed for its cGMP-dependence. In those assays, cyclic GMP was shown to promote the levels of autophosphorylation of the soluble protein kinase (Szmidt-Jaworska *et al*., 2003). Enzyme activity of this soluble protein kinase was shown to increase two-folds in the presence of cGMP, with *Pharbitis nil* histones used as substrates for the phosphorylation (Szmidt-Jaworska *et al*., 2003). The *Pharbitis nil* protein kinase has since been found to cross-react with antibodies raised against the animal protein kinase G (Pk-G) (Szmidt-Jaworska *et al*., 2003), suggesting a structural similarity between this kinase and the animal Pk-G. The Pk-G is a cGMP-dependent protein kinase that is a major effector of cGMP actions in both animals and yeasts (Szmidt-Jaworska *et al*., 2003).

Incubation of *Pharbitis nil* protein kinase with no substrate but in the presence or absence of cGMP showed that the protein kinase could not undergo any significant levels of autophosphorylation in the absence of cGMP but very high levels of autophosphorylation in the presence of cGMP (Szmidt-Jaworska *et al*., 2003). Furthermore, the levels of autophosphorylation for the kinase increased in a cGMP concentration-dependent manner (Szmidt-Jaworska *et al*., 2003), where maximal autophosphorylation was reached at 1.0 µM cGMP concentration. The fact that the

activities of protein kinases in plants appear to be regulated by cGMP, further demonstrates the importance of cGMP in plant signal transduction pathways.

1.5.10 Plant Disease Resistance may be Mediated by cGMP

Plant resistance to pathogenic diseases is suggested to be mediated by a nitric oxide-cGMP-dependent signal transduction pathway (Durner *et al*., 1998; Klessig *et al*., 2000). Infection of tobacco mosaic virus (TMV) resistant *Nicotiana tabacum* with the TMV has been shown to increase the enzymatic activity of nitric oxide synthase by at least 5 times when compared to uninfected or TMV-susceptible plants (Durner *et al*., 1998; Klessig *et al*., 2000). This demonstrated that the recognition of a pathogen by plants could lead to elevation of nitric oxide levels and hence implying that nitric oxide was involved in responses to the virus.

Artificially-induced nitric oxide elevations from a nitric oxide donor S-nitroso-L-glutathione were shown to increase expression and activity of the *PAL* gene in *Nicotiana tabacum*, a gene that is normally expressed early in response to a number of stress stimuli (Durner *et al*., 1998; Klessig *et al*., 2000). The increases in expression and activity of this gene were found to be more than 8 times upon treatment of the plants with the S-nitroso-L-glutathione and that such increases were also mimicked by the cell-permeable cGMP analogue, 8-Br-cGMP (Durner *et al*., 1998; Klessig *et al*., 2000) thus implying a cGMP action downstream of the nitric oxide pathway.

The guanylyl cyclase inhibitors, 6-(phenylamino)-5,8-quinolinedione and 1H-[1,2,4]oxadiazolo[4,3-a]quinoxalin-1-one inhibited the induction of the *PAL* gene expression by S-nitroso-L-glutathione in *Nicotiana tabacum* plants (Durner *et al*.,

1998; Klessig *et al*., 2000) further strengthening the suggestion that nitric oxide was responsible for the stimulation of guanylate cyclase activity in response to pathogen attack thus resulting in elevation of cGMP levels and consequent activation of the defense gene expressions. The observation was consistent with the other observations that showed that the induction of nitric oxide synthesis resulted in more than 10 times elevation of cGMP levels in *Nicotiana tabacum* with a concomitant rapid transient increase in *PAL* gene induction (Durner *et al*., 1998).

1.5.11 Modulation of AtPNP-A-induced Stomatal Opening by cGMP

Pharmawati *et al*., (2001) showed that immunoreactive PNPs from *Hedera helix* could induce stomatal opening in *Solanum tuberosum* leaves that was accompanied with elevations in cGMP levels of the guard cells (Pharmawati *et al*., 2001). They also showed that such stomatal opening in *Solanum tuberosum* was inhibited by the guanylate cyclase inhibitor, 6-(phenylamino)-5,8-quinolinedione which also inhibited the observed immunoreactive PNP-induced cGMP elevations (Pharmawati *et al*., 2001). Findings of this study first demonstrated that plant natriuretic peptides were not species specific in their action since a plant natriuretic peptide from one species had the same effect on another different plant species, and secondly, that the immunoreactive PNP-induced stomatal opening in *Solanum tuberosum* was modulated by the second messenger cGMP.

The fact that both the stomatal opening and the cGMP elevation induced by plant natriuretic peptides were inhibited by 6-(phenylamino)-5,8-quinolinedione served as an indication of the dependence of plant natriuretic peptide-induced stomatal opening on activation of guanylyl cylclase-catalyzed synthesis of cGMP by plant natriuretic

peptides. Plant natriuretic peptides therefore most likely stimulate guanylyl cyclase activity, which then elevates cGMP levels and triggering a signal transduction pathway that will lead to stomatal opening. This can occur via promotion of K^+ influx followed by water uptake into guard cells, probably by direct or Ca^{2+}-mediated inward gating of K^+ channels, resulting in stomatal opening. The opening of stomata induced by plant natriuretic peptides appears to require the presence of intracellular cytosolic free Ca^{2+} because ethylene glycol-bis(β-aminoethyl ether)-N,N,N',N'-tetraacetic acid (a calcium chelator) and ruthenium red (an inhibitor of intracellular Ca^{2+} release) inhibited stomatal opening by plant natriuretic peptides (Pharmawati *et al*., 2001). These Ca^{2+}-specific inhibitors also inhibited stomatal opening induced by application of 8-Br-cGMP, a cell-permeable analog of cGMP (Pharmawati *et al*., 2001).

It has been shown that the enzyme H^+-ATPase plays a role in promoting stomatal opening via ATP hydrolysis (Kinoshita *et al*., 1995) and consequent promotion of H^+ efflux out of guard cells (Suwastika and Gehring, 1999; Pharmawati *et al*., 2001). The resulting cellular hyperpolarization leads to K^+ influx into guard cells followed by water uptake that leads to stomatal opening (Kinoshita *et al*., 1995; Briskin and Gawienowski, 1996; Suwastika and Gehring, 1999; Pharmawati *et al*., 2001). Elevation of intracellular Ca^{2+} levels inhibited this H^+-ATPase effect (Kinoshita *et al*., 1995; Shimazaki *et al*., 1999) and this observation was supported by the observed closure of stomata upon exposure of guard cells to high Ca^{2+} concentrations (Shimazaki *et al*., 1999) but was in contrast with Ca^{2+}-dependent stomatal opening induced by plant natriuretic peptides (Suwastika and Gehring, 1999; Pharmawati *et al*., 2001).

However, plant natriuretic peptides appeared to stimulate both the H^+-ATPase and Ca^{2+}-dependent cGMP-mediated stomatal opening (Suwastika and Gehring, 1999; Pharmawati *et al*., 2001). It thus appears that plant natriuretic peptides affect stomatal opening via a cGMP-dependent signalling pathway that requires Ca^{2+} but is independent of the stimulation of the H^+-ATPase. The independence of plant natriuretic peptide-induced stomatal opening from the H^+-ATPase-induced stomatal opening is supported by two observations. First, cGMP inhibited the H^+-ATPase that lead to stomatal opening (Suwastika and Gehring, 1999; Pharmawati *et al*., 2001). Therefore, the cGMP-mediated stomatal opening has to be independent of the H^+-ATPase-mediated stomatal opening. Second, Ca^{2+} inhibited the H^+-ATPase but has been shown to be required for the cGMP-mediated stomatal opening induced by plant natriuretic peptides (Suwastika and Gehring, 1999; Pharmawati *et al*., 2001).

1.5.12 Mediation of AtPNP-A-induced Protoplast Cell Volume Increases by cGMP

Native and synthetic PNPs have previously been shown to induce cell volume increases through osmoticum-dependent net water uptake in *Solanum tuberosum* and *Arabidopsis thaliana* MCPs (Maryani *et al*., 2001; Morse *et al*., 2004; Wang *et al*., 2007). Using three different guanylate cyclase inhibitors (LY 83583, ODQ and NS 2028) that have different modes of action, Wang *et al*., (2007) demonstrated that those inhibitors could reduce protoplast cell volume increases induced by recombinant AtPNP-A (26-126) and its synthetic peptide A (33-66) in *Arabidopsis thaliana*. LY 83583 is a redox-sensitive dye that is a cell permeable competitive inhibitor of soluble guanylate cyclases and acts by generating superoxide anion radicals (Mulsch *et al*., 1988). ODQ and NS 2028 are analogues that are specific irreversible inhibitors of

soluble guanylate cyclase *in vitro* and thought to act at the haem-binding pocket and hence can be reversed in intact cells (Garthwaite *et al*., 1995; Schrammel *et al*., 1996; Olesen *et al*., 1998). The use of several inhibitors was targeted at assuring that heterologous pharmacological agents do not cause misleading results. In addition, Wang *et al*., (2007) also showed that the membrane permeable analogue of cGMP, 8-Br-cGMP, could increase the AtPNP-A- and peptide A-induced protoplast volume increases at a concentration of 0.1 μM but not at 10 μM (probably due to an overriding feedback system of 8-Br-cGMP at the higher concentrations or possibly its toxicity). Taken together, these findings strongly supported a role for guanylate cyclase activity in relaying the AtPNP-A signalling via the second messenger cGMP.

1.6. Guanylate Cyclases

Guanylate cyclases (GCs) are enzymes that are capable of converting guanosine-5′-triphosphate (GTP) to cyclic 3′, 5′-guanosine monophosphate (cGMP). Cyclic GMP participates in cell signalling by i) stimulating the activity of kinases that belong to the protein kinase G family; ii) altering the conductance of cGMP-gated ion channels and iii) changing the activity of cGMP-regulated phosphodiesterases (Schaap, 2005). In animals, two general major classes of guanylate cyclases (GCs) are known and these are the soluble GCs and particulate GCs (Lucas *et al*., 2000). The particulate GCs serve as receptors for natriuretic peptides and exhibit highly conserved domain structures which include an N-terminal extracellular binding domain, a hydrophobic transmembrane domain, a regulatory domain that shows homology to protein kinases, a hinge region and an intracellular domain at the C-terminal of the protein on the cytoplasmic side of the cell (in which the GC catalytic domain resides) (Lucas *et al*., 2000). Soluble GCs are heterodimeric proteins consisting of 2 subunits (α- and β-

subunits) where generally both subunits are required for the catalytic activity of the molecule (Lucas *et al*., 2000). Each of the subunits has a regulatory domain at the N-terminus and a catalytic domain at the C-terminus (Lucas *et al*., 2000) while the β-subunit also contains a heme domain that acts as a binding site for nitric oxide (Namiki *et al*., 2001).

In higher plants, the first protein with *in vitro* GC activity (AtGC1) was identified in 2003 by Ludidi and Gehring when they carried out a blast search on the *Arabidopsis* genome using a search motif; ([RKS][YFW][GCTH][VIL][FV]X[DNA]X[VIL] X{4}[KR]) that was designed based on conserved and functionally-assigned amino acids in the catalytic centres of annotated and known prokaryotic and eukaryotic GCs (Ludidi and Gehring, 2003). Their querying returned seven candidates including AtGC1 (Ludidi and Gehring, 2003). The AtGC1 was then characterized and eventually found to be a bifunctional protein possessing the GC activity (Ludidi and Gehring, 2003) and a proteinase activity (Ludidi, personal communication). The other six remaining candidates were however found to lack the glycine-rich sequences that are commonly found on the N-terminus of the catalytic centres of all annotated GCs (Ludidi and Gehring, 2003). Some detailed analysis of those six molecules then further revealed that two of them were kinases while the other two were wall associated kinase-like molecules (WAKLs) (Ludidi and Gehring, 2003). One of the two WAKLs (At1g79680) was finally termed AtWAKL10 because of the unusualness of its domain organization, which resembled that of natriuretic peptide (NP) receptors (Ludidi and Gehring, 2003). Like NP receptors, AtWAKL10 has an extracellular N-terminal ligand-binding domain, a single trans-membrane region, and an intracellular C-terminal guanylate cyclase/kinase domain (Maack, 1992; Ludidi and Gehring,

2003). This resemblance in domain organization between AtWAKL10 and ANP receptors may also suggest for a functional homology between these two molecules and even further proposing AtWAKL10 as a potential plant natriuretic peptide (PNP) receptor. This is particularly tempting since the application of ANP or PNP to plant cells results in cGMP transents (Pharmawati *et al*., 1998a).

Work in this thesis will seek to elucidate the mechanisms of action of plant natriuretic peptides. It will involve the expression of a biologically active recombinant plant natriuretic peptide from *Arabidopsis thaliana* (AtPNP-A) followed by an assessment of its physiological effects in a Cape sage, *Plectranthus ecklonii* Benth. The possible systemic action of the recombinant AtPNP-A in the sage shall also be assessed and ascertained. Finally, a probable functional link between AtPNP-A and another recombinant *Arabidopsis thaliana* molecule (AtWAKL10) suspected to be a possible AtPNP-A receptor, will be explored.

Chapter 2

Preparation of a Biologically Active Recombinant Natriuretic Peptide

Abstract

Immunological studies in plants have revealed the presence of a novel class of plant molecules that are recognized by antibodies generated against vertebrate atrial natriuretic peptides (ANPs). Functional properties of these immunoanalogues, commonly known as immunoreactant plant natriuretic peptides (irPNPs), have been characterized and the irPNPs have been shown to be involved in maintenance of plant cellular and physiological homeostasis. In an attempt to further characterize the functional properties of these immunoreactant PNPs, we prepared a biologically active recombinant plant natriuretic peptide from *Arabidopsis thaliana* (AtPNP-A) by impirically optimizing its expression, purification and refolding properties. The biological activity of the prepared recombinant AtPNP-A was demonstrated by showing its ability to induce net water uptake into *Arabidopsis thaliana* protoplasts.

2.1 Introduction

Expression of recombinant proteins in prokaryotic systems, especially in *Escherichia coli*, plays a major role in the efficient production of genetically-engineered proteins particularly when their biological functions do not depend on post-translational modifications such as glycosylation (Li *et al*., 2003; Li *et al*., 2004). Use of prokaryotic systems often results in very high rates of protein expression and

frequently leading to accumulation of insoluble polypeptides aggregates, often termed "inclusion bodies" (Lilie *et al*., 1998).

The expression of recombinant proteins in the form of inclusion bodies has however its own advantages (Lilie *et al*., 1998). Firstly, about 30-50% of the total protein would be the recombinant proteins. Secondly, the recombinant proteins are largely protected from proteolytic degradation by host cell enzymes. Thirdly, during purification, cell disruption can be carried out under denaturing conditions with no detrimental effects on the recombinant proteins. Fourthly, due to their sizes, densities and insolubilities, inclusion bodies can be easily purified from the soluble host proteins through centrifugation, filtration, or size-exclusion chromatography. This in turn reduces the number of separation steps and at the same time increasing the yield of the purified and desired protein products. Fifthly, if the recombinant proteins are toxic to the host cells, their expression in form of inactive inclusion bodies would increase the viability of the cells and subsequently the overall yield of the targeted recombinant products. Lastly, the expression of recombinant proteins as inclusion bodies can be directly observed and monitored through the use of phase contrast microscopy thereby avoiding a requirement for their initial identification by such methods like gel electrophoresis (Lilie *et al*., 1998; Li *et al*., 2003; Li *et al*., 2004).

In most cases, the major challenge associated with the expression of recombinant proteins as inclusion bodies is on converting them into soluble and correctly refolded biologically active products (Li *et al*., 2003; Li *et al*., 2004). However, a number of different methods have so far been developed and described to tackle this problem (Rudolph and Lilie, 1996; Mukhopadhyay, 1997). These include dialysis, slow

dilution, rapid dilution, pulse renaturation, as well as chromatography (Lilie *et al*., 1998; Li *et al*., 2003; Li *et al*., 2004). In all these methods, the purified inclusion bodies are first solubilized in high concentrations of a denaturing agent such as urea or guanidine-HCl followed by a controlled removal of the denaturant and in this case, allowing the inclusion bodies to refold into native and active forms (Li *et al*., 2003; Li *et al*., 2004). The one major challenge during this process occurs when protein aggregation tends to precede protein refolding (De Bernardez Clark *et al*., 1998; Li *et al*., 2003; Li *et al*., 2004). However, this problem can be overcomed by allowing the refolding process to progress in the presence of refolding agents such as NaCl, glucose, poly-ethyl glycol, non-detergent sulfobetaine, reduced glutathione and oxidized glutathione that in turn would effectively promote and facilitate the refolding properties of the recombinant proteins (Li *et al*., 2003; Li *et al*., 2004).

Empirical optimization of the expression, purification and refolding strategies for most recombinant proteins produced in several bacterial expression systems usually results in high levels of purified products with improved functional properties (Li *et al*., 2003; Li *et al*., 2004). Here we report the preparation of a biologically active recombinant natriuretic peptide from *Arabidopsis thaliana* (AtPNP-A) using a pCRT7/TOPO TA expression system (Invitrogen) and a QIAexpress purification/refolding system (Qiagen). These two systems are specifically designed (especially when properly optimized) to allow for high expression levels of recombinant proteins in form of inclusion bodies, their rapid purification as well as their subsequent and effective refolding into biologically active molecules (The QIAexpressionist, 2003).

2.2 Materials and Methods

2.2.1 Source of the Recombinant AtPNP-A Insert

The insert for the recombinant AtPNP-A was provided by Dr. Monique Morse (Department of Biotechnology, University of the Western Cape) in the form of a construct (pCRT7/NT-TOPO-AtPNP-A) transformed into BL21 Star pLysS *E. coli* cells (Invitrogen). Before protein expression was undertaken, the pCRT7/NT-TOPO-AtPNP-A construct was checked to verify if it was carrying the correct AtPNP-A insert. The verification process involved isolation of the pCRT7/NT-TOPO-AtPNP-A construct from the transformed BL21 Star pLysS *E. coli* cells followed by a re-amplification of the anticipated AtPNP-A insert by polymerase chain reaction (PCR).

2.2.2 Isolation and Purification of the pCRT7/NT-TOPO-AtPNP-A Construct

The pCRT7/NT-TOPO-AtPNP-A construct was isolated from the BL 21 Star pLysS *E. coli* cells (invitrogen) by inoculating 10 ml of double strength yeast-tryptone medium (1.6% (w/v) tryptone powder, 1% (w/v) yeast extract, 0.5% (w/v) NaCl) supplemented with 100 µg/ml ampicillin and 34 µg/ml chloramphenicol with a 200 µl culture of these cells. The inoculated media was then incubated at 37°C overnight in an orbital shaker (New Brunswick Scientific) rotating at 200 rpm. The next morning, the culture was centrifuged at 12 x 4 *g* for 5 minutes to harvest the cells. The supernatant was discarded while the pellet was resuspended into 200 µl GTE solution and left to stand at room temperature for 5 minutes.

In order to lyse the cells, 400 µl of 0.2 M NaOH/1% (w/v) SDS solution were added followed by a gentle mixing through finger-tapping before the mixture was left to

incubate on ice for 5 minutes. After this 5-minute incubation, 300 µl of 3 M KAc were then added followed by a thorough mixing before the mixture was again left to incubate on ice for 5 minutes. At this stage, a coarse white precipitate of cell debris and chromosomal DNA was formed and this precipitate was pelleted out through centrifugation at 12 x 4 *g* for 5 minutes. The clear supernatant was then carefully transferred to a fresh tube while the pellet was discarded. To the clear supernatant, 600 µl of isopropanol were added followed by incubation of the mixture at -20°C for 30 minutes. The mixture was then centrifuged at 12 x 4 *g* for 5 minutes to pellet the plasmid DNA. The supernatant was discarded while the pellet was air-dried to drive out all the isopropanol. The pellet was then dissolved into 100 µl of sterile water.

In order to get rid of RNA, a 0.1 volume of 10 mg/ml RNAse A was added to this DNA solution followed by a 30-minute incubation at 37°C. The plasmid DNA was further purified by adding an equal volume of phenol to its solution followed by a vigorous mixing through vortexing. The mixture was then partitioned through centrifugation at 8.28 x 4 *g* for 5 minutes. The upper phase of the clarified fractions was carefully collected into a fresh tube while the rest of the solution was discarded. The steps involving the addition of phenol, vortexing, centrifugation and collection of the upper phase were repeated once more with the first collected clarified upper phase. To the second collected clarified upper phase, a 0.1 volume of 3 M KAc and a 0.6 volume of isopropanol were then added followed by a 30-minute incubation at -20°C. The cleaned plasmid DNA was then pelleted out through centrifugation at 12 x 4 *g* for 5 minutes. The pellet was then washed twice by adding 500 µl of 70% (v/v) ethanol followed by centrifugation at 12 x 4 *g* for 5 minutes. The washed plasmid DNA wash then resuspended into 100 µl of 10 mM Tris buffer; pH 8.0 and stored at -

20°C. An aliquot of this solution was electrophoretically resolved on a 0.8% (w/v) agarose gel and examined under UV light to determine both the yield and expected size of the purified plasmid DNA.

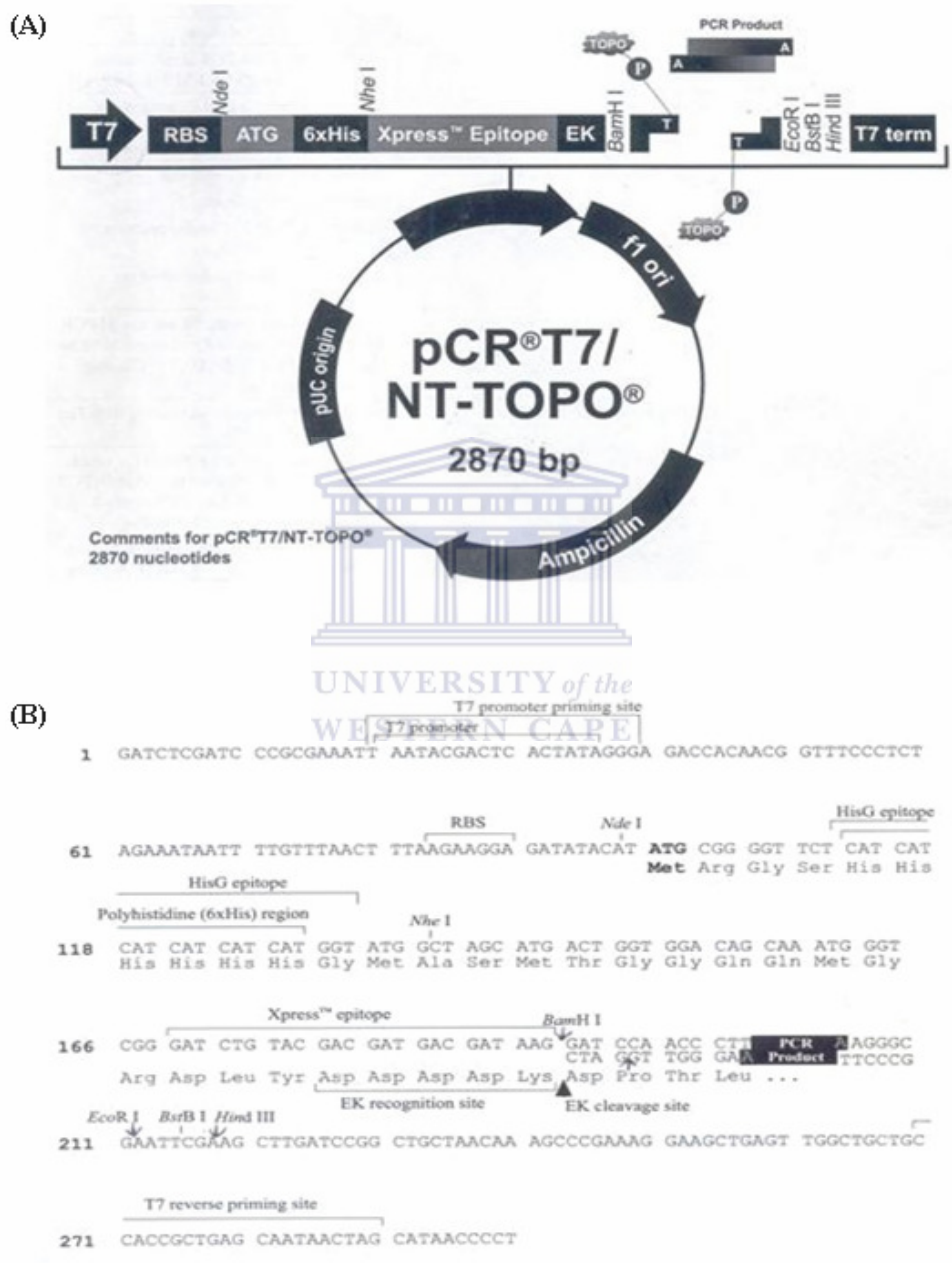

Figure 2.1: Features of the pCR®T7 TOPO® TA expression vector. (**A**) Physical map of the vector showing the various features that makes it ideal as an expression vector. (**B**) Sequence map of the vector showing the cloning site. The AtPNP-A insert was cloned as a PCR product between the *Bam* HI and *Hind* III restriction sites. (Figure from Invitrogen manual).

2.2.3 Verification of the Presence of the AtPNP-A Insert in the Plasmid Construct

In order to verify the presence of the correct recombinant AtPNP-A insert in the plasmid construct, a re-amplification of the anticipated insert fragment was carried out by polymerase chain reaction (PCR) using specific primers; (forward) 5′GAT ATC GGA TCC GCT CAA GGA AAA GCT GTC TAT TAC G3′ incorporating a *Bam* HI restriction site and (reverse) 5′ACT AAG AAG CTT TTA CGG TGT GTA TAC GAC ACG AAT G3′ incorporating a *Hind* III restriction site. The isolated and purified pCRT7/NT-TOPO-AtPNP-A construct was used as the template DNA for the insert re-amplification in a 50 µl standard reaction mixture containing; 30 ng template DNA, 1X *Taq* + $MgCl_2$ reaction buffer, 20 mM dNTPs mix, 1 Unit Econo*Taq* DNA Polymerase (Fermentas), and 0.5 µM forward and 0.5 µM reverse primers. The reaction mixture was then incubated in 0.2 ml thin-walled reaction tubes in a Mastercycler (Eppendorf) and processed successively as follows: 1 cycle of initial denaturation at 94°C for 2 minutes, followed by 30 cycles of denaturation at 94°C for 30 seconds, annealing at 67°C for 30 seconds, elongation at 72°C for 50 seconds, and 1 cycle of final elongation at 72°C for 7 minutes. After the final round of elongation, the solution was kept at 4°C. An aliquot of this solution was electrophoretically resolved on a 0.8% (w/v) agarose gel and examined under UV light to determine both the yield and expected size of the amplified PCR product. The resultant PCR product was further verified by sequencing before protein expression was initiated.

2.2.4 Expression of the Recombinant AtPNP-A

For improved expression of the recombinant AtPNP-A, 200 µl of a glycerol stock of BL 21 Star pLysS *E. coli* cells habouring the pCRT7/NT-TOPO-AtPNP-A construct

vector were transferred into 10 ml double strength yeast-tryptone medium supplemented with 100 µg/ml ampicillin and 34 µg/ml chloramphenicol. The culture was incubated at 37°C overnight in an orbital shaker at 200 rpm. The next morning, 1 ml of this overnight culture was then transferred into 50 ml double strength yeast-tryptone medium containing the appropriate antibiotics. The culture was incubated at 37°C shaking at 200 rpm until an OD_{600} of 0.6 to 0.7. An aliquot (1 ml) of this culture was then collected to check for "leaky expression" by sodium dodecyl sulphate polyacrylamide gel electrophoresis (SDS-PAGE). For induction, 0.5 mM IPTG was added and the culture left to grow for a further 3 hours. At the end of the 3 hours, another 1 ml aliquot was also collected for analysis of the overall expression levels by SDS-PAGE. The rest of the culture was then harvested through centrifugation at 12 x 4 *g* for 30 minutes.

2.2.5 Purification of the Recombinant AtPNP-A

2.2.5.1 Preparation of a cleared cell lysate

A cleared lysate of the recombinant AtPNP-A was prepared under denaturing conditions by resuspending the harvested cells into a lysis buffer (8 M urea, 100 mM NaH_2PO_4, 10 mM Tris-Cl; pH 8.0, 500 mM NaCl, 20 mM β-mercaptoethanol, and 7.5% (v/v) glycerol) at a ratio of 1 g pellet weight to every 10 ml buffer volume. The contents were thoroughly mixed at room temperature for 1 hour using a magnetic stirrer before being spun at 12 x 4 *g* for 15 minutes. The supernatant was then collected as a cleared lysate and its aliquot (1 ml) saved for analysis by SDS-PAGE.

2.2.5.2 Binding of the recombinant AtPNP-A onto the Ni-NTA beads

In order to bind the denatured recombinant AtPNP-A onto the Ni-NTA beads (Qiagen), 2 ml of the beads were first equilibrated for 30 minutes into 10 column volumes (20 ml) of lysis buffer supplemented with 35 mM imidazole. The equilibrated beads were then transferred to the recombinant protein lysate (that was also supplemented with 35 mM imidazole) at a ratio of 1 ml beads to every 35 ml lysate. The contents were gently mixed on a rotary mixer (Breda Scientific) at 4.0 rpm for 1 hour at room temperature. The contents were then spun at 12 x 4 *g* for 1 minute at room temperature in order to separate the beads from the lysate. The supernatant was discarded as a 'flow-through' with its aliquot (1 ml) saved for analysis by SDS-PAGE.

2.2.5.3 Washing of the Ni-NTA beads binding the recombinant AtPNP-A

After binding the recombinant AtPNP-A onto the Ni-NTA beads, unbound bacterial proteins were then washed off by resuspending the bound beads into 10 column volumes of wash buffer (8 M urea, 100 mM NaH_2PO_4, 10 mM Tris-Cl; pH 8.0, 500 mM NaCl, 20 mM β-mercaptoethanol, 7.5% (v/v) glycerol, and 40 mM imidazole), and allowing the mixture to stand at room temperature for 5 minutes before spinning it at 12 x 4 *g* for 1 minute. The supernatant was discarded as a 'first wash' and its aliquot (1 ml) saved for analysis by SDS-PAGE. The washing step was repeated three more times with aliquots (1 ml) for each wash also saved for analysis by SDS-PAGE. Furthermore, an aliquot (20 µl) of the washed bound beads was also collected for analysis by SDS-PAGE.

2.2.6 Refolding of the Purified and Denatured Recombinant AtPNP-A

2.2.6.1 Preparation of a refolding column

The washed beads carrying the bound and purified recombinant AtPNP-A were first resuspended into 10 column volumes of gradient buffer (8 M urea, 200 mM NaCl, 50 mM Tris-Cl; pH 8.0, and 20 mM β-mercaptoethanol) before the whole slurry was carefully loaded into an empty XK16 column (Amersham Biosciences). Proper loading was achieved by pouring the slurry from the top part of the column while a small tap positioned on its bottom part was kept closed. The beads were then allowed to sediment by draining 8 column volumes of the buffer through the tap before the loaded column was connected to an AKTA fast protein liquid chromatography (FPLC) machine (Amersham Biosciences) for the initiation of a refolding gradient system.

2.2.6.2 The linear gradient system

A gradual and linear refolding gradient system was created and run on the FPLC machine based on parameters listed in table 2.1 below. In this system, the 8 M urea gradient buffer was slowly and linearly diluted to approximately 0 M urea concentration with a refolding buffer (200 mM NaCl, 50 mM Tris-Cl; pH 8.0, 500 mM glucose, 0.05% (w/v) poly-ethyl glycol, 4 mM reduced glutathione, 0.04 mM oxidized glutathione, 100 mM non-detergent sulfobateine, and 0.5 mM phenylmethanesulfonylfluoride).

Table 2.1: Parameter settings for a FPLC-controlled linear gradient system.

Variable	Value
Column volume (cv)	2.00 ml
Flow rate	1.00 ml/min
Column pressure limit	2.80 MPa
Averaging time for UV	1.30 min
System pump for automatic pressure and flow regulation	Normal
Starting concentration of buffer B	0.00%
Targeted concentration of buffer B	100.00%
Equilibrate column with	4.00 cv
Length of gradient	50.00 cv
Gradient delay with	5.00 ml
Clean after gradient with	5.00 cv

The listed conditions were used to run a 100-minute long linear gradient for the refolding of the denatured recombinant AtPNP-A into a biologically active molecule.

2.2.7 Elution of the Refolded Recombinant AtPNP-A

In order to elute the refolded recombinant AtPNP-A from the Ni-NTA beads, the bound beads in the XK16 column were first washed with 10 column volumes of washing buffer (200 mM NaCl, 50 mM Tris-Cl; pH 8.0, 20% (v/v) glycerol, and 0.5 mM phenylmethanesulfonylfluoride). This washing step was carried to remove most of the residual refolding agents prior to elution. After the wash, the refolded recombinant protein was then eluted with 4 column volumes of elution buffer (200 mM NaCl, 50 mM Tris-Cl; pH 8.0, 250 mM imidazole, 20% (v/v) glycerol, and 0.5 mM phenylmethanesulfonylfluoride) using an elution process that was linked to the FPLC system.

2.2.8 Concentration and Desalting of the Eluted Recombinant AtPNP-A

The eluted recombinant AtPNP-A was both concentrated and desalted by spinning at 12 x 4 *g* for 2 hours in YM-3 centriplus filtration devices (Millipore) with a molecular weight cut off point of 3.0 kDa. The final protein concentration was then determined by the Bradford method (Bradford, 1976). An aliquot (20 µl) of this final recombinant product was also analyzed by SDS-PAGE.

2.2.9 Determination of the Biological Activity of the Recombinant AtPNP-A

2.2.9.1 Preparation of cell protoplasts

Cell protoplasts were prepared using *Arabidopsis thaliana* suspension cultures at mid-log phase and growing in Murashige and Skoog basal salt with minimum organics (MSMO) (4.43 g MSMO, 50 µl kinetin, 3 g sucrose, 500 µl naphthaline acetic acid; pH 5.7 and made up to 1 L), where 20 ml of the culture were transferred into a 50 ml polypropylene tube followed by centrifugation at 2.89 x 4 *g* for 10 minutes at 23°C. The supernatant was discarded followed by the addition of an enzymatic solution (0.8% (w/v) cellulase (Fluka), 0.2% (w/v) pectinase (Worthington), 0.08% (w/v) pectolyase (Sigma) made up in 400 mM sorbitol; pH 4.8) to the pellet. The tube was covered in foil and then placed into a shaking incubator rotating at 135 rpm at 37°C for 3 hours. After this incubation, another 1 ml of the enzymatic solution was further added to the cells followed by a 2-hour incubating under similar conditions. The digested cell walls were then filtered through a gauze followed by a spinning of the filtrate at 2.89 x 4 *g* for 15 minutes at room temperature. The supernatant was discarded while the pellet (protoplasts) were re-suspended into 2 ml of 400 mM

sorbitol, pH 4.8 and kept on ice. Cells were kept in 400 mM sorbitol at pH 4.8 in order to block them from rapturing since this solution has an osmotic potential that is equivalent (iso-osmotic) to that of protoplasts.

2.2.9.2 Cell volume measurements

The prepared protoplasts were then treated with 150 ng/ml AtPNP-A (except for the controls that were treated with equal volumes of water) and incubated at 23°C for 15 minutes. The protoplasts were then visualized under a microscope fitted with a calibrated ocular micrometer. Randomly selected cells (controls and treatments) with volume increases of ≥50 µm in size were then photographed followed by analysis of their size changes by a one-way analysis of variance (ANOVA) and paired Student *t* test assuming a spherical shape of a cell. Differences between controls and treatments were then ascertained.

2.3 Results

AtPNP-A, a recombinant plant natriuretic peptide from *Arabidopsis thaliana* was synthesized using a prokaryotic expression system. The expressed AtPNP-A is a 102 amino acid fragment that does not contain the N-terminal signal peptide required for secretion of the protein into the extracellular space and is shown in blue in Fig. 2.2 below.

MAVKFVVVMIVFAQILAPIAEAAQGKAVYY

DPPYTRSACYGTQRETLVVGVKNNLWQNGR

ACGRRYRVRCIGATYNFDRACTGRTVDVKV

VDFCREPCNGDLNLSRDAFRVIANTDAGNI

RVVYTP

Figure 2.2: The complete amino acid sequence of recombinant AtPNP-A. The black sequence represents the signal peptide (amino acid 1-24) that is required for its secretion into the extracellular space but not for its biological activity. The cysteine residues (red) are highly conserved in PNP-like molecules (AtPNP-A, AtPNP-B and CjBAp12). The arrows delineate the domain critical for natriuretic peptide-like biological activity of the molecule (Morse *et al*., 2004). The blue sequence (amino acid 26-126) represents the section that was cloned as an insert into the pCRT7/NT-TOPO vector system for protein expression. (Figure from Morse *et al*., 2004).

Before AtPNP-A expression was undertaken, the pCRT7/NT-TOPO-AtPNP-A construct was checked to verify if it was carrying the correct size of the AtPNP-A insert. The process involved isolation of the pCRT7/NT-TOPO-AtPNP-A construct from the transformed BL21 Star pLysS *E. coli* cells followed by a re-amplification of the AtPNP-A insert by polymerase chain reaction (PCR). Fig. 2.3 below shows the agarose gel resolutions of the isolated pCRT7/NT-TOPO-AtPNP-A construct (Slide A) and the re-amplified AtPNP-A insert fragment (Slide B). As is shown in slide B, the expected 306-base pair fragment that encodes for the 102 amino acid AtPNP-A sequence lacking the signal peptide was re-amplified thereby verifying the presence of a correct AtPNP-A insert size in the vector construct. The correct base sequences for the amplified AtPNP-A insert fragment were later confirmed through DNA sequencing.

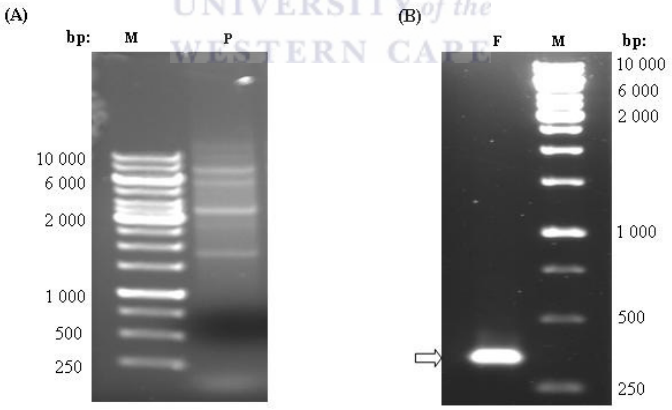

Figure 2.3: Verification of the correct AtPNP-A insert in the pCRT7/NT-TOPO-AtPNP-A construct. The pCRT7/NT-TOPO-AtPNP-A construct was first isolated from the BL 21 Star pLysS *E. coli* cells and used as a template for a re-amplification of the AtPNP-A insert by polymerase chain reaction. (**A**) The isolated pCRT7/NT-TOPO-AtPNP-A construct and (**B**) the re-amplified AtPNP-A insert as resolved by electrophoresis on a 0.8% agarose gel. (M) is a 1 kb DNA ladder, (P) is the plasmid construct, and (F) is the amplified insert fragment. The PCR product is marked by the arrow.

The expression system used to generate recombinant AtPNP-A was capable of producing it as a His-tagged fusion product with an approximate size of 15.5 kDa (Fig. 2.4A). The expression conditions used with this system largely favoured over-expression of the recombinant protein resulting in the generation and accumulation of insoluble inclusion bodies (Lilie *et al*., 1998). Therefore, purification of this protein was then undertaken on an Ni-NTA affinity system (Stempfer *et al*., 1996; Lindwall *et al*., 2000) under denaturing conditions (The QIAexpressionist, 2003), where partial purification of the recombinant AtPNP-A was achieved (Fig. 2.4B).

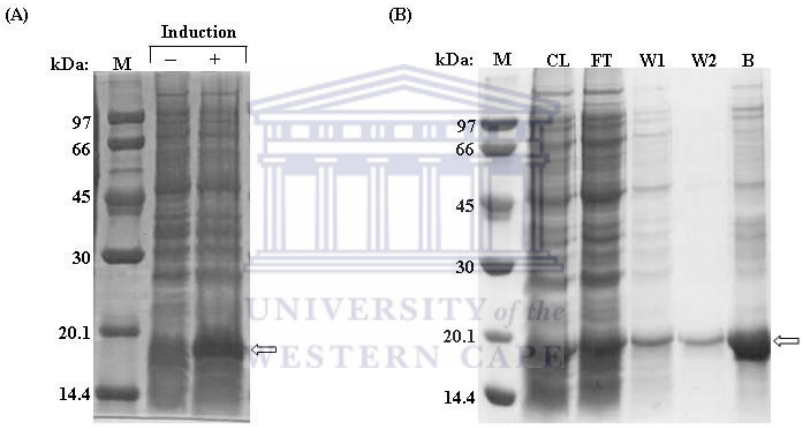

Figure 2.4: Expression and purification of recombinant AtPNP-A. (**A**) SDS PAGE of uninduced (-) and induced (+) proteins from *E. coli* BL21 Star pLysS cells (Invitrogen) habouring the pCRT7/NT-TOPO-AtPNP-A expression construct. (**B**) Gel resolution of the recombinant AtPNP-A fractions collected from different steps of its purification procedure. (CL) is the cleared lysate after solubilization of the inclusion bodies in 8 M urea buffer, (FT) is the flow-through of the cleared lysate after it was passed through the Ni-NTA agarose matrix, (W1) is the first wash of the bound AtPNP-A with wash buffer, (W2) is the second wash, and (B) is the purified and bound recombinant AtPNP-A. The arrows mark the recombinant AtPNP-A bands while (M) represents the low molecular weight markers.

In order to facilitate a regaining of biological activity for the purified and denatured recombinant AtPNP-A, the recombinant protein was passed through a refolding process that was linked to an FPLC system set to run at a flow rate of 1 ml/min. During this process, an 8 M urea buffer into which the recombinant AtPNP-A was resuspended was slowly diluted over a 100-minute time period with a non-denaturing refolding buffer to a final concentration of 0 M urea. As is shown in Fig. 2.5 below, a linear refolding gradient system was achieved over the 100 minutes refolding time period and is represented by the linear green line stretching between the 0 ml and 100 ml volumes of the non-denaturing refolding buffer.

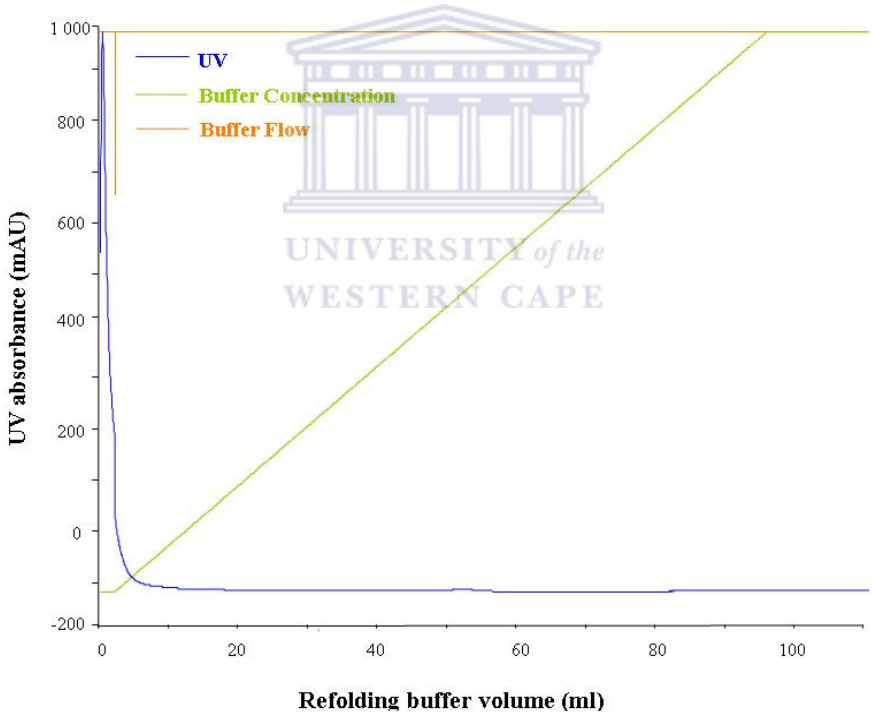

Figure 2.5: Refolding of the purified and denatured recombinant AtPNP-A. The purified and denatured protein was refolded while it was still bound onto the Ni-NTA agarose matrix using an FPLC-controlled linear gradient system set to run at a flow rate of 1 ml/min. An 8 M urea buffer resuspending the bound and purified recombinant AtPNP-A was gradually diluted with a non-denaturing refolding buffer to 0 M urea final concentration. The green line (linear) shows a gradual concentration increase (0-100%) of the dilution buffer during the refolding process, while the buffer flow (orange) and UV status (blue) remained steady.

The refolded purified recombinant AtPNP-A was finally eluted off the Ni-NTA agarose matrix with 250 mM imidazole using an elution process that was linked to an FPLC system and set to pass the elution buffer at a flow rate of 1 ml/min. The eluted protein fraction that was eluted with 8 ml of the elution buffer over 8 minutes is represented by the blue peak in Fig. 2.6 below.

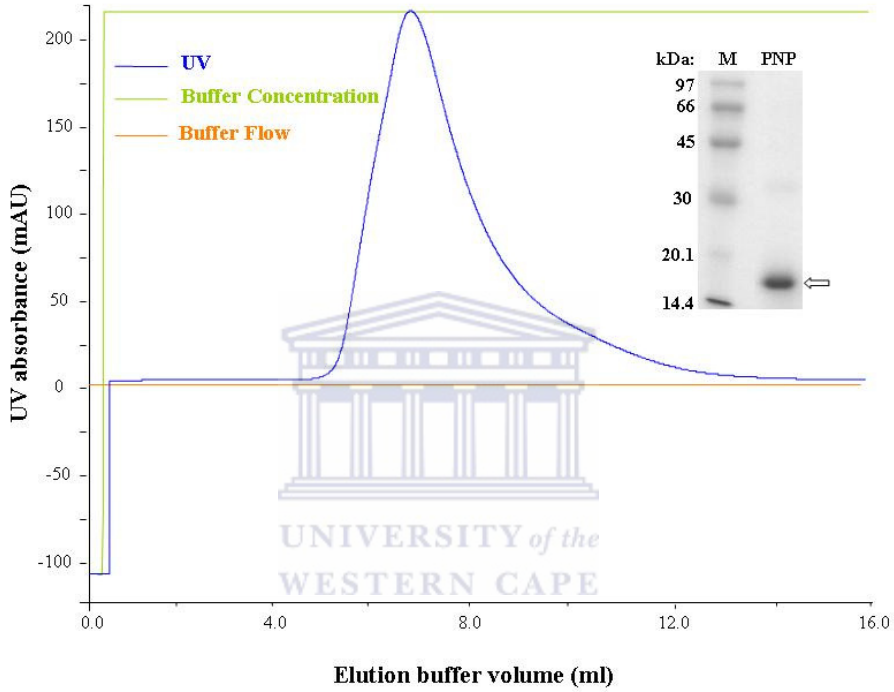

Figure 2.6: Elution of the refolded recombinant AtPNP-A from the Ni-NTA agarose matrix. The protein was eluted with 8 ml of 250 mM imidazole in an elution process that was controlled by an FPLC system and set to operate at a flow rate of 1 ml/min. The blue curve represents both the quantity and quality of the protein fraction that was eluted by the system when both the elution buffer flow (orange) and its concentration (green) were kept at steady states. Inset: SDS-PAGE of the eluted protein fraction where (M) is the low molecular weight marker while the arrow marks the refolded purified recombinant AtPNP-A.

In order to test if the refolded recombinant AtPNP-A had regained its biological function, its eluted fraction was assessed in a protoplast assay system (Maryani *et al*., 2001; Morse *et al*., 2004; Wang *et al*., 2007) as is shown in Fig. 2.7 below. Treatment of protoplasts with the recombinant AtPNP-A resulted in induction of cell swelling thereby demonstrating that the protein was biologically active.

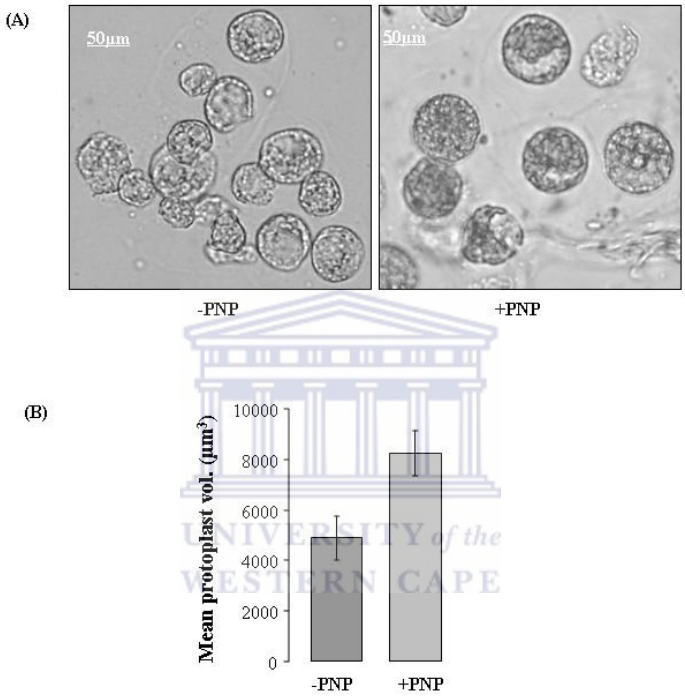

Figure 2.7: Effects of recombinant AtPNP-A on protoplast cell volumes. (**A**) *Arabidopsis thaliana* protoplasts were treated with H_2O (left image) and 150 ng/ml recombinant AtPNP-A (right image) for 15 minutes at 23°C and then viewed under a microscope fitted with a calibrated ocular micrometer. (**B**) Graphical representation of randomly selected protoplasts with cell volume increases of ≥50 µm as analyzed by ANOVA and paired Student *t* test assuming a spherical shape of cells. The graphs represent the differences in mean ± SE of protoplasts treated (+PNP) and not treated (-PNP) with the recombinant AtPNP-A.

2.4 Discussion

A primary consideration for recombinant protein expression and purification is the experimental purpose for which the protein will be used. For biochemical and structural studies, it is important to optimize conditions for the expression of soluble and functionally active proteins, whereas for antigen production, where protein activity is not a primary consideration, the recombinant protein can be expressed either in its native or denatured form (The QIAexpressionist, 2003). However, when an over-expression of a recombinant protein required for biochemical or structural studies occurs, then its production in form of inclusion bodies may be inevitable (Lilie *et al*., 1998). This means that such inclusion bodies need to be purified under denaturing conditions followed by a refolding process that allows the expressed recombinant protein to regain its biological function before being used for either biochemical or structural studies (The QIAexpressionist, 2003; Anant, 2008). A wide variety of heterologous expression systems for the expression of recombinant proteins as inclusion bodies and the subsequent refolding of such inclusion bodies into native and active forms of protein have already been developed and are currently in use (Rudolph and Lilie, 1996; Mukhopadhyay, 1997; Lilie *et al*., 1998; Li *et al*., 2003; Li *et al*., 2004). What is required when using these expression systems is to empirically optimize their expression conditions so that they suite the individual recombinant protein involved (Rudolph and Lilie, 1996; Mukhopadhyay, 1997; Lilie *et al*., 1998; Li *et al*., 2003; Li *et al*., 2004).

In this study, a biologically active recombinant plant natriuretic peptide (PNP) from *Arabidopsis thaliana* (AtPNP-A) was prepared by empirically optimizing its expression, purification and refolding properties. Optimization of the expression

conditions resulted in over-expression of the recombinant AtPNP-A as is shown in Fig. 2.4A. Since over-expression of recombinant proteins can favour formation of inclusion bodies (Lilie *et al*., 1998), the recombinant AtPNP-A was mostly recovered in form of these insoluble aggregates. For the purpose of purification, the recombinant AtPNP-A was then first solubilized in 8 M urea buffer supplemented with other solubilization agents such as 20 mM β-mercaptoethanol and 7.5% (v/v) glycerol followed by its purification on a Ni-NTA affinity matrix (Rudolph and Lilie, 1996; Mukhopadhyay, 1997; Lilie *et al*., 1998; Li *et al*., 2003; The QIAexpressionist, 2003; Li *et al*., 2004). Purification of the recombinant AtPNP-A on the Ni-NTA affinity matrix was made possible by the fact that the recombinant protein was expressed using a pCRT7/TOPO TA expression system that adds a negatively-charged 6 x histidine tag (His-tag) to its N-terminus end thereby facilitating its binding to the affinity matrix (Lilie *et al*., 1998; The QIAexpressionist, 2003). Furthermore, solubilization of the recombinant AtPNP-A into 8 M urea buffer resulted in the "stretching out" of the His-tags thereby enhancing the binding of the protein onto the affinity matrix (Anant, 2008). The optimized purification conditions resulted in partial purification of the recombinant AtPNP-A as is shown in Fig. 2.4B.

The purified and denatured recombinant AtPNP-A was then refolded while it was still bound to the Ni-NTA affinity matrix. The keeping of proteins onto a solid support during the refolding process (Stempfer *et al*., 1996; Lindwall *et al*., 2000) has an added advantage of preventing molecules from diffusing towards each other and forming aggregates or mis-folded products (Holzinger *et al*., 1996; Li *et al*., 2003; Li *et al*., 2004). In addition, the refolding process was systematically linked to an automated fast protein liquid chromatography (FPLC) system (Fig. 2.5) that in turn

enhanced both the process control as well as the overall product output (Li *et al*., 2003; Li *et al*., 2004). Furthermore, the refolding buffer was supplemented with a number refolding agents that include glucose, NaCl, reduced and oxidized glutathione, non-detergent sulfobetaine, and poly-ethyl glycol that are reported to improve the final outcome of the refolding process (Wingfield *et al*., 1995; Lilie *et al*., 1998; Novagen, 1998; Umetsu *et al*., 2003; Vincentelli *et al*., 2004).

The activity of the refolded recombinant AtPNP-A (Fig. 2.6) was tested using an *Arabidopsis thaliana* protoplast assay system in which the protein was shown to induce significant protoplast swelling thereby demonstrating biological activity (Fig. 2.7). Recombinant AtPNP-A has previously been shown to promote cellular volume increases in *Arabidopsis thaliana* mesophyl cell protoplasts through an osmoticum-dependent water uptake that is both time-dependent and dose-dependent (Morse *et al*., 2004; Wang *et al*., 2007).

Chapter 3

Physiological Roles of a Recombinant Plant Natriuretic Peptide

Abstract

Plant natriuretic peptides (PNPs) and vertebrate artrial natriuretic peptides (ANPs) are immunoanalogues that elicit common biological responses in plants and therefore, can also be viewed as functional analogues. Vertebrate ANPs are a highly-conserved and well-studied group of hormones with a role in regulation of salt and water balances in animals. In an endeavour to gain further understanding into the physiological roles of PNPs in plants, we have used a biologically active recombinant PNP from *Arabidopsis thaliana* (AtPNP-A) in physiological studies of a soft South African perennial forest sage, *Plectranthus ecklonii* and showed that the recombinant protein can slow down the process of photosynthesis while at the same time, promoting respiration, transpiration as well as net water uptake and retention capacities, thus demonstrating its important physiological roles in plant growth and homeostasis.

3.1 Introduction

The growing number of peptide molecules identified in plants (Pearce *et al*., 1991; Matsubayashi and Sakagami, 1996; van de Sande *et al*., 1996; Fletcher *et al*., 1999; Schofer *et al*., 1999; Garcia-Olmedo *et al*., 2001; Pearce *et al*., 2001; Casson *et al*., 2002) has led to a reassessment of the role of peptide hormones, as well as further exploration to discover novel peptide families involved in plant signalling. The immunoaffinity purification of novel, biologically active proteins from *Hedera helix* (Billington *et al*., 1997) and *Solanum tuberosum* (Maryani *et al*., 2001) with

antibodies directed against a vertebrate atrial natriuretic peptide (ANP) have previously been reported and the proteins were termed immunoreactant plant natriuretic peptides (irPNPs) (Gehring, 1999). Subsequently, N- and C-terminal sequences of an irPNP from *Solanum tuberosum* (StPNP) were also obtained (Maryani *et al*., 2001) which in turn, lead to the identification and isolation of two *Arabidopsis thaliana* homologues (AtPNP-A and AtPNP-B) (Ludidi *et al*., 2002). Functional analyses of these plant natriuretic peptides (PNPs) have linked them to a number of physiological processes vital for maintenance of cellular homeostasis and growth in plants. These processes include promotion of radial water movements out of the xylem tissue (Suwastika and Gehring, 1998), concentration-dependent induction of stomatal guard cell movements (Billington *et al*., 1997), modulation of ion fluxes in conductive tissue (Pharmawati *et al*., 1999; Ludidi *et al*., 2004) and the control of osmoticum-dependent cellular water transport (Maryani *et al*., 2001; Morse *et al*., 2004; Wang, 2007). While these important responses to PNPs were detected in isolated plant tissues, here we report whole plant assaying methods and further demonstrate the physiological roles of PNPs in whole plants.

These methods make use of an infra-red gas analyzer (IRGA) (LC*pro*+, ADC Bioscientific, England) (refer to Fig. 3.1 below), which is a portable, field use device designed for plant physiological studies (LCi User Guide, 2000; LC*pro*+, 2005). Its purpose is to measure plant leaf environments and their associated physiological processes such as photosynthesis and respiration (LCi User Guide, 2000; LC*pro*+, 2005). The device comprises of two components; the main console and the leaf chamber that are connected to each other by an 'umbilical cord' (Fig. 3.1). The console contains a display, keypad, and a microprocessor-controlled operating system

with a signal conditioning air supply unit and a data card. The leaf chamber has two movable jaws into which plant leaves are trapped during assaying. Furthermore, the leaf chamber is mounted with several sensors for detection and control of chamber environmental conditions. Factors such as temperature, light (photosynthetically active radiation), pressure, carbon dioxide and water vapour can be easily controlled both automatically and independently to be either above or below ambient states (LCi User Guide, 2000; LC*pro*+, 2005).

When a plant leaf is enclosed into the leaf chamber, the console supplies air to the chamber via the "umbilical" cord at a controlled flow rate. Carbon dioxide and water vapour concentrations in the flowing air are first measured prior to their entrance into the chamber. This is then followed by their even distribution, with a small fan, over both surfaces of the leaf before being allowed to leave the chamber back to the console. The discharged air is again analyzed for both its carbon dioxide and water vapour concentrations before leaving the leaf chamber. The measured and calculated concentration differences are then sent to the console for display on the screen. It is from this information that the rates of several physiological processes such as photosynthesis, respiration and transpiration can be determined by this device (LCi User Guide, 2000; LC*pro*+, 2005).

Figure 3.1: The physical components of an infra-red gas analyzer (IRGA). The device is a portable, field-use piece of equipment designed to measure plant leaf environments and their associated physiological processes. It comprises of the main console and the leaf chamber connected to each other with an "umbilical" cord. The main console contains a keypad, a display and a microprocessor-controlled operating system with a signal conditioning air supply unit and a data card. The leaf chamber has some movable jaws into which plant leaves are trapped during their physiological analysis and is also mounted with several sensors for detection and control of the chamber environment. (Figure from LC*pro*+ manual).

Therefore, in an attempt to gain further understanding into the physiological roles of PNPs in plants, the IRGA was used to assess the *in planta* effects of a recombinant PNP from *Arabidopsis thaliana* (AtPNP-A) on photosynthesis, respiration, transpiration, photosynthetic water-use efficiency, photon yield, light compensation point, ribulose-1,5-biphosphate carboxylase activity, electron transport capacity, stomatal CO_2 conductance, and substomatal CO_2 concentration in a soft South African perennial forest sage *Plectranthus ecklonii* Benth. These *in planta* assays were also further complemented by the determination of the effects of the recombinant AtPNP-A on water potential, stomatal conductance and net water uptake and retention capacities in detached *Plectranthus ecklonii* leaves. In addition, the diurnal and circadian gene expression patterns of AtPNP-A in *Arabidopsis thaliana* as well as its expression profiles in various plant tissues were examined bioinformatically.

3.2 Materials and Methods

3.2.1 Source of Recombinant Protein and Plants used in the Assays

All physiological assays outlined in this Chapter were carried out in 8 months old soft South African perennial forest sages, *Plectranthus ecklonii* Benth (Fig. 3.1 below), a species that has previously been used to test responses to native and recombinant PNPs from different species (Maryani *et al*., 2003; Gottig *et al*., 2008) using the biologically active recombinant AtPNP-A (see Chapter 2). The *Plectranthus ecklonii* plants were supplied by the Department of Biodiversity and Conservation Biology, University of the Western Cape, in well-watered potting soils that had been kept under atmosphere-controlled green house conditions for the entire 8 months. Assays were then carried out during the day under laboratory-controlled conditions.

Figure 3.2: The soft South African perennial forest sage, *Plectranthus ecklonii* Benth. *Plectranthus ecklonii* is a soft, erect, and fast growing plant that is very attractive and popular as a garden or home ornamental and is best grown under shady conditions. It has fairly large leaves (74-190 x 35-115 mm) arranged in opposite pairs on square stems (van Jaarsveld, 2001).

3.2.2 Measurement of Photosynthesis, Transpiration, Stomatal CO_2 Conductance, and Sub-stomatal CO_2 Concentration

Assays were carried out during day time (0900 to 1600 hours) under shady laboratory conditions (2.0 - 4.0 µmol photons $m^{-2}s^{-1}$) at 24°C in 6 different *Plectranthus ecklonii* plants on a single pair of young fully-expanded leaves of each plant. One leaf of the selected pair of leaves was treated with 50 µl of a 100 µg/ml recombinant AtPNP-A sample while the leaf opposite was treated with 50 µl sterile distilled H_2O to act as a control. Leaf treatments were done by applying 25 µl of the protein sample (or H_2O) to the abaxial surface and another 25 µl of the same sample (or H_2O) to the adaxial surface followed by an even distribution of the samples across both surfaces through gentle spreading with the long flat side of a sterile pipette tip. Each treated leaf was then immediately enclosed in the leaf chamber of the portable infra-red gas analyzer (IRGA) (LCpro+, ADC Bioscientific Ltd, Herts, England) (Fig. 3.1) which was set to keep all environmental factors at ambient states except for the light source which was then varied between 0 and 1600 µmol photons $m^{-2}s^{-1}$ during the assaying period. At each selected light level, the IRGA console was capable of detecting and displaying on its screen the rates of photosynthesis, transpiration and stomatal CO_2 conductance as well as the levels of sub-stomatal CO_2 concentration in the treated leaves. The corresponding steady readings at every selected light level for each physiological process were recorded and presented as instructed by the LCpro+ user guide (ADC Bioscientific Ltd).

3.2.3 Determination of the Apparent Ribulose-1,5-biphosphate Carboxylase Activity and the Electron Transport Capacity

Leaf treatments as described in section 3.2.2 above were done followed by measurement of the leaf photosynthetic rates with the IRGA set to vary carbon dioxide concentration between 0 and 2000 ppm during the assaying period while all other environmental conditions were fixed at ambient states. A photosynthetic CO_2-response curve was then constructed by plotting the obtained photosynthetic response values against their corresponding selected CO_2 concentrations. From this curve, the apparent ribulose-1,5-biphosphate carboxylase (rubisco) activity (an enzyme capable of fixing CO_2 into complex sugars by combining it with an intermediate molecule, ribulose-1,5-biphosphate to produce a 3-carbon molecule, glyceraldehyde-3-phosphate (G3P) (Goodwin and Mercer, 1983; Forbes and Watson, 1992; Mathews *et al*., 1999) was then calculated from the slope of its CO_2-limiting section as the value of the slope (Von Caemmerer and Farquhar, 1981; Watanabe *et al*., 1994; Valentine *et al*., 2002). From the same curve, the electron transport capacity, which refers to the total number of electrons (e^-) liberated from the photo-oxidation of H_2O that are then transferred by an electron transport system to the reduced nicotinamide adenine dinucleotide phosphate (NADPH) for the ultimate fixation of CO_2 into complex sugars (Goodwin and Mercer, 1983; Forbes and Watson, 1992; Mathews *et al*., 1999), was determined from its CO_2-non-limiting section as the value of the highest photosynthetic rate attained on the curve (Von Caemmerer and Farquhar, 1981; Watanabe *et al*., 1994; Valentine *et al*., 2002).

3.2.4 Determination of Apparent Photosynthetic Photon Yield, Photosynthetic Light Compensation Point, and Leaf Dark Respiration

Following the measurement of the photosynthetic rate of a leaf as is described in section 3.2.2, a photosynthetic light-response curve for the leaf was constructed by plotting the obtained photosynthetic response values against their corresponding selected light levels. From this curve, the apparent photosynthetic photon yield, which is a measure of the total amount of light energy required during the light-dependent stage of photosynthesis for complete oxidation of H_2O (Goodwin and Mercer, 1983; Forbes and Watson, 1992; Mathews *et al*., 1999), was then calculated from the slope of its light-limiting section as the gradient value of the slope (Valentine *et al*., 2006; Mortimer *et al*., 2008). Using the same curve, the photosynthetic light compensation point, which represents the light level at which the processes of photosynthesis and respiration are equal (Goodwin and Mercer, 1983; Forbes and Watson, 1992; Mathews *et al*., 1999), was also determined at its *x*-axis intercept as the value of the intercept (Valentine *et al*., 2002; Mortimer *et al*., 2003). Leaf dark respiration was determined from the same curve at its *y*-axis intercept as the value of the intercept (Valentine and Kleinert, 2007).

3.2.5 Determination of the Photosynthetic Water-use Efficiency

The photosynthetic water-use efficiency (**a/e**), which is a measure of how much of the total amount of water taken up by a plant is utilized for photosynthetic purposes (Goodwin and Mercer, 1983; Forbes and Watson, 1992; Mathews *et al*., 1999), for a leaf treated with either recombinant AtPNP-A or H_2O as outlined in section 3.2.2, was calculated as the relative ratio between its photosynthetic rate (**a**) and its

corresponding transpiration rate (**e**) for each selected light level (Mortimer *et al*., 2003).

3.2.6 Measurement of Leaf Xylem Water Potential

Leaf xylem water potentials (XWP) were measured using a pressure bomb (PNS instruments Co. Oregon, USA). Measurements were also taken during day time (0900 to 1600 hours) under shady laboratory conditions (2.0 - 4.0 µmol photons $m^{-2}s^{-1}$) at 24°C in 6 different *Plectranthus ecklonii* plants on a single pair of young fully-expanded leaves of each plant. One leaf of the selected pair of leaves was evenly treated on both sides with 50 µl of a 100 µg/ml recombinant AtPNP-A sample while the leaf opposite was similarly treated with 50 µl sterile distilled H_2O (control). Each treated leaf was then immediately detached from the plant and fitted air-tight into the pressure bomb, with its leaf part inside the pressure chamber and the cut surface of its petiole protruding out of the chamber. Pressure was then gradually increased in the chamber until the xylem sap had evenly covered the cut surface of the leaf petiole. At this point, the pressure supply was then turned off and its corresponding value recorded as the leaf XWP.

3.2.7 Determination of Relative Net Water Transport and Retention Capacities

Net water transport was determined during day time (0900 to 1600 hours) under shady laboratory conditions (2.0 - 4.0 µmol photons $m^{-2}s^{-1}$) at 24°C in 6 different *Plectranthus ecklonii* plants on a single pair of young fully-expanded leaves of each plant. The two leaves of each selected pair of leaves per plant were first detached from their plant by cutting them off with a sterile blade ensuring that their petioles

were of the same length followed by measurement of their relative fresh weights on an analytical balance (Cape Scientific Services, Cape Town, RSA). One leaf was then evenly treated with a 100 µg/ml recombinant AtPNP-A sample by applying 25 µl of the protein sample to its abaxial surface and another 25 µl of the same sample to its adaxial surface followed by a gentle distribution of the samples with the long flat side of a sterile pipette tip. The other leaf was also similarly treated with a total of 50 µl sterile distilled H_2O to act as a control. Petioles of the treated leaves were then separately immersed into pre-weighed water contained in Eppendorf tubes before the settings were left to stand for 2 hours at room temperature (24°C).

At the end of the 2 hours, both leaves were then carefully removed from their respective tubes and their relative weights measured again. Similarly, the relative weights of the water in the two respective tubes were also re-measured. From these measurements, the relative net water transport capacity for each leaf was determined as the difference between its initial and final tube water weights while its relative net water retention capacity was calculated as the difference between its initial and final fresh weights.

3.2.8 Measurement of Leaf Stomatal Conductance

Stomatal conductances were measured with a leaf porometer (Decagon devices Inc.) during day time (0900 to 1600 hours) under shady laboratory conditions (2.0 - 4.0 µmol photons $m^{-2}s^{-1}$) at 24°C on the sets of leaves described above (section 3.2.7) during the 2-hour period at 30-minute time intervals. Measurements were taken by trapping a leaf into the jaws of the porometer with the leaf underside always facing the device sensor. Corresponding readings were then displayed on the device screen

for recording. Initial readings (0 minute) for the leaves were taken before the leaves were treated with either the recombinant AtPNP-A or sterile distilled H_2O.

3.2.9 Determination of the Diurnal and Circadian Expression Pattern of AtPNP-A

The diurnal and circadian gene expression pattern of AtPNP-A were analyzed in *Arabidopsis thaliana* rosette leaves using the Diurnal project web tool (Mockler *et al*., 2007). The data used for this analysis were obtained from a microarray dataset (Blasing *et al*., 2005), where *Arabidopsis thaliana* plants was grown in soil at 22°C and under growth conditions that included a 12-hour light cycle (130 µE) and a 12-hour dark cycle for 35 days, at which time flowering had not commenced. Typically, five replicate samples, each containing three rosettes, were collected 4, 8, and 12 hours into the light period and 4, 8, and 12 hours into the night, and three independent biological experiments for each cycle were performed at 2-month intervals.

3.2.10 Determination of AtPNP-A Expression Profiles in Various Plant Tissues

In order to reveal the expression patterns of AtPNP-A in various plant tissues, the anatomy tool in Genevestigator (Zimmermann *et al*., 2004) was used, which calculates how strongly a gene is expressed in different anatomy parts. The data used for the expression analysis of AtPNP-A was obtained from various microarray experiments and the average signal intensity values were then calculated for each type of plant tissue.

3.2.11 Statistical Analysis

Results of all assayed physiological processes were based on the means of the six replicates where results from corresponding responses for each process were subjected to analysis of variance (ANOVA) (Super-Anova, Statsgraphics Version 7, 1993, Statsgraphics Corporation, USA). Where the ANOVA revealed significant differences between treatments, the means (n = 6) were separated using a *post hoc* Student Newman Kuehls (SNK), multiple range test ($p \leq 0.05$).

3.3 Results

The effects of recombinant AtPNP-A on photosynthesis and other photosynthetic-related parameters were assessed in *Plactranthus ecklonii* leaves and the findings are shown in Fig.3.3 below. In panel A, leaves were treated with 50 µl of 100 µg/ml recombinant AtPNP-A (+PNP) while controls (-PNP) were treated with an equal volume of H_2O followed by measurement of photosynthetic rates in µmol CO_2 $m^{-2}\cdot s^{-1}$ at different light intensity levels ranging from 0-1600 µmol photons $m^{-2}\cdot s^{-1}$. The panel represents the photosynthetic rates obtained during the initial light intensity levels of 0-350 µmol photons $m^{-2}\cdot s^{-1}$. Treatment of plant leaves with the recombinant AtPNP-A resulted in significant decreases in photosynthetic rates and this effect of the protein was light intensity-dependent but less pronounced at higher irradiances. Within the first 2 minutes of AtPNP-A treatment, the photosynthetic rates for the treated leaves were strongly reduced to -5.6 µmol CO_2 $m^{-2}\cdot s^{-1}$ at 0 µmol photons $m^{-2}\cdot s^{-1}$ light levels followed by sharp increases of up to 0.1 µmol CO_2 $m^{-2}\cdot s^{-1}$ at 100 µmol photons $m^{-2}\cdot s^{-1}$ irradiances that lasted for 2 minutes before gradually remaining steady up to 2.0 µmol CO_2 $m^{-2}\cdot s^{-1}$ at 350 µmol photons $m^{-2}\cdot s^{-1}$ light levels for the next 5 minutes as compared to control leaves whose photosynthetic rates were -0.2, 0.3 and

3.5 µmol CO_2 $m^{-2}\cdot s^{-1}$ at 0, 100 and 350 µmol photons $m^{-2}\cdot s^{-1}$ light intensity levels respectively in the same time intervals.

Panel B shows the relative photosynthetic water-use efficiencies for the same sets of treated leaves (+PNP) and controls (-PNP) calculated in µmol H_2O $m^{-2}\cdot s^{-1}\cdot$µmol CO_2 $m^{-2}\cdot s^{-1}$ over the same light intensity range of 0-350 µmol photons $m^{-2}\cdot s^{-1}$. Leaf treatment with the recombinant AtPNP-A had almost a similar effect on the water-use efficiencies of *Plectranthus ecklonii* leaves as was with its photosynthetic rates. Within the first 2 minutes of AtPNP-A treatment, the water-use efficiencies were significantly decreased to -4.9 µmol H_2O $m^{-2}\cdot s^{-1}\cdot$µmol CO_2 $m^{-2}\cdot s^{-1}$ at 0 µmol photons $m^{-2}\cdot s^{-1}$ followed by a sharp increase to -0.1 µmol H_2O $m^{-2}\cdot s^{-1}\cdot$µmol CO_2 $m^{-2}\cdot s^{-1}$ at 100 µmol photons $m^{-2}\cdot s^{-1}$ that lasted for 2 minutes and then a gradual 5-minute increase of up to 1.25 µmol H_2O $m^{-2}\cdot s^{-1}\cdot$µmol CO_2 $m^{-2}\cdot s^{-1}$ at 350 µmol photons $m^{-2}\cdot s^{-1}$ when compared to control leaves whose values were -0.3, 1.2 and 6.0 µmol H_2O $m^{-2}\cdot s^{-1}\cdot$µmol CO_2 $m^{-2}\cdot s^{-1}$ at the three respective light intensity levels and within the same time intervals.

Panel C represents the apparent photosynthetic photon yields calculated in µmol CO_2 $m^{-2}\cdot s^{-1}\cdot$µmol $photon^{-1}$ $m^{-2}\cdot s^{-1}$ for the same set of *Plectranthus ecklonii* leaves treated with recombinant AtPNP-A (+PNP) and their controls (-PNP). Treatment of leaves with the recombinant AtPNP-A resulted in a significant reduction of their apparent photosynthetic photon yields from 0.022 µmol CO_2 $m^{-2}\cdot s^{-1}\cdot$µmol $photon^{-1}$ $m^{-2}\cdot s^{-1}$ to 0.013 µmol CO_2 $m^{-2}\cdot s^{-1}\cdot$µmol $photon^{-1}$ $m^{-2}\cdot s^{-1}$. This reduction in apparent photosynthetic photon yields for treated leaves was almost half that of control leaves and was observed within the first 2 minutes of leaf treatment with the recombinant

AtPNP-A. Panel D represents the relative light compensation points calculated in µmol photons $m^{-2}\cdot s^{-1}$ for the same set of treated leaves (+PNP) and their controls. Treatment of leaves with the recombinant protein resulted in a significant increase of their light compensation points from 25 µmol photons $m^{-2}\cdot s^{-1}$ to 95 µmol photons $m^{-2}\cdot s^{-1}$. This increase in light compensation points for treated leaves was almost four times higher than in controls and was also observed within the first 2 minutes of leaf treatment with the recombinant AtPNP-A.

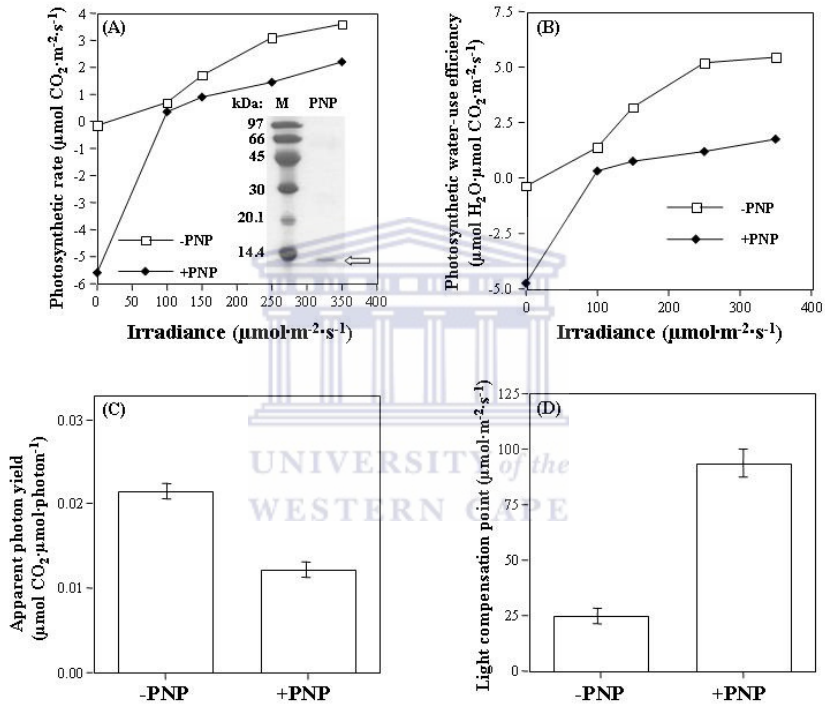

Figure 3.3: The effects of recombinant AtPNP-A on photosynthesis in *Plectranthus ecklonii* when light intensity is a limiting factor. Abaxial and adaxial surfaces of *Plectranthus ecklonii* leaves were evenly treated with 50 µl of 100 µg/ml recombinant AtPNP-A (50 µl of H_2O for control leaves) followed by measurement of the photosynthetic rates over a light intensity range of 0-1600 µmol photons $m^{-2}\cdot s^{-1}$. (**A**) Overall rates of photosynthesis for the treated (+PNP) and control (-PNP) leaves determined by plotting light-response curves for the different photosynthetic values obtained during the assaying process. Inset: SDS-PAGE of the recombinant AtPNP-A protein that was used in the assays, where (M) is the low molecular weight marker, while the arrow is marking the AtPNP-A. (**B**) Relative photosynthetic water-use efficiencies (**a/e**) for the treated (+PNP) and control (-PNP) leaves calculated as the relative ratios between the photosynthetic rates (**a**) and corresponding transpiration rates (**e**) for each light level. (**C**) Apparent photosynthetic photon yields for the treated (+PNP) and control (-PNP) leaves calculated as slopes of the light-limiting parts of the photosynthetic light-response curves. (**D**) Relative light compensation points for the treated (+PNP) and control (-PNP) leaves determined as the *x*-axis intercepts of the photosynthetic light-response curves. Error bars represent the standard errors (SE) of the means (n = 6) of the different response values obtained and analyzed by ANOVA.

The effects of recombinant AtPNP-A on the process of photosynthesis in *Plectranthus ecklonii* was also assessed using an alternative method and the results are as shown in Fig. 3.4 below. In panel A, *Plectranthus ecklonii* leaves were treated with 50 µl of 100 µg/ml recombinant AtPNP-A (+PNP) while controls (-PNP) were treated with an equal volume of H_2O followed by measurement of photosynthetic rates in µmol CO_2 $m^{-2}\cdot s^{-1}$ at different CO_2 concentrations ranging from 0-2000 ppm. The panel represents the photosynthetic rates obtained during the initial CO_2 concentration range of 0-500 ppm. As was with the light-dependent photosynthetic rates, treatment of *Plectranthus ecklonii* leaves with the recombinant AtPNP-A resulted in significant decreases in the rates of photosynthesis. At 0 ppm and 2 minutes after leaf treatment with the recombinant AtPNP-A, the photosynthetic rates of treated leaves were 0.05 µmol CO_2 $m^{-2}\cdot s^{-1}$ while those of control leaves were 0.9 µmol CO_2 $m^{-2}\cdot s^{-1}$, at 150 ppm and 4 minutes after leaf treatment, the photosynthetic rates of treated leaves were 0.3 µmol CO_2 $m^{-2}\cdot s^{-1}$ while those of control leaves were 1.5 µmol CO_2 $m^{-2}\cdot s^{-1}$ and at 500 ppm and 7 minutes after leaf treatment, the photosynthetic rates of treated leaves were 0.4 µmol CO_2 $m^{-2}\cdot s^{-1}$ compared to 3.2 µmol CO_2 $m^{-2}\cdot s^{-1}$ for control leaves. This outcome showed that the effect of the protein on photosynthesis was CO_2-independent and more pronounced at higher CO_2 concentrations.

Panels B and C represent the levels of photosynthetic rubisco activities and electron transport capacities in µmol CO_2 $m^{-2}\cdot s^{-1}$ respectively for the same set of *Plectranthus ecklonii* leaves treated with recombinant AtPNP-A (+PNP) and their controls (-PNP). In both panels, treatment of leaves with the recombinant AtPNP-A resulted in significant reduction of both parameters, where the rubisco activities for treated leaves were reduced to almost three times less than those of controls (0.0022 µmol CO_2 m^{-}

$^{2}\cdot s^{-1}$ for treatments compared to 0.0058 µmol CO_2 $m^{-2}\cdot s^{-1}$ for controls) while the electron transport capacities for treated leaves were reduced to almost six times less than those of controls (0.125 µmol CO_2 $m^{-2}\cdot s^{-1}$ for treatments compared to 0.70 µmol CO_2 $m^{-2}\cdot s^{-1}$ for controls). These effects of recombinant AtPNP-A on both parameters were observed within the first 2 minutes of leaf treatment with the recombinant protein.

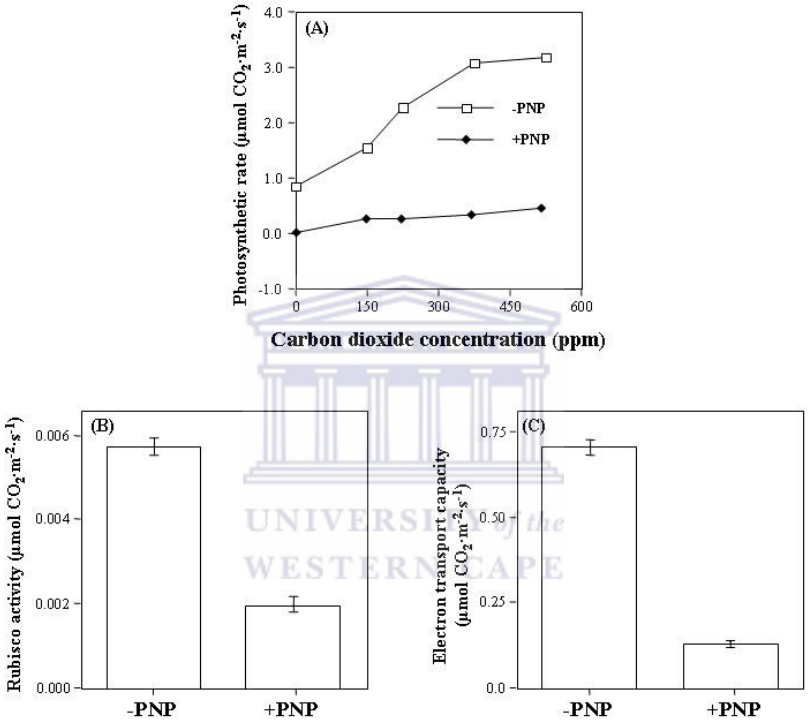

Figure 3.4: The effects of recombinant AtPNP-A on photosynthesis in *Plectranthus ecklonii* when carbon dioxide concentration is a limiting factor. Upper and lower surfaces of *Plectranthus ecklonii* leaves were evenly treated with 50 µl of 100 µg/ml recombinant AtPNP-A (50 µl of H_2O for control leaves) followed by measurement of the photosynthetic rates over a carbon dioxide concentration range of 0-2000 ppm. (**A**) Overall rates of photosynthetic for the treated (+PNP) and control (-PNP) leaves determined by plotting CO_2-response curves for the different photosynthetic values obtained during the assaying process. (**B**) Relative photosynthetic rubisco activities for the treated (+PNP) and control (-PNP) leaves calculated as slopes of the CO_2-limiting parts of the photosynthetic CO_2-response curves. (**C**) Relative photosynthetic electron transport capacities for the treated (+PNP) and control (-PNP) leaves determined as the highest photosynthetic rates reached on the CO_2-non-limiting parts of the photosynthetic CO_2-response curves. Error bars represent the standard errors (SE) of the means (n = 6) of the different response values obtained and analyzed by ANOVA.

Recombinant AtPNP-A was also assessed to check if it had any physiological effects on the respiratory processes of *Plectranthus ecklonii* leaves described in Fig. 3.3 and the results are as is shown in Fig 3.5 below. In panel A, the respiratory responses for leaves treated with 50 µl of 100 µg/ml recombinant AtPNP-A (+PNP) and their controls (-PNP) are represented in µmol CO_2 $m^{-2}\cdot s^{-1}$. The responses show that treatment of leaves with the recombinant protein resulted in significant increases in respiratory responses that were at least three-fold higher than those of controls. Treated leaves showed respiratory responses of 1.6 µmol CO_2 $m^{-2}\cdot s^{-1}$ within the first 2 minutes of their treatment with the recombinant AtPNP-A while control leaves showed respiratory responses of 5.5 µmol CO_2 $m^{-2}\cdot s^{-1}$ within the same time period.

Panels B and C represent the levels of the sub-stomatal CO_2 concentrations in ppm and rates of stomatal CO_2 conductances in µmol CO_2 $m^{-2}\cdot s^{-1}$ respectively for the same set of *Plectranthus ecklonii* leaves treated with recombinant AtPNP-A (+PNP) and their controls (-PNP) recorded over the initial light intensity range of 0-350 µmol photons $m^{-2}\cdot s^{-1}$. In both panels, leaves treated with the recombinant AtPNP-A produced significantly higher responses than their controls. In panel B, treatment of leaves with the recombinant protein resulted in gradual response increases that were light-independent and more pronounced at higher irradiances. At 0 µmol photons $m^{-2}\cdot s^{-1}$ and 2 minutes after leaf treatment with the recombinant AtPNP-A, the sub-stomatal CO_2 concentrations of treated leaves were 370 ppm while those of control leaves were 355 ppm, at 100 µmol photons $m^{-2}\cdot s^{-1}$ and 4 minutes after leaf treatment, the sub-stomatal CO_2 concentrations of treated were 375 ppm while those of control leaves were 340 ppm and at 350 µmol photons $m^{-2}\cdot s^{-1}$ and 7 minutes after leaf treatment, the sub-stomatal CO_2 concentrations of treated leaves were 379 ppm

compared to 260 ppm for control leaves. In panel C, the treatment of leaves with recombinant AtPNP-A resulted in highly significant response increases that were light-dependent and more pronounced throughout all light intensity levels. At 0 µmol photons $m^{-2}\cdot s^{-1}$ and 2 minutes after leaf treatment with the recombinant AtPNP-A, the stomatal CO_2 conductances of treated leaves were 0.35 µmol CO_2 $m^{-2}\cdot s^{-1}$ while those of control leaves were 0.06 µmol CO_2 $m^{-2}\cdot s^{-1}$, at 150 µmol photons $m^{-2}\cdot s^{-1}$ and 4.5 minutes after leaf treatment, the stomatal CO_2 conductances of treated were 0.46 µmol CO_2 $m^{-2}\cdot s^{-1}$ while those of control leaves were 0.095 µmol CO_2 $m^{-2}\cdot s^{-1}$ and at 350 µmol photons $m^{-2}\cdot s^{-1}$ and 7 minutes after leaf treatment, the stomatal CO_2 conductances of treated leaves were 0.43 µmol CO_2 $m^{-2}\cdot s^{-1}$ compared to 0.11 µmol CO_2 $m^{-2}\cdot s^{-1}$ for control leaves.

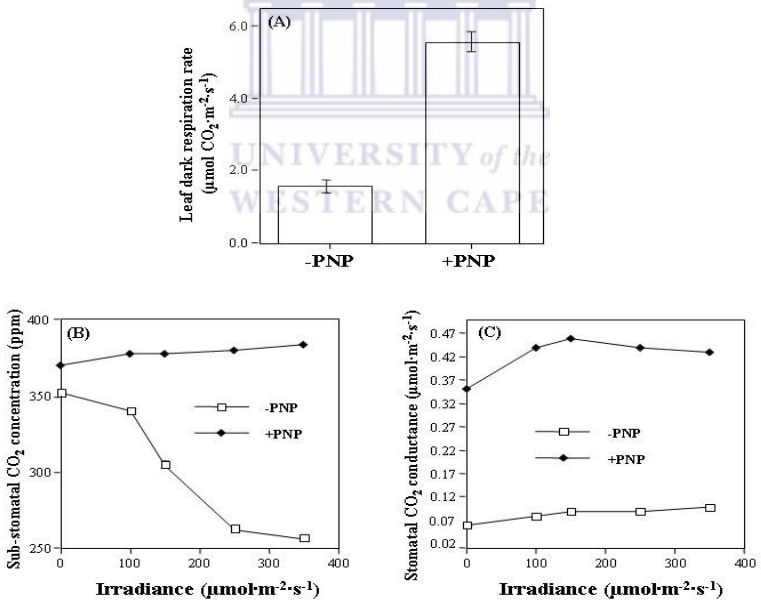

Figure 3.5: The effects of recombinant AtPNP-A on leaf respiration in *Plectranthus ecklonii*. Leaves of the *Plectranthus ecklonii* were treated and analyzed as described in the legend to Fig. 3.3. (**A**) Leaf dark respiration levels for the treated (+PNP) and control (-PNP) leaves determined as the *y*-axis intercepts of the photosynthetic light-response curves. (**B**) Sub-stomatal CO_2 concentrations for the treated (+PNP) and control (-PNP) leaves determined by plotting light-response curves for the different sub-stomatal CO_2 concentration values obtained during the assaying process. (**C**) Stomatal CO_2 conductances for the treated (+PNP) and control (-PNP) leaves determined by plotting light-response curves for the different stomatal CO_2 conductance values obtained during the assaying process. Error bars represent the standard errors (SE) of the means (n = 6) of the different response values obtained and analyzed by ANOVA.

Recombinant AtPNP-A was also assessed for its physiological effects on the process of transpiration in *Plectranthus ecklonii* (Fig 3.6). Panel A shows the transpiration rates in µmol H_2O $m^{-2}\cdot s^{-1}$ of the *Plectranthus ecklonii* leaves treated with 50 µl recombinant AtPNP-A (+PNP) and their controls (-PNP) recorded over the initial light intensity range of 0-350 µmol photons $m^{-2}\cdot s^{-1}$. Treatment of plant leaves with the recombinant AtPNP-A resulted in significant increases in the rates of transpiration and such increases were inversely light-dependent and less pronounced at higher intensities. Within the first 2 minutes of leaf treatment with recombinant AtPNP-A, transpiration rates for treated leaves were significantly increased to 1.21 µmol H_2O $m^{-2}\cdot s^{-1}$ at 0 µmol photons $m^{-2}\cdot s^{-1}$ light levels followed by gradual decreases of up to 1.01 µmol H_2O $m^{-2}\cdot s^{-1}$ at 350 µmol photons $m^{-2}\cdot s^{-1}$ light levels that lasted for 7 minutes as compared to control leaves whose transpiration rates started at 0.31 µmol H_2O $m^{-2}\cdot s^{-1}$ at 0 µmol photons $m^{-2}\cdot s^{-1}$ light intensity levels and 2 minutes from the time of their treatment with H_2O and then in 7 minutes time, gradually increased to 0.65 µmol H_2O $m^{-2}\cdot s^{-1}$ at 150 µmol photons $m^{-2}\cdot s^{-1}$.

Panel B and C represent the leaf water potentials in mPa and net water transport in $ml\cdot g^{-1}$ fresh leaf weight respectively for *Plectranthus ecklonii* leaves treated with 50 µl recombinant AtPNP-A (+PNP) and their controls (-PNP). Both panels show that treatment of leaves with the recombinant AtPNP-A resulted in significant increases of both parameters with increases that were almost two-fold stronger in treated leaves than in control leaves. In panel B, the leaf water potentials of treated leaves were increased from -0.25 to -0.46 mPa after 2 minutes of their treatment with the recombinant AtPNP-A while in panel C, the net water transport capacities for treated

leaves were increased from 0.12 to 0.22 $ml \cdot g^{-1}$ fresh leaf weight 2 hours after their treatment with the recombinant AtPNP-A.

Panel D shows trends of the transpiration rates described in Panel A when the rates of transpiration for leaves treated with 50 µl recombinant AtPNP-A (+PNP) and their controls (-PNP) were recorded as stomatal conductances in µmol H_2O $m^{-2} \cdot s^{-1}$ over a time period of 120 minutes in day light. The results show that leaves treated with the recombinant AtPNP-A first gained rapid transpiration rates of up to 90 µmol H_2O $m^{-2} \cdot s^{-1}$ (compared to 65 µmol H_2O $m^{-2} \cdot s^{-1}$ for controls) that lasted for over 30 minutes followed by gradual decreases in transpiration rates that were even lower than those of controls between 50 and 120 minutes.

Panel E represents changes in leaf weights for the same sets of leaves described in panel D recorded with comparison to their standardized original leaf weights (CONT) over a 2-hour time period. In relation to their original sizes (CONT), leaves treated with the recombinant AtPNP-A (+PNP) gained 1.8% of their original weight while those treated with H_2O lost 0.6% of their original weight.

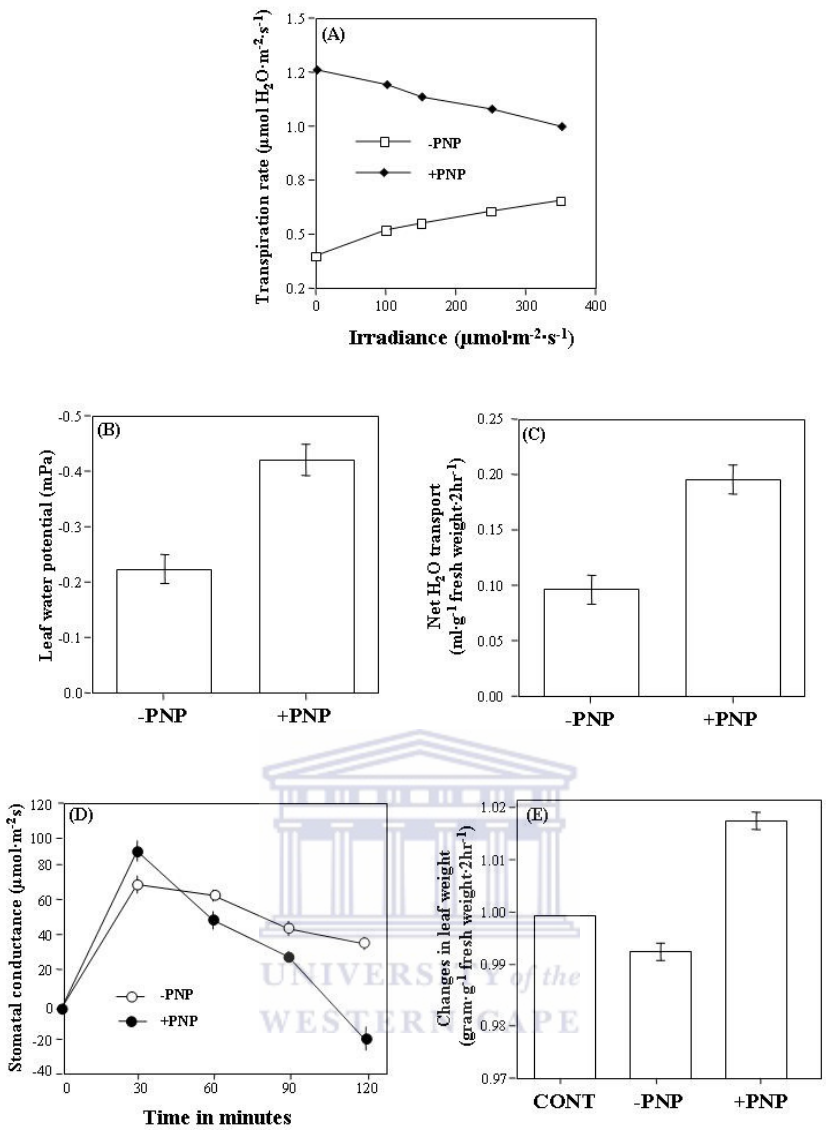

Figure 3.6: The effects of recombinant AtPNP-A on transpiration in *Plectranthus ecklonii*. (**A**) Transpiration rates for *Plectranthus ecklonii* leaves treated with 50 µl recombinant AtPNP-A (+PNP) and controls (-PNP) treated with 50 µl of H_2O as determined by plotting light-response curves for the different transpiration responses obtained during the assaying process. (**B**) Leaf water potentials for leaves treated with 50 µl recombinant AtPNP-A (+PNP) and their controls (-PNP) determined as the ability for a leaf to take up H_2O. (**C**) Net water transport capacities for leaves treated with 50 µl recombinant AtPNP-A (+PNP) and their controls (-PNP) calculated in ml/g fresh leaf weight as the total amount of water taken up by a leaf over a period of 2 hours. (**D**) Stomatal conductances for leaves treated with 50 µl recombinant AtPNP-A (+PNP) and their controls (-PNP) determined as the amount of water vapour lost from the leaf surface over a period of 2 hours. (**E**) Net water retention capacities for leaves treated with 50 µl recombinant AtPNP-A (+PNP) and their controls (-PNP) determined as changes in leaf weights in ml/g fresh leaf weight over a period of 2 hours. Error bars represent the standard errors (SE) of the means (n = 6) of the different response values obtained and analyzed by ANOVA.

A web based tool, The Diurnal Project (Mockler *et al*., 2007) was used to find out how the AtPNP-A was expressed during the diurnal cycle in *Arabidopsis. thaliana*. Plants were exposed to a 12-hour light cycle (130 µE) and 12-hour dark cycle and AtPNP-A expression detected in rosettes of the plant. Analysis of the results showed that AtPNP-A expression was steadily increased from 0.19 to 0.97 normalised gcRMAATH1 during the 12-hour light cycle, which was then followed by a consistent decrease in expression of up to 0.125 normalised gcRMAATH1 during the 12-hour dark cycle (Fig 3.7). This observation was again readily detected during the next 24-hour light/dark cycle, which could lead to the conclusion that AtPNP-A expression was high during day-time and low in darkness.

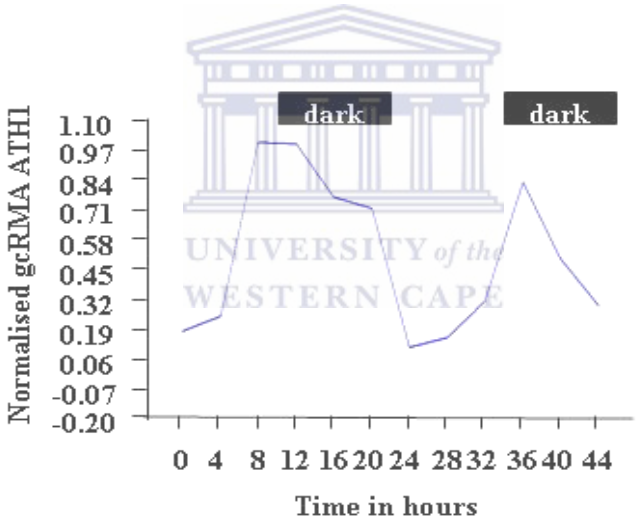

Figure 3.7: AtPNP-A expression in the diurnal cycle. Expression of AtPNP-A during the light cycle (130 µE) showed a steady increase while during the dark cycle its expression indicated a decreased profile (data obtained from The Diurnal Project Mockler *et al*., 2007).

Genevestigator (Zimmermann *et al*., 2004) analysis of the *AtPNP-A* gene using the anatomy tool showed that AtPNP-A was expressed in many plant tissues which included stamens, petioles, hypocotyls and leaves. There was however, an immensely elevated expression of AtPNP-A in the sepals of up to 3500 arbitrary fluorescence units as compared to most investigated plant tissues whose expression levels were all below 1000 fluorescence units (Fig 3.8). This therefore indicated that AtPNP-A has a much higher level of expression in sepals than in any other plant tissue investigated.

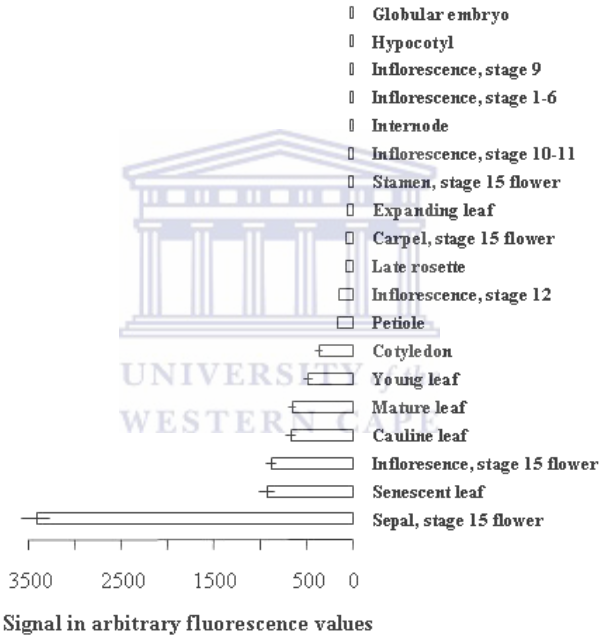

Figure 3.8: Expression profile of AtPNP-A in different plant tissues. *AtPNP-A* gene expression in various parts of the plant showed considerably elevated expression levels of AtPNP-A in the sepals (data obtained from Genevestigator anatomy tool Zimmermann *et al*., 2004).

3.4 Discussion

Plant natriuretic peptides (PNPs) are a class of extracellular, systemically mobile molecules that elicit a number of plant responses important for growth and maintenance of cellular homeostasis (Gehring and Irving, 2003). Here, it was demonstrated that the treatment of *Plectranthus ecklonii* leaves with a biologically active recombinant PNP from *Arabidopsis thaliana* (AtPNP-A) does lead to significant changes in photosynthesis and respiration. The recombinant AtPNP-A was shown to down-regulate photosynthesis (Figs. 3.3A and 3.4A) and at the same time, up-regulate respiration (Fig. 3.5A). Concurring with these effects, recombinant AtPNP-A was also shown to reduce the photosynthetic water-use efficiencies (Fig. 3.3 B), apparent photon yields (Fig. 3.3C), electron transport capacities (Fig. 3.4B) and rubisco activities (Fig. 3.4C) of the *Plectranthus ecklonii* leaves while at the same time, it increased their light compensation points (Fig. 3.3D), sub-stomatal CO_2 concentrations (Fig. 3.5B) and stomatal CO_2 conductances (Fig. 3.5C).

In nature, the balance between the rates of photosynthesis and respiration is mainly governed by light since it is the main factor that provides the energy required for photosynthesis (Forbes and Watson, 1992). The light intensity level at which the rates of photosynthesis and respiration balance one another, and at which net assimilation rate is therefore zero, is the light compensation point (Forbes and Watson, 1992). Above the light compensation point, photosynthesis is higher than respiration with a positive net assimilation rate while below the compensation point, respiration is higher than photosynthesis with a negative net assimilation rate (Forbes and Watson, 1992). In absolute darkness, the rate of photosynthesis is zero while respiration continues so that the net assimilation rate is negative (Forbes and Watson,

1992). In this study, the treatment of *Plectranthus ecklonii* leaves with recombinant AtPNP-A in the presence of light resulted in increased light compensation points (Fig. 3.3D) thus a shifted in favour of respiration at the expense of photosynthesis. The same leaf treatment in total darkness resulted in substantial increases in dark respiration (Fig.3.5A).

However, the manner in which photosynthesis and respiration are affected by recombinant AtPNP-A in *Plectranthus ecklonii* leaves is noteworthy. Under most physiological conditions, the down-regulation of photosynthesis is usually associated with lower sub-stomatal CO_2 concentrations and stomatal CO_2 conductances (Forbes and Watson, 1992), and this was not the case here. This then brings to the fore a possibility that photosynthesis could have been limited by other factors such as the utilisation of its light reaction products, such as the reduced nicotinamide adenine dinucleotide phosphate (NADPH), by respiration (Niyogi, 2000). NADPH is required by photosynthesis as a source of electrons for the fixation of CO_2 (Forbes and Watson, 1992), and therefore its possible utilisation by respiration would cause a decrease in photosynthesis. Such a decrease in photosynthesis is always associated with decreases in apparent photon yields, water-use efficiencies, electron transport capacities and rubisco activities, those parameters whose rates are directly proportional to the amount of CO_2 fixed, (Forbes and Watson, 1992), of which was the case in this study.

Naturally, the mopping-up of NADPH from photosynthesis by respiration (photorespiration and/chlororespiration) and other processes in plants is a safe way of dissipating excess photons and electrons, thereby protecting the photosynthetic

apparatus from light-induced damages caused by the inevitable generation of reactive intermediates and by-products (Niyogi, 2000). Such generation of reactive intermediates and by-products in plants generally occurs as a result of diurnal and seasonal fluctuations in light intensities, as well as environmental stresses such as cold, drought, salinity, and nutrient deficiency, that limit CO_2 fixation and resulting in the absorption of more light energy than can be utilized productively by photosynthesis (Niyogi, 2000). Hence if photosynthesis in *Plectranthus ecklonii* is down-regulated by recombinant AtPNP-A through the utilization of NADPH by respiration, then this implies a very important role for AtPNP-A in plant cellular homeostasis as the protein would be able to protect plants from the light-induced damages caused by the inevitable generation of reactive intermediates and by-products whenever they are susceptible to such situations through the dissipation of excess photons and electrons in form of NADPH via respiration.

In general, the application of recombinant AtPNP-A to *Plectranthus ecklonii* leaves appears to favour catabolic reactions. Such an effect of AtPNP-A on respiration was also recently observed in a collaborative research project with the Institute for Plant Biotechnology (University of Stellenbosch, RSA) where treatment of *Plectranthus ecklonii* leaf discs with the recombinant AtPNP-A was shown to result in significant reduction in starch, sucrose, glucose and fructose contents (Gavin George, personal communication). These observations are consistent with the promotion of respiration by recombinant AtPNP-A in *Plectranthus ecklonii* leaves, where the carbohydrate levels are reduced as a consequence of increased cellular catabolism. In addition, the diurnal and circadian expression patterns of AtPNP-A also showed that *AtPNP-A* gene expression steadily increases during the light cycle and then decreases at night

(Fig 3.7). Since starch formation is higher during the day (due to photosynthesis) than at night (Forbes and Watson, 1992), this could be another indication that AtPNP-A plays a role in aiding the breakdown of starch and sugars into CO_2 and H_2O during respiration. Furthermore, expression profiling studies of the *AtPNP-A* gene in the entire plant showed that AtPNP-A expression is highest in sepals as compared to other parts of the Arabidopsis plant (Fig. 3.8). This again further links AtPNP-A to the high metabolic activities found in sepals that might be associated with processes such as flower development (Robels and Pelaz, 2005; Blázquez *et al*., 2006), flower movements (opening and closing) (Bynum and Smith, 2001), fruit development (Robels and Pelaz, 2005), seed formation (Kohler and Makarevich, 2006) as well as fruit ripening (Giovannoni, 2007).

The response - down-regulated photosynthesis and up-regulated respiration - has recently been reported to occur in *Arabidopsis thaliana* leaves during infection by a virulent strain of *Pseudomonas syringae* (Bonfig *et al*., 2006). Using chlorophyll fluorescence imaging to compare the effects of infection by virulent and avirulent strains of *Pseudomonas syringae* on photosynthesis and sink metabolism in *Arabidopsis thaliana* leaves, inoculation of leaves with the virulent but not the avirulent strain resulted in down-regulation of photosynthetic genes and up-regulation of vacuolar invertases with increased quantum yields of the dissipated non-regulated energy (Bonfig *et al*., 2006). A co-ordinated regulation of defence mechanisms, photosynthesis and sink metabolism has been shown to be independently mediated by sugars and defence-related stimuli (Ehness *et al*., 1997; Sinha *et al*., 2002; Berger *et al*., 2006). Suppression of host photosynthesis during infections is a defense mechanism employed by plants aimed at preventing successful invasion and/or

spreading of the pathogens (Berger *et al*., 2006) since under such conditions, the availability and supply of photosynthetic assimilates to pathogens would be strongly limited. On the other hand, the sink strengths of plants are typically increased during infections to satisfy the energy requirements of the activation of the cascade of defense reactions with assimilates mobilized for these reactions (Roitsch and Gonzalez, 2004; Bonfig *et al*., 2006).

A similar pattern where photosynthesis is slowed down while respiration is promoted has also been reported in previous studies that involved an assessment of the effects of wounding on photosynthesis, sink metabolism, and defense responses in *Chenopodium rubrum* leaves (Ehness *et al*., 1997). In these studies, the effects of wounding on photosynthesis, sink metabolism, and defense responses were determined by analyzing the regulation of mRNAs for representative enzymes involved in key pathways of these three processes (Ehness *et al*., 1997). The mRNAs for phenylalanine ammonia-lyase, a key enzyme of defense response, and for the sink-specific extracellular invertase were induced while the mRNA for the Calvin cycle enzyme ribulose bisphosphate carboxylase was repressed (Ehness *et al*., 1997).

Recently, studies using a combination of expression correlation analysis, meta-analysis of gene expression profiles in response to specific stimuli and in selected mutants, as well as promoter content analysis to infer the biological role of AtPNP-A in *Arabidopsis thaliana*, have indicated that AtPNP-A expression was significantly correlated with that of genes involved in the systemic acquired resistance (SAR), defence response pathways, and in response to various abiotic (*e.g*., osmotic stress and K^+ starvation) and biotic (*e.g*., pathogen infections) stimuli (Meier *et al*., 2008b).

This induced expression of *AtPNP-A* by SAR elicitors and AtPNP-A secretion into the apoplast (Boudart *et al*., 2005) was similar to that of pathogen related (PR) proteins and strongly implicates AtPNP-A in defence responses (and SAR in particular) which may involve the modification of cellular ion and water homeostasis (Meier *et al*., 2008b). This conclusion is consistent with the observed coordinated regulation of photosynthesis and respiration by recombinant AtPNP-A in *Plectranthus ecklonii* leaves and is also expected to affect cellular water and ion homeostasis.

In addition to having an effect on photosynthesis and respiration, recombinant AtPNP-A also had significant effects on the process of transpiration in *Plectranthus ecklonii*. The rates of transpiration were promoted (Fig. 3.6A) in leaves treated with the recombinant AtPNP-A and this observation was further confirmed by the promotion of the relative xylem water potentials (Fig. 3.6B), net water transport capacities (Fig. 3.6C) as well as stomatal H_2O conductances (Fig. 3.6D).

When recombinant AtPNP-A was assessed for its effect on leaf weights during transpiration in *Plectranthus ecklonii*, it was noted that it could promote significant weight gains (Fig. 3.6E) leading to a conclusion that recombinant AtPNP-A causes net water uptake and retention. Regulations of net water uptake in plant cells by PNPs have previously been reported for irPNPs and AtPNP-A that were shown to cause protoplast swelling due to net water uptake in *Solanum tuberosum* and *Arabidopsis thaliana* mesophyl protoplasts respectively, (Maryani *et al*., 2001; Morse *et al*., 2004; Wang, 2007) thus affecting cell volumes and cell weights.

Chapter 4

A Recombinant Plant Natriuretic Peptide has a Systemic Mode of Action Associated with the Vascular System

Abstract

Plant natriuretic peptides (PNPs) have previously been shown to affect a number of biological processes in plants at nanomolar concentrations and evidence from several lines of cellular and physiological studies have suggested that they may have a systemic mode of action. In an attempt to elucidate the mode of action of these PNPs, we have used a biologically active recombinant PNP from *Arabidopsis thaliana* (AtPNP-A) and demonstrated that respiratory response signals initiated in one leaf of a soft South African perennial forest sage, *Plectranthus ecklonii* by treating it with the recombinant protein could be systemically transmitted to other surrounding leaves on the same plant. We also showed that chilling of petiole segments between the treated leaf and its neighbouring leaves would weaken and delay the transmission of the respiratory response signals. In addition, chilling had similar effects on the transmission of AtPNP-A-induced net water transport signals from petiole ends to leaf surfaces of the *Plectranthus ecklonii* leaves. Taken together, these findings demonstrated a systemic mode of action for the recombinant AtPNP-A in *Plectranthus ecklonii* which was closely associated with the phloem tissue.

4.1 Introduction

Several lines of evidence from a number of studies have suggested that plant natriuretic peptides (PNPs) may have a systemic mode of action in plants. Firstly, PNPs are structurally (Ludidi *et al*., 2002; Gehring and Irving, 2003) and functionally (Pharmawati *et al*., 1998b; Suwastika and Gehring, 1998) related to ANPs. ANPs are hormonal molecules with a systemic mode of action in vertebrates (deBold *et al*., 1981). Secondly, amino acid sequence comparisons and structural modelling predicted that PNPs do not contain the putative polysaccharide-binding C-terminal domain typical for the related expansins that act on cell walls (Linder and Teeri, 1997; Barre and Rouge, 2002; Ludidi *et al*., 2002). The absence of such a domain in PNPs presumably results in their increased extracellular mobility, which in turn is a precondition to a systemic mode of action.

Thirdly, PNPs were shown to be associated with the conductive tissues as was demonstrated by *in situ* immunoreactivity and immunofluorescence assays of *Hedera helix* and *Solanum tuberosum* probed with anti-human atrial natriuretic peptide antibodies and anti-potato natriuretic peptide antibodies respectively (Maryani *et al*., 2003). Furthermore, biologically active PNPs were also isolated from xylem exudates of *Plectranthus ciliatus* (Maryani *et al*., 2003), whereby the concentrated exudates could promote stomatal opening in *Arabidopsis thaliana* (Maryani *et al*., 2003), thus further supporting the idea that PNPs are systemically mobile.

Fourthly, an Arabidopsis PNP has previously been identified in the apoplastic fluid of Arabidopsis rosettes using a proteomic and bioinformatic approach (Boudart *et al*., 2005) thus reaffirming its extracellular location which is also a precondition to a

systemic mode of action. Lastly, PNP has recently been identified in differentiating phloem tissues of *Arabidopsis thaliana* leaves and inflorescence stems using a microarray analyses approach that was based on a predicted increase in vascular-related gene expression in response to an auxin transport inhibitor-induced vascular overgrowth (Wenzel *et al*., 2008).

Recent findings from our work (Chapter 3) using a recombinant *Arabidopsis thaliana* PNP (AtPNP-A) to assess its effects on various physiological processes in *Plectranthus ecklonii* have shown that the recombinant AtPNP-A can enhance leaf respiration and net water transport. Based on these two findings, two physiological assaying methods that involved the tracing of AtPNP-A induced leaf respiration and net water transport response signals in *Plectranthus ecklonii* were hereby developed and used to demonstrate a phloem-dependent systemic mode of action for the recombinant AtPNP-A.

4.2 Materials and Methods

4.2.1 Source of Recombinant Protein and Plants used in the Assays

The systemic assays were carried out in 8 months old soft South African perennial forest sages, *Plectranthus ecklonii* Benth (refer to Fig 3.1 in Chapter 3), a species that has previously been used to test responses to native and recombinant PNPs from different species (Maryani *et al*., 2003; Gottig *et al*., 2008) using the biologically active recombinant AtPNP-A (see Chapter 2). The *Plectranthus ecklonii* plants were supplied by the Department of Biodiversity and Conservation Biology, University of the Western Cape, in well-watered potting soils that had been kept under atmosphere-controlled green house conditions for the entire 8 months. Assays were then carried out during the day under laboratory-controlled conditions.

4.2.2 Respiratory Response Assays

4.2.2.1 Induction of leaf respiration by recombinant AtPNP-A at high light intensities in Plectranthus ecklonii

Recombinant AtPNP-A was first assessed for its ability to induce leaf respiration at the photosynthetic saturating light intensity level (Forbes and Watson, 1992) of *Plectranthus ecklonii* of 1300 µmol photons $m^{-2} \cdot s^{-1}$. Respiratory responses were measured in 6 different *Plectranthus ecklonii* plants (refer to Fig 3.2 in Chapter 3) using a portable infra-red gas analyzer (IRGA) (LCpro+, ADC Bioscientific Ltd, Herts, England) (refer to Fig 3.1 in Chapter 3). Measurements were taken during day time (0900 to 1600 hours) under shady laboratory conditions (2.0 - 4.0 µmol photons $m^{-2}s^{-1}$) at 24°C on a single pair of young fully-expanded leaves of each plant. One

leaf of the selected pair of leaves was treated with 50 µl of a 100 µg/ml recombinant AtPNP-A sample while the leaf opposite was also similarly treated with 50 µl sterile distilled H_2O to act as a control. Leaf treatments were done by applying 25 µl of the protein sample (or H_2O) to the abaxial surface and another 25 µl of the same sample (or H_2O) to the adaxial surface followed by an even distribution of the samples across both surfaces through gentle spreading with the long flat side of a sterile pipette tip. Each treated leaf was then immediately enclosed into the leaf chamber of the IRGA which was set to take respiratory readings at a light intensity level of 1300 µmol photons $m^{-2} \cdot s^{-1}$ while keeping all other environmental factors at ambient states. Readings were recorded at 2-minute intervals for 8 minutes. Initial readings (0 seconds) for the leaves were taken before the leaves were treated with either the recombinant AtPNP-A or sterile distilled H_2O.

As a positive control for this assay, another experiment that was meant to measure leaf dark respiration was also similarly set as described above with an exception that the IRGA was set to take respiratory readings at 0 µmol photons $m^{-2} \cdot s^{-1}$ light intensity level. In order to maximize the effectiveness of this control experiment, all assays were conducted while the leaf chamber was completely covered with a piece of black cloth so as to exclude light (Valentine *et al*., 2002).

4.2.2.2 Assessment of the systemic nature of the AtPNP-A-induced respiratory responses in Plectranthus ecklonii

Assays were carried out during day time (0900 to 1600 hours) under shady conditions (2.0 - 4.0 µmol photons $m^{-2}s^{-1}$) at 24°C in 6 different *Plectranthus ecklonii* plants. For each plant, three adjacent pairs of young fully-expanded leaves were selected and four leaves on these three pairs marked 1 to 4 as is shown in Fig. 4.1 below. An IRGA set to take respiratory readings at 1300 µmol photons $m^{-2}\cdot s^{-1}$ light intensity level while keeping all other environmental factors at ambient states was then used to measure the basal respiratory responses of each of the four marked leaves by enclosing each one of them into the leaf chamber followed by the recording of the corresponding respiratory readings. One leaf of the middle pair (leaf 1) was then treated with 50 µl of a 100 µg/ml recombinant AtPNP-A sample by applying 25 µl of the protein sample to its abaxial surface and another 25 µl of the same sample to its adaxial surface followed by an even distribution of the samples across both surfaces with the long flat side of a sterile pipette tip. This treatment was made to induce leaf respiration in the leaf. The treated leaf was then immediately enclosed into the leaf chamber of an IRGA which was set to take respiratory readings at 1300 µmol photons $m^{-2}\cdot s^{-1}$ light intensity level while keeping all other environmental factors at ambient states. Similar measurements were then taken from one leaf on the lower pair (leaf 2), the opposite leaf on the middle pair (leaf 3) and one leaf on the upper pair (leaf 4) at 5-minute intervals for 20 minutes. These measurements were taken to check if the respiratory response initiated in leaf 1 was being transmitted to leaves 2, 3 or 4 and if so, whether such a transmission was time-dependent. The overall leaf respiration response for each individual leaf at each time point was finally calculated as the

difference between the respiratory reading at that particular time point and the basal respiratory reading of that leaf.

Figure 4.1: The assaying scheme used to assess the systemic action of recombinant AtPNP-A in *Plectranthus ecklonii*. Leaf 1 was evenly treated with 50 µl of a 100 µg/ml recombinant AtPNP-A sample (refer to section 4.2.2.2) to initiate a respiratory response signals. The possible transmission of this respiratory response signal was then assessed by monitoring the induction of respiratory responses in leaves 2, 3, and 4 at 5-minute intervals over 20 minutes. All respiratory response measurements were taken with an IRGA set to take readings at 1300 µmol photons $m^{-2} \cdot s^{-1}$ light intensity level.

4.2.2.3 The effects of petiole chilling on the transmission of AtPNP-A-induced respiratory responses in Plectranthus ecklonii

The assays in section 4.2.2.2 above were repeated as previously described except that part of the petiole segments of leaves 2, 3 and 4 (points marked A, B and C respectively in Fig. 4.2 below) were chilled down with ice-cold rings during the entire assaying period. The chilling was done using a small 3-way peristaltic pump (Pharmacia Fine Chemicals) that circulated ice-cold H_2O around each leaf petiole

(cold girdling) in 1.0 mm (internal diameter) x 0.8 mm (wall thickness) plastic tubings (Pharmacia Fine Chemicals) at a flow rate of 1.0 ml/min during the assaying period. Overall leaf respiration responses for leaves 2, 3 and 4 in this assay were then calculated as previously described in section 4.2.2.2. The relative strengths and rates of these responses were then analyzed by comparing them with the relative strengths and rates of the respiratory responses obtained in section 4.2.2.2 for the same sets of leaves (2, 3 and 4).

Figure 4.2: The assaying regime used to determine the effect of petiole chilling on the transmission of an AtPNP-A-induced respiratory response signals in *Plectranthus ecklonii*. The assaying scheme described in Fig. 4.1 above was repeated while part of the petiole segments of leaves 2, 3 and 4 (marked A, B and C respectively) were chilled down with ice-cold rings (cold girdling) during the entire assaying period (for the chilling procedure, refer to section 4.2.2.3). The respiratory responses obtained in leaves 2, 3 and 4 under this chilling effect were then analyzed by comparing them with the respiratory responses obtained for the same sets of leaves (2, 3, and 4) without chilling (see Fig. 4.1).

4.2.3 Net Water Transport Response Assays

4.2.3.1 Measurement of net water transport in Plectranthus ecklonii

Net water transport was determined in 6 different *Plectranthus ecklonii* plants on a single pair of young fully-expanded leaves of each plant. The two leaves of each selected pair of leaves per plant were first detached from their plant by cutting them off with a sterile blade ensuring that their petioles were of the same length followed by measurement of their relative fresh weights on an analytical balance (Cape Scientific Services, Cape Town, RSA). The petiole of one leaf was then immersed into an Eppendorf tube containing pre-weighed H_2O that was pre-treated with recombinant AtPNP-A to a final protein concentration of 100 µg/ml while the petiole of the other leaf was immersed into an Eppendorf tube containing untreated pre-weighed H_2O (control). Solutions in both tubes were covered with a thin layer of mineral oil in order to minimize evapouration. The settings were then left to stand for 2 hours at room temperature (24°C), and at 2.0 - 4.0 µmol photons $m^{-2}s^{-1}$ room light intensity levels. At the end of the 2 hours, both leaves were then carefully removed from their respective tubes and their relative new fresh weights measured. Similarly, the relative new weights of their tube water were also re-measured. The relative net water transport for each leaf was then determined as the calculated difference between its initial and final tube water weights expressed in ml/g fresh leaf weight.

As a control for this assay, another experiment was also similarly set as described above except that no protein was added into the tube water. Instead, one leaf was evenly treated on its surfaces with 50 µl of a 100 µg/ml recombinant AtPNP-A sample by applying 25 µl of the protein sample to its abaxial surface and another 25

µl of the same sample to its adaxial surface followed by a gentle distribution of the samples with the long flat side of a sterile pipette tip while the other leaf was also similarly treated with a total of 50 µl sterile distilled H_2O to act as a control. The relative net water transport capacities of the two leaves in this control experiment were as well calculated and determined as is previously explained for the experimental set ups.

4.2.3.2 The effects of petiole chilling on AtPNP-A-induced net water transport in Plectranthus ecklonii

The experimental assay described above (section 4.2.3.1) was repeated with parts of the leaf petiole segments chilled down (cold girdling) as described in section 4.2.2.3. The relative net water transport capacities of the leaves in this assay were then determined and their levels compared to those obtained in section 4.2.3.1.

4.2.4 Statistical Analysis

Results of all assayed physiological processes were based on the means of the six replicates where results from corresponding responses for each process were subjected to analysis of variance (ANOVA) (Super-Anova, Statsgraphics Version 7, 1993, Statsgraphics Corporation, USA). Where the ANOVA revealed significant differences between treatments, the means (n = 6) were separated using a *post hoc* Student Newman Kuehls (SNK), multiple range test ($p \leq 0.05$).

4.3 Results

Recombinant AtPNP-A was first tested for its ability to induce leaf respiration at the photosynthetic saturating light intensity level (Forbes and Watson, 1992) of *Plectranthus ecklonii* of 1300 µmol photons $m^{-2}\cdot s^{-1}$. A positive control experiment whereby respiratory responses were measured in the absence of light was also s*et al*ongside this experiment. Leaves were treated with 50 µl of 100 µg/ml recombinant AtPNP-A (+PNP) and their controls (-PNP) with equal volume of H_2O followed by measurement and recording of respiratory rates in µmol CO_2 $m^{-2}\cdot s^{-1}$ at 1300 µmol photons $m^{-2}\cdot s^{-1}$ and 0 µmol photons $m^{-2}\cdot s^{-1}$ as is shown in Fig.4.3 below. Panel A shows the respiratory responses induced in the *Plectranthus ecklonii* leaves by the recombinant AtPNP-A at their photosynthetic saturating light intensity level of 1300 µmol photons $m^{-2}\cdot s^{-1}$. Treatment of leaves with the recombinant AtPNP-A resulted in a significant increase of their respiratory rates from -2.6 µmol CO_2 $m^{-2}\cdot s^{-1}$ to 3.4 µmol CO_2 $m^{-2}\cdot s^{-1}$ that lasted for 4 minutes followed by a gradual decrease to 1.8 µmol CO_2 $m^{-2}\cdot s^{-1}$ that also lasted for 4 minutes as compared to respiratory rates of control leaves that only rose from -1.2 µmol CO_2 $m^{-2}\cdot s^{-1}$ to -0.2 µmol CO_2 $m^{-2}\cdot s^{-1}$ during the first 4 minutes and then falling down to -0.8 µmol CO_2 $m^{-2}\cdot s^{-1}$ in the last 4 minutes.

Panel B shows the respiratory responses induced in the *Plectranthus ecklonii* leaves by the recombinant AtPNP-A in the absence of light (0 µmol photons $m^{-2}\cdot s^{-1}$). Treatment of leaves with the recombinant AtPNP-A resulted in a rapid increase of their respiratory rates from 0.2 µmol CO_2 $m^{-2}\cdot s^{-1}$ to 5.9 µmol CO_2 $m^{-2}\cdot s^{-1}$ that lasted for 6 minutes followed by a 2-minute gradual decrease to 5.2 µmol CO_2 $m^{-2}\cdot s^{-1}$ as compared to respiratory rates of control leaves that only rose from 0.1 µmol CO_2 $m^{-2}\cdot s^{-1}$ to 1.4 µmol CO_2 $m^{-2}\cdot s^{-1}$ during the first 6 minutes that was then followed by a 2-

minute decrease to 0.9 µmol CO_2 $m^{-2}\cdot s^{-1}$. These results indicated that the recombinant AtPNP-A had the potential to induce leaf respiration in *Plectranthus ecklonii* leaves at their photosynthetic saturating light intensity level of 1300 µmol photons $m^{-2}\cdot s^{-1}$.

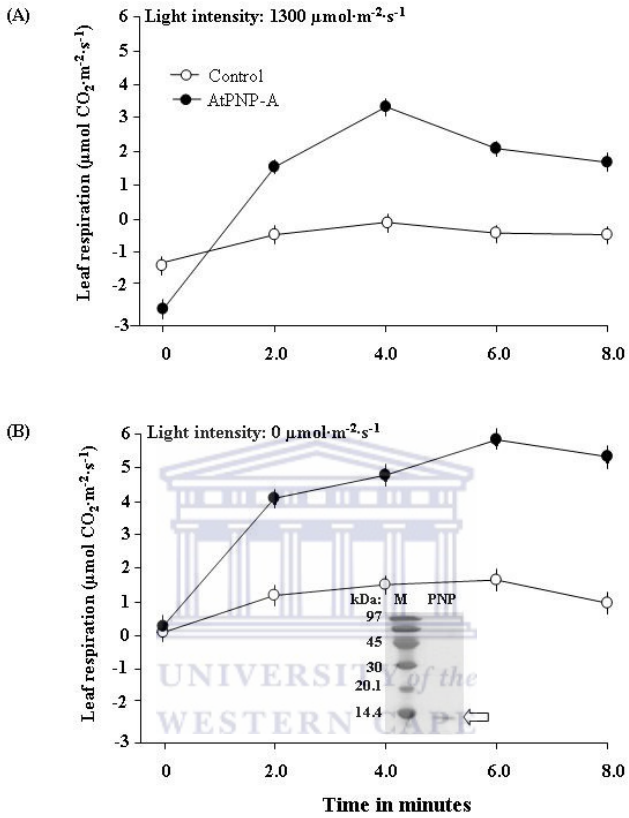

Figure 4.3: A comparison of recombinant AtPNP-A's potentials to induce leaf respiration in *Plectranthus ecklonii* in the presence and absence of light. *Plectranthus ecklonii* leaves were evenly treated on both surfaces with 50 µl of 100 µg/ml recombinant AtPNP-A (50 µl of H_2O for control leaves) followed by measurement and recording of respiratory responses at 1300 and 0 µmol photons $m^{-2}\cdot s^{-1}$ light levels at 2-minute intervals over a time period of 8 minutes. (**A**) Respiratory responses recorded at 1300 µmol photons $m^{-2}\cdot s^{-1}$ light levels. (**B**) Respiratory responses recorded at 0 µmol photons $m^{-2}\cdot s^{-1}$ light levels (dark respiration rate). Inset: SDS-PAGE of the recombinant AtPNP-A protein that was used in the assays, where (M) is the low molecular weight marker, while the arrow is marking the AtPNP-A. Error bars represent the standard errors (SE) of the means (n = 6) of the obtained respiratory responses as analyzed by ANOVA.

The ability of the recombinant AtPNP-A to induce leaf respiration in the presence of light was then exploited as a response signal to assess for the possible downward and/or upward systemic actions of this protein in *Plectranthus ecklonii*. A single leaf on the *Plectranthus ecklonii* plant was treated with 50 µl of 100 µg/ml recombinant AtPNP-A to initiate a respiratory response followed by measurement and recording of any possible transmitted respiratory responses in other leaves surrounding the treated leaf at 1300 µmol photons $m^{-2}\cdot s^{-1}$ light intensity level at different time intervals as is shown in Fig.4.4 below (for the measurement regimes, refer to Fig. 4.1).

Panels A, B and C show the respiratory responses recorded after 5, 10 and 15 minutes of leaf treatment respectively in leaves opposite, above and below the treated leaf and in relation to the respiratory responses induced in the treated control leaf itself. After 5 minutes of treating the control leaf with the recombinant AtPNP-A, a respiratory response of 0.4 µmol CO_2 $m^{-2}\cdot s^{-1}$ was only recorded in the lower leaf (Panel A), then after the next 5 minutes, respiratory responses of 3.2 µmol CO_2 $m^{-2}\cdot s^{-1}$ and 1.1 µmol CO_2 $m^{-2}\cdot s^{-1}$ were then recorded in the lower and upper leaves respectively (Panel B) and finally, after the next 5 minutes, respiratory responses of 3.1 µmol CO_2 $m^{-2}\cdot s^{-1}$, 1.0 µmol CO_2 $m^{-2}\cdot s^{-1}$ and 0.5 µmol CO_2 $m^{-2}\cdot s^{-1}$ were recorded in the lower, upper and opposite leaves respectively (Panel C). These results indicated that the respiratory response signals induced in the control leaf by the recombinant AtPNP-A were transmitted first to the lower leaf after 5 minutes, then to the upper leaf after 10 minutes and lastly to the opposite leaf after 15 minutes thereby proposing a systemic action for the recombinant AtPNP-A which could have been either along the phloem or xylem vessels (Cronshaw, 1981; Goodwin and Mercer, 1983; Oparka, 1990) of the *Plectranthus ecklonii* plant.

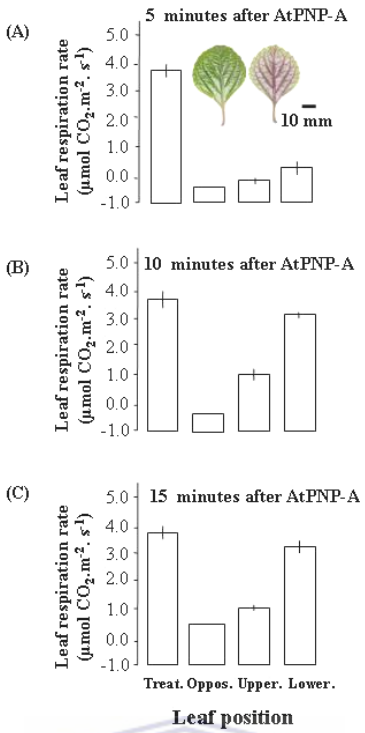

Figure 4.4: Assessment of the systemic action of recombinant AtPNP-A in *Plectranthus ecklonii*. A respiratory response signal was initiated in one *Plectranthus ecklonii* leaf by evenly treating its abaxial and adaxial surfaces with 50 µl of 100 µg/ml recombinant AtPNP-A followed by measurement of the transmitted respiratory response signals in leaves below, above and opposite the treated leaf at 1300 µmol photons $m^{-2} \cdot s^{-1}$ light intensity levels for 20 minutes at 5-minute intervals (for the treatment regime, also refer to Fig. 4.1). The bars represent the mean ± SE (n = 6) of the response signals detected after (**A**) 5 minutes, (**B**) 10 minutes and (**C**) 15 minutes in the three neighbouring leaves of the treated leaf and in comparison to the respiratory response signals generated by the treated leaf itself as analyzed by ANOVA.

Phloem transport in plants has been shown to be affected by cold or ice treatment (Webb, 1967; Giaquinta and Geiger, 1973; Lang and Minchin, 1986; Grusak *et al*., 1989; Hannah *et al*., 2001; Peuke *et al*., 2006), and in order to check and verify if the transmission of the AtPNP-A induced respiratory response signals in *Plectranthus ecklonii* were phloem-dependent, the experiment described in Fig. 4.4 above was repeated while part of the petiole segments of the three neighbouring leaves to the treated leaf were chilled down with ice-cold rings through cold girdling (for the chilling regime refer to Fig. 4.2).

Panels A and B show the respiratory responses obtained with and without chilling for the lower and upper leaves respectively. In the lower leaf, the detection of the respiratory response signals was delayed from 5 minutes to 10 minutes by chilling and after those 10 minutes, the strengths of the transmitted respiratory response signals were weakened from 1.9 µmol CO_2 $m^{-2}\cdot s^{-1}$ to 0.5 µmol CO_2 $m^{-2}\cdot s^{-1}$. In the upper leaf, the detection of the respiratory response signals was also delayed from 10 minutes to 15 minutes by the chilling effect and after those 15 minutes, the strengths of the transmitted respiratory response signals were also weakened from 1.5 µmol CO_2 $m^{-2}\cdot s^{-1}$ to 1.3 µmol CO_2 $m^{-2}\cdot s^{-1}$. The results therefore verified that the transmission of the AtPNP-A induced respiratory response signals in *Plectranthus ecklonii* from the treated leaf to its neighbouring leaves was indeed phloem-dependent.

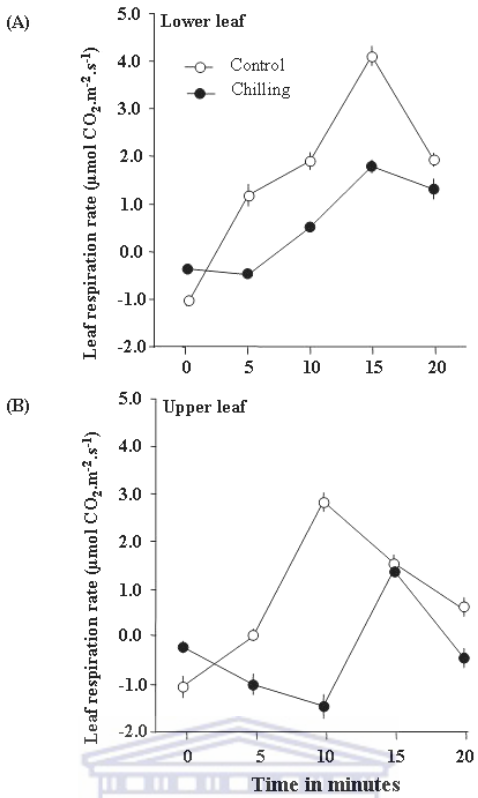

Figure 4.5: The effect of low temperature on transmission of recombinant AtPNP-A-induced respiratory response signals in *Plectranthus ecklonii*. The assay described in Fig. 4.4 above was repeated while parts of the leaf petiole segments of the three neighbouring leaves to the treated leaf were chilled down by placing ice cold rings around them (for the chilling regime, refer to Fig. 4.2). The effect of chilling was then assessed by comparing the respiratory response signals generated under chilling and those generated without chilling for the three neighbouring leaves. (**A**) Respiratory response signals detected with and without chilling in the lower leaf. (**B**) Respiratory response signals detected with and without chilling in the upper leaf. Error bars represent the standard errors (SE) of the means (n = 6) of the obtained respiratory response signals as analyzed by ANOVA.

Recombinant AtPNP-A was also assessed if it could induce net water transport in detached *Plectranthus ecklonii* leaves when applied on their petiole ends. A pair of leaves was detached from the *Plectranthus ecklonii* plant by cutting off the leaves with a sterile blade and ensuring that their petioles were of the same length. Relative net fresh weights of these leaves were then determined using an analytical balance (Cape Scientific Services, Cape Town, RSA). A petiole end of one leaf was immersed into an Eppendorf tube containing pre-weighed H_2O that was pre-treated with recombinant AtPNP-A to a final protein concentration of 100 µg/ml while the petiole end of the other leaf was immersed into an Eppendorf tube containing untreated pre-weighed H_2O (control). The settings were then left to stand for 2 hours at room temperature (24°C). Alongside this experiment, a positive control experiment was also set using a pair of detached *Plectranthus ecklonii* leaves whose relative net fresh weights were also noted. One leaf was evenly treated on its abaxial and adaxial surfaces with 50 µl of a 100 µg/ml recombinant AtPNP-A sample while the other leaf was also similarly treated with 50 µl sterile distilled H_2O (control). Petiole ends of the treated leaves were then separately immersed into Eppendorf tubes containing untreated pre-weighed H_2O and also left to stand for 2 hours at room temperature (24°C). At the end of the 2 hours, all leaves were then carefully removed from their respective tubes followed by a re-measurement of their respective tube H_2O weights. The relative net water transport for each leaf was then determined as the calculated difference between its initial and final tube H_2O weights expressed in ml/g fresh leaf weight and are presented in Fig. 4.6 below.

The results show that application of the recombinant AtPNP-A on the petiole ends of leaves could induce net water transport responses that were even higher than those

induced when the protein was applied on leaf surfaces. Water transport was increased from 0.1 ml·g^{-1} fresh leaf weight to 0.24 ml·g^{-1} fresh leaf weight after 2 hours in leaves treated with the recombinant AtPNP-A on petiole ends while for leaves treated with the recombinant protein on leaf surfaces, water transport was only increased from 0.1 ml·g^{-1} fresh leaf weight to 0.18 ml·g^{-1} fresh leaf weight and over the same time period. This outcome proposed an AtPNP-A signaling system in the *Plectranthus ecklonii* leaves that could have been along the phloem or xylem tissue (Cronshaw, 1981; Goodwin and Mercer, 1983; Oparka, 1990).

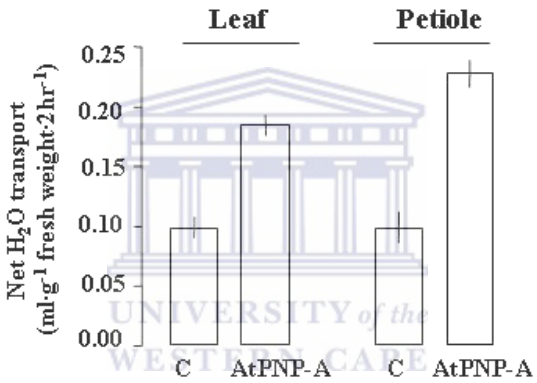

Figure 4.6: Assessment of the AtPNP-A's ability to induce net water transport in *Plectranthus ecklonii*. Two pairs of *Plectranthus ecklonii* leaves were detached from the plant followed by measurement of their net fresh weights with an analytical balance (Cape Scientific Services, Cape Town, RSA). The petiole end of one leaf from the first pair was then immersed into an Eppendorf tube containing pre-weighed water pre-treated with recombinant AtPNP-A to a final protein concentration of 100 µg/ml while the petiole end of the other leaf was immersed into an Eppendorf tube containing untreated pre-weighed water to act as a control. The settings were then allowed to stand for 2 hours at room temperature (24°C). As a positive control, one leaf from the second pair was evenly treated on both surfaces with 50 µl of 100 µg/ml recombinant AtPNP-A while the other leaf was also similarly treated with 50 µl of H_2O to act as a control followed by the immersing of their petiole ends into separate Eppendorf tubes contained pre-weighed water. The settings were also allowed to stand for 2 hours at room temperature (24°C). At the end of the 2 hours, all the leaves were then carefully removed from the tubes and their tube water re-weighed. Differences between their initial and final tube water weights were then considered as their relative net water transport capacities expressed in ml per gram fresh leaf weight. The bars represent the mean ± SE (n = 6) of the relative net water transport capacities for the different *Plectranthus ecklonii* leaves as analyzed by ANOVA.

In order to check and verify if the proposed recombinant AtPNP-A signaling system in *Plectranthus ecklonii* leaves was phloem-dependent, the experiment describing the protein's ability to induce net water transport when applied on petiole ends of leaves in Fig. 4.6 above was repeated while part of the petiole segments of all leaves were chilled down with ice-cold rings through cold girdling (for the chilling regime refer to Fig. 4.2). As is shown in Fig. 4.7 below, the chilling effect could significantly reduce net water transport in the *Plectranthus ecklonii* leaves from 0.24 $ml \cdot g^{-1}$ fresh leaf weight to 0.19 $ml \cdot g^{-1}$ fresh leaf weight over 2 hours, and thereby verifying a phloem-dependent AtPNP-A signaling system in the *Plectranthus ecklonii* leaves.

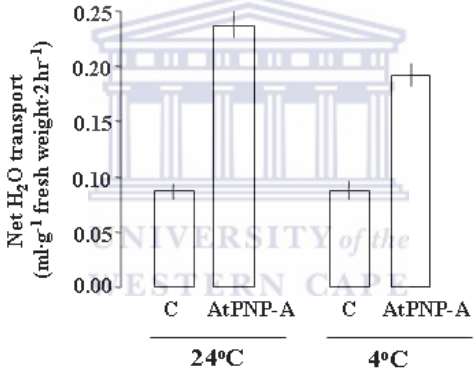

Figure 4.7: The effect of petiole chilling on the induction of net water transport by recombinant AtPNP-A in *Plectranthus ecklonii*. The assay described for the experimental pair of leaves in Fig. 4.6 above was repeated while part of the leaf petiole were chilled down with ice-cold rings through cold girdling (for the chilling procedure, refer to section 4.2.2.3). The relative net water transport capacities for the leaves were then calculated and the effect of chilling assessed by comparing their values with those obtained without chilling. The bars represent the mean ± SE (n = 6) of the relative net water transport capacities for the different *Plectranthus ecklonii* leaves as analyzed by ANOVA.

4.4 Discussion

One of the most important features that have allowed higher plants to withstand dry land conditions is the presence of the vascular system (xylem and phloem tissues) which transports water, photo-assimilates, nutrients and signals over long distances within the plants (Peuke *et al*., 2006). While the xylem functions mainly as an upward conductive tissue for water and minerals, the phloem tissue is responsible for the transport of metabolic products and for the recycling of mineral nutrients from the shoot to the root or within the shoot from mature leaves to younger growing parts (Peuke *et al*., 2006). The phloem can be divided into three functional areas; the loading phloem, the transport phloem and the unloading phloem (van Bel, 1993, 2003a, b). While the loading phloem is responsible for active loading of photo-assimilates into the phloem tissue, the unloading phloem delivers assimilates to sink tissues, and the transport phloem translocates water and solutes from source to sink tissues (van Bel, 1993, 2003a, b). In the transport phloem, which generally can be found from the main leaf veins downwards, release as well as loading (retrieval) of sugars take place and along the way, the transport phloem provides the surrounding tissues with assimilates for processes such as maintenance and growth (van Bel, 1993, 2003a, b; Lalonde *et al*., 2003; Gould *et al*., 2004).

Long-distance phloem transport within intact plant systems is especially difficult to measure because only few techniques are suitable and because of the extreme sensitivity of the phloem tissue to wounding (Peuke *et al*., 2006). Additionally, the small vessel sizes, the slow flow velocities and the small flowing volume per unit of cross-section make measurement of phloem flow a technically challenging enterprise (Peuke *et al*., 2006). In a number of studies, dyes or radioactive tracers are applied or

injected to investigate transport in the phloem (Patrick, 1997; Knoblauch and van Bel, 1998; Oparka and Turgeon, 1999; Komor, 2000). Currently, the method that has been most successful in providing detailed, non-invasive information on the characteristics of water transport in the phloem of intact plants is nuclear magnetic resonance (NMR) flow imaging.

Transport of assimilates in the phloem tissue has been shown to be affected by cold or ice treatment (Webb, 1967; Giaquinta and Geiger, 1973; Lang and Minchin, 1986; Grusak *et al*., 1989; Pickard and Minchin, 1990; Hannah *et al*., 2001), application of heat (Gould *et al*., 2004), vibrations (Minchin and Thorpe, 1984; Pickard and Minchin, 1990), as well as electric or osmotic shocking (Pickard and Minchin, 1990). In the case of cold treatment, the effect was found to be a 'reversible inhibition' and not a 'total stoppage' of the phloem transport (Giaquinta and Geiger, 1973; Lang and Minchin, 1986; Grusak *et al*., 1989; Hannah *et al*., 2001) due to the effect of low temperature on the physiological processes of active cells of the phloem tissue (Webb, 1967). For instance, cold girdling of the *Ricinus communis* hypocotyl using ice-cold water was demonstrated to inhibit phloem mass flow in less than 15 - 30 minutes from the time of cold treatment (Peuke *et al*., 2006). Thus cold treatment of the phloem can be used as a tool in plant physiology to verify phloem transport in plants.

In this study, a non-invasive technique that uses an infra-red gas analyser (IRGA) to measure respiratory responses in *Plectranthus ecklonii* leaves was used to demonstrate that the transmission of respiratory response signals initiated in one leaf through treatment with a biologically active recombinant PNP from *Arabidopsis thaliana* (AtPNP-A) to the other neighbouring leaves was systemic and time-

dependent (Fig. 4.4). Furthermore, when the same experiment was repeated while petiole segments of the neighbouring leaves to the AtPNP-A treated leaf were cold-girdled with ice-cold water, it was demonstrated that the chilling effect could significantly reduce the strengths and rates of signal transmission (Fig. 4.5). In addition, the same effects of cold-girdling leaf petioles with ice-cold water were also demonstrated on the transmission of AtPNP-A induced net water transport response signals in the same plant (Fig. 4.7). Taken together, these findings firstly, demonstrated a systemic mode of action for the recombinant AtPNP-A in *Plectranthus ecklonii*, and secondly, confirmed that such a systemic action was phloem-dependent.

Evidences obtained in this study may suggest two possible ways through which the AtPNP-A induced response signals could be transmitted in the phloem of *Plectranthus ecklonii*; either as an AtPNP-A-dependent messenger or as AtPNP-A itself. There is evidence that suggests that proteins can move in the phloem. Firstly, a number of non-cell-autonomous proteins (NCAPs) with molecular weights ranging from 43 kDa to more than 100 kDa have been identified in the phloem saps of several angiosperms (Lough and Lucas, 2006; Turgeon and Wolf, 2009) that include *Cucurbita maxima* (Balachandran *et al*., 1997; Walz *et al*., 2004; Petersen *et al*., 2005), *Ricinus communis* (Schobert *et al*., 2000), wheat (Fisher *et al*., 1992), lupin (Marentes and Grusak, 1998) and several monocotyledonous and dicotyledonous plants (Schobert *et al*., 1998). Secondly, PNPs have been shown to be associated with the phloem tissues of *Hedera helix* and *Solanum tuberosum* as was demonstrated by *in situ* immunoreactivity and immunofluorescence assays of *Hedera helix* and *Solanum tuberosum* probed with anti-human atrial natriuretic peptide antibodies and

anti-potato natriuretic peptide antibodies respectively (Maryani *et al*., 2003). Lastly, PNP has recently been identified in differentiating phloem tissues of *Arabidopsis thaliana* leaves and inflorescence stems using a microarray analyses approach that was based on a predicted increase in vascular-related gene expression in response to an auxin transport inhibitor-induced vascular overgrowth (Wenzel *et al*., 2008).

Previous evidence has suggested a facilitated and regulated protein movement into sieve elements from the neighbouring companion cells through modification of the plasmodesmata that interconnect the two tissues (Balachandran *et al*., 1997; Turgeon and Wolf, 2009). This modification of the plasmodesmata might facilitate movement of recombinant AtPNP-A into the phloem after uptake from the leaf surfaces (possibly through the stomata) via the apoplatic space in the experiment described here (Fig.4.4). AtPNP-A has previously been identified in the apoplastic fluid of Arabidopsis rosettes using a proteomic and bioinformatic approach (Boudart *et al*., 2005) thus reaffirming its extracellular location which is a precondition to a systemic mode of action. AtPNP-A signaling may also have occurred through an autocrine effect of the molecule, where its application on the leaf cells could have induced the expression of more AtPNP-A, which then may have moved into the phloem tissue to affect the observed long-range effect.

By combining all the information generated in this study with information already known on PNPs in plants, a general model on the role and action of these peptides can be proposed Fig. 4.8 (adapted after Meier *et al*., 2008a).

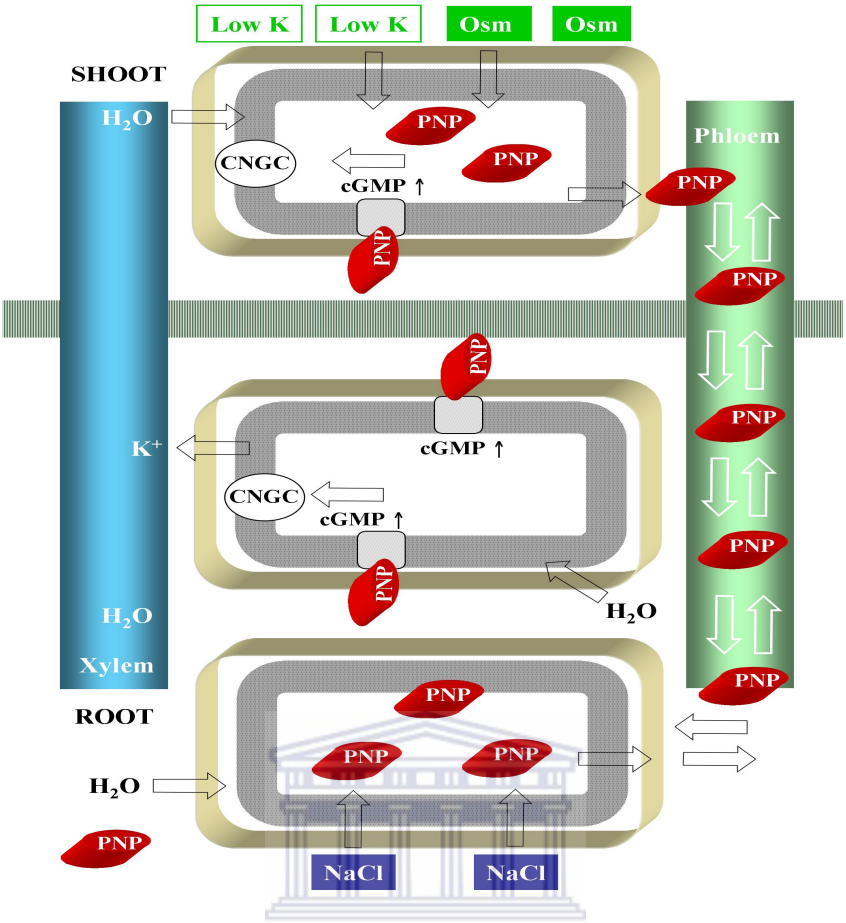

Figure 4.8: A proposed model for the systemic mode of action for PNPs in plants. The model is essentially based on data from *Arabidopsis thaliana* and represents two major spatial components, the root and the shoot and proposes that AtPNP-A plays a role in the signaling between the two. The root/shoot boundary is indicated by a horizontal bar. The xylem (blue) functions mainly as a conductive tissue for water and minerals from the roots to the stems and leaves. The phloem (light green) transports nutrients as well as organic molecules like PNPs down from the leaves to the stems and roots and also up from the roots to the stems and leaves. The AtPNP-A transcription inducing stresses are NaCl in the root and low K^+ and high osmotic pressure in the shoot. Proposed specific PNP receptors are the light grey boxes where the binding of the protein is proposed to increase cGMP levels, which in turn affects various cellular processes notably, the regulation of cyclic nucleotide-gated channels (CNGCs), K^+ release and activation of aquaporins. (Figure modified after Meier *et al.*, 2008a).

We propose that in order to gain further insights into the mode of action of the recombinant AtPNP-A, a number of additional experiments need to be performed and they will make use of radioactively or fluorescently labeled AtPNP-A to trace the molecule *in vivo* and *in planta*.

Chapter 5

A Recombinant Wall-associated Receptor Kinase-like Molecule has *in vitro* Guanylate Cyclase and Kinase Activities and a Role in Plant Defense Mechanisms

Abstract

Plants, like animals, also possess functional guanylate cyclases (GCs) that are crucial for several signaling transduction pathways. When the first plant GC (AtGC1) was discovered in *Arabidopsis thaliana*, another potential GC candidate belonging to a family of wall associated kinase-like molecules (WAKLs) was also identified. This molecule, termed AtWAKL10, had a domain organization resembling that of vertebrate natriuretic peptide receptors (having an extracellular ligand-binding domain and an intracellular guanylate cyclase/kinase domain). This resemblance in domain organization between these two molecules also suggested for a functional homology between them and furthermore, proposing AtWAKL10 to be a potential plant natriuretic peptide receptor. Based on these two ideas, we therefore prepared a biologically active recombinant form of AtWAKL10 and demonstrated that this molecule could function as a GC and a kinase *in vitro* (bi-functional) with a role in plant pathogen-defense mechanisms.

5.1 Introduction

Vascular plants possess a specialised class of protein molecules that are known to physically link the extracellular matrix to the plasma membranes and thus facilitating communication between the two compartments (Kohorn, 1999, 2000). These include

cellulose synthases (Pear *et al*., 1996), a class of arabinogalactan proteins that are reversibly attached to the plasma membrane via a glycosyl phosphatidyl inositol anchor (Oxley and Bacic, 1999; Svetek *et al*., 1999), pectines, which are glycolytic enzymes with transmembrane domains (Nicol *et al*., 1998), and wall-associated kinases (WAKs) (He *et al*., 1996; He *et al*., 1999; Anderson *et al*., 2001). These molecules do not only physically link the extracellular matrices to the plasma membranes but can also act as communicating signal transducers. Communication between the cytoplasm and the cell wall is essential during processes such as cell expansion during elongation growth (Cosgrove *et al*., 1997) as well as during pathogen infection. These processes would normally lead to altered biosynthesis and modifications of the cell wall components that are accompanied with downstream cytoplasmic events such as systemic acquired resistance (Kohorn, 1999).

WAKs represent a unique group of receptor-like molecules, whose an N-terminus domain is tightly linked to the cell wall, followed by a transmembrane domain that separates the extracellular sequence from the intracellular carboxyl cytoplasmic serine/threonine protein kinase domain (He *et al*., 1996). Their extracellular domain is similar in organization to those of vertebrate epidermal growth factors (EGF)-like molecules (He *et al*., 1996). WAK structure strongly suggests a role in cell wall-membrane binding and signalling systems (Anderson *et al*., 2001; Kohorn, 2001). Amino acid variability within the N-terminus domains of most WAK isoforms may be indicative of their distinct interactions with various cell wall components (He *et al*., 1996). Similarly, amino acid identity among their kinase domains also suggests that they may elicit similar cytoplasmic events (He *et al*., 1996).

Different WAK isoforms (WAK 1-5) are expressed in different and specific plant organs such as root apical meristems, expanding leaves, organ junctions, and shoot apical meristems (He *et al*., 1999). WAK expression occurs in response to various biotic and abiotic stimuli, thus suggesting that this family of proteins may serve to mediate fundamental processes that depend on cell wall and plasma membrane interactions (He *et al*., 1999). To date, WAKs have been shown to be involved in pathogen-related responses and defence-related signalling in angiosperms (He *et al*., 1998; Maleck *et al*., 2000b), where their induction is necessary for plants to survive high levels of salicylic acid (SA) (He *et al*., 1998). Perhaps not surprisingly, WAKs have also been linked to cell expansion and elongation in Arabidopsis (Lally *et al*., 2001; Wagner and Kohorn, 2001).

Reiterative database searches (BLAST) that used the *WAK1* cDNA or WAK1 protein sequences as a query, identified a family containing 22 genes in Arabidopsis that were closely related to *WAK*s (Verica and He, 2002). These sequences were then referred to as *WAK*-like genes (*WAKL*s 1-22) (Shiu and Bleecker, 2001b, a, 2003). Of the 22 *WAKL* genes, five were predicted to exclusively encode WAKL proteins, while the remaining 17 were found to share similar intron-exon organizations with the *WAK*s, where each had three exons and two introns (Verica and He, 2002). These 17 *WAKL* genes together with the 5 known *WAK* genes (He *et al*., 1999) could be divided into four separate groups based on pair-wise comparisons of their predicted protein sequences (Verica and He, 2002). It is conceivable that the large number of genes in this family may provide plants with a potential to recognize and respond to a diverse types of ligands (Verica and He, 2002) under pathogen attacks or a continuously changing cell wall environment.

We have latetly proposed a catalytic domain search motif based on residues with defined roles in catalysis of guanosine 5′-triphosphate (GTP) to guanosine 3′,5′-cyclic monophosphate (cGMP) and identified a number of candidate guanylate cyclases (GCs) (Ludidi and Gehring, 2003). One of these is a wall associated kinase-like protein (WAKL10; At1g79680). Here we show that a biologically active recombinant WAKL10 molecule from *Arabidopsis thaliana* (AtWAKL10) functions as a GC and a kinase *in vitro* with a role in plant defense mechanisms.

5.2 Material and Methods

5.2.1 Search Motif

The search motif that was used for the identification of AtWAKL10 was designed based on conserved and functionally-assigned amino acids found in the catalytic centres of annotated and known prokaryotic and eukaryotic GCs (Ludidi and Gehring, 2003). Several guanylate cyclases were retrieved from NCBI followed by alignment of their catalytic domains using Clustal X (Thompson *et al*., 1997). Alignments at the catalytic centres of their catalytic domains were then used to derive the search motif. The derived search motif was then tested for its accuracy and specificity to detect nucleotide cyclases by querying the Protein Information Resource (www.nbrf.georgetown.edu) using the Pattern Match option on the PIR-NREF link. The confirmed search motif was finally used to query the Arabidopsis Information Resource database (www.arabidopsis.org) and GenBank using the Patmatch link in The Arabidopsis Information Resource (Altschul *et al*., 1997).

5.2.2 Preparation and Cloning of the AtWAKL10 Insert

The AtWAKL10 insert was prepared from *Arabidopsis thaliana* cDNA where total RNA was extracted from 3 week old *Arabidopsis thaliana* ecotype Col. seedlings using the RNeasy plant mini kit (Qiagen) in combination with DNase treatment using an RNase-free DNase Set (Qiagen) as instructed by the manufacturer. The AtWAKL10 cDNA was then synthesised from the total RNA through reverse transcriptase polymerase chain reaction (RT-PCR) where amplification was performed with the specific primers (forward) 5′GAT ATC GGA TCC GCT CAA GGA AAA GCT GTC TAT TAC G 3′ incorporating a *Sac* I restriction site and (reverse) 5′ACT AAG AAG CTT TTA CGG TGT GTA TAC GAC ACG AAT G 3′ incorporating a *Xho* I restriction site using the Access RT-PCR System (Promega) as instructed by the manufacturer. The PCR product was then cloned into the cloning site of a pCRT7/NT-TOPO vector (Invitrogen) to produce a pCRT7/NT-TOPO-AtWAKL10 fusion expression construct with an N-terminal 6xHis purification tag. The clone was then maintained in TOPO10 F′ *Escherichia coli* cells (Invitrogen). Single colonies of these cells were selected with their clones virtually analyzed and confirmed by DNA sequencing.

5.2.3 Protein Expression

For expression of the recombinant AtWAKL10, *E. coli* BL 21 Star pLys S cells (Invitrogen) were transformed with the pCRT7/NT-TOPO-AtWAKL10 construct and grown in double strength yeast-tryptone media containing 100 µg/ml ampicillin and 34 µg/ml chloramphenicol on an orbital shaker at 200 rpm at 37°C. The expression of the recombinant was then induced by adding 1 mM isopropyl-β-D-

thiogalactopyranoside (IPTG) at an optical density (OD_{600}) of 0.6 of the cell culture. The induced cultures were then left to grow for a further 3 hours at 37°C.

5.2.4 Cyclic Nucleotide Assays

To determine the *in vivo* activity of the recombinant AtWAKL10, its expression profile outlined in section 5.2.3 above was repeated and when the cell culture was at an optical density (OD_{600}) of 0.5, 1 mM IPTG together with 1 mM 3-isobutyl-1-methyl xanthine (IBMX) were then added followed by a further incubation for 3 hours at 37°C. While IPTG was added to induce protein expression, IBMX was added to inhibit cGMP degradation by phosphodiesterases. At the end of the 3 hours, cGMP was extracted from the induced cells following an extraction procedure for suspension cells as is described in the cGMP enzymeimmunoassay Biotrak (EIA) system (Amersham Biosciences, Little Chalfont, UK). The extracted cGMP was then measured by a cGMP enzymeimmunoassay Biotrak (EIA) system based on the acetylation protocol as is described in the manufacturer's manual (Amersham Biosciences, Little Chalfont, UK).

To determine the activity of this recombinant protein *in vitro*, the AtWAKL10 protein expressed by the transformed *E. coli* BL 21 Star pLys S cells (Invitrogen) as a result of IPTG induction (section 5.2.3), was first purified followed by its assessment for the GC activity. The expressed protein was purified on an Ni-NTA affinity system (Qiagen) under denaturing conditions and refolded with an FPLC-linked linear gradient system as is described in sections 2.2.4 and 2.2.5 of Chapter 2 of this thesis (The QIAexpressionist, 2003). Protein activity was then assessed by adding 1.0 µg purified recombinant AtWAKL10 into a reaction system containing 50 mM Tris-HCl;

pH 8.0, 2 mM IBMX, 5 mM Mg^{2+} and/or 5 mM Mn^{2+} and 1 mM GTP followed by incubations at room temperature for time intervals of between 0 to 20 minutes. At the end of each selected time point, reactions were terminated by adding 4 mM EDTA and rapid chilling at 4°C for 10 minutes. The terminated reactions were then clarified through centrifugation at 14 500 rpm for 10 minutes. The respective supernatants were then collected and their cGMP product levels measured by enzymeimmunoassay Biotrak (EIA) system based on the acetylation protocol as is described in the manufacturer's manual (Amersham Biosciences, Little Chalfont, UK). The effect of 1 mM ATP (as an additive to the reaction system) on the GC activity of this recombinant protein was also assessed and determined with the same assaying system.

Although the anti-cGMP antibody in the enzymeimmunoassay system is known to be highly specific for cGMP with an approximately 10^6 times lower affinity for cAMP, it was sought to verify this method with mass spectrometry, a method capable of specifically and sensitively detecting cGMP levels at fentomolar concentrations. Therefore, a Waters API Q-TOF Ultima mass spectrometer (Waters Microsep, Johannesburg, South Africa) that was capable of detecting cGMP in its acetylated form followed by the interpretation of results in the W-mode was used. Samples were introduced into the machine with a Waters Acquity UPLC at a flow rate of 180 ml/min. Separation was then achieved in a Phenomenex Synergi (Torrance, CA) 4 µm Fusion-RP (250 x 2.0 mm) column when a gradient of solvent ''A'' (0.1% (v/v) formic acid) and solvent ''B'' (100% (v/v) acetonitrile) was applied over 18 minutes. During the first 7 minutes, the solvent composition was kept at 100% (v/v) ''A'' followed by a linear gradient of up to 80% (v/v) ''B'' for 3 minutes, and then a re-equilibration to the initial conditions. An electrospray ionisation in the negative mode

was used at a cone voltage of 35 V resulting in the detection of molecules with the ultimate generation of the respective mass chromatograms.

5.2.5 Kinase Assays

The kinase activity for the recombinant AtWAKL10 were assessed *in vitro* by measuring its ability to direct the phosphorylation of a special substrate peptide as described in the Omnia™ Ser/Thr-Recombinant Kit (BioSource). A 50 µl reaction system containing 0.1 ng purified recombinant AtWAKL10, 1x reaction buffer, 1 mM ATP, 0.2 mM DTT, and 25 µM Ser/Thr-peptide was prepared. This was followed by an instant measurement of the phosphorylation activity in form of fluorescence signals at 460 nm (λ_{em} 460) after a reaction excitation at 360 nm (λ_{ex} 360). All activity readings were recorded in form of relative fluorescence units (RFUs) on a Modulus Microplate Reader (Turner BioSystems) after every 1 minute over a 60-minute time range at 30°C. The effects of 1 mM GTP and 1 µM cGMP (as separate additives to the reaction system) on the kinase activity of the recombinant AtWAKL10 were also assessed and ascertained with the same assaying system. Furthermore, GTP was also tested as a possible substrate for the kinase domain of this recombinant protein.

5.2.6 Analysis of Pathogen Responses and Defense Mechanisms

The role of AtWAKL10 in pathogen response mechanisms was determined using a bioinformatics approach as described by Meier and Gehring (2008). The approach is based on the fact that since it is well established that genes do not function alone but in networks that function coherently to achieve a common biological response, then inferences into the functional roles of individual genes can be gained by their association with other genes with more precisely defined functions (Meier and Gehring, 2008). It involved the use of a sequential web-based tool termed "Genevestigator" (www.genevestigator.ethz.ch) that integrates information from different databases followed by the association of the function of the *AtWAKL10* with a network of those genes and additionally, by identifying the specific biological processes in which all such genes collectively function (Meier and Gehring, 2008).

The analysis was performed across all of the 322 available Ath1 22K microarrays from the NASC/GARNet dataset which contains probe sets that recognise 21 891 Arabidopsis genes and thus providing a more complete representation of the Arabidopsis genome than the alternative 8K chip. In brief, the approach began by performing a global gene expression correlation analysis of the *AtWAKL10* to identify those other genes whose expression was most strongly correlated with its expression. In doing so, its expression correlated gene group (ECGG) was established. This ECGG was then subjected to a gene ontology (GO) analysis, stimulus specific expression analysis and promoter content analysis. By doing so, the process therefore managed to link the *AtWAKL10* with the other plant genes with which it was commonly co-expressed and at the same time, identifying the specific conditions that could commonly induce the expression of its ECGG. Furthermore, the process could

also identify the putative regulatory elements that were enriched in the promoters of the ECGG and thus could most likely be responsible for coordinating their common transcriptional responses. All the retrieved expression responses for the *AtWAKL10* were finally presented as microarray expression profiling data from where further insights were then deduced.

5.3 Results

An alignment of representative catalytic domains of annotated guanylate cyclases from different prokaryotes and eukaryotes was used to derive a 14-mer search motif (Fig. 5.1A) (Ludidi and Gehring, 2003) that was later used to identify AtWAKL10 using a "Patmatch" link to search the Arabidopsis genome database. When a replacement of a glycine residue at the functionally unassigned but conserved position in the catalytic centre of the search motif was permitted, the blast search returned seven candidates (Ludidi and Gehring, 2003) of which one was AtWAKL10 (Fig. 5.1B). Amino acid sequence analysis of known guanylate cyclases through alignment of their catalytic domains revealed that most annotated GCs had a glycine-rich N-terminal domain of the catalytic centre (Ludidi and Gehring, 2003). However, AtWAKL10 did not contain this characteristic domain and a close analysis of its structural organization further revealed that its GC domain was embedded within its kinase domain (Fig. 5.1C).

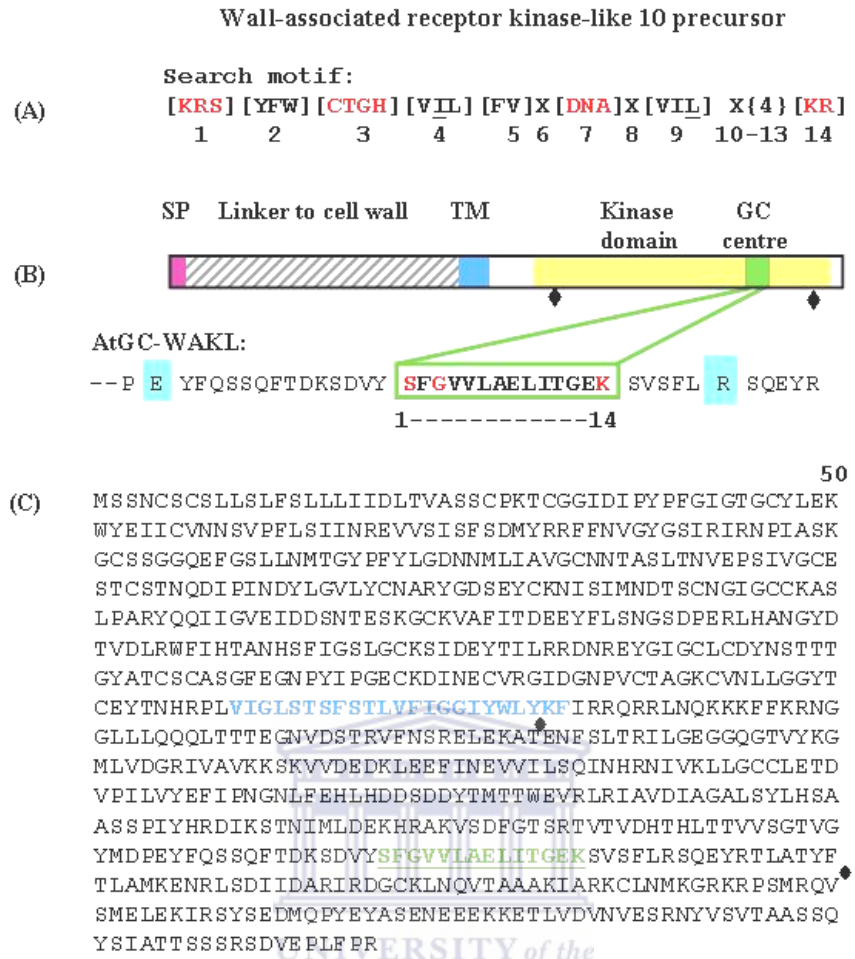

Figure 5.1: Structural features of the AtWAKL10 domain organization. (**A**) The 14 amino acid long search motif generated based on conserved and functionally-assigned amino acids in the catalytic centres of annotated GCs. Amino acid substitutions in the search motif are in square brackets ([ ]); X represents any amino acid and curly brackets ({ }) define the number of amino acids. Red amino acids are functionally assigned residues [1: Arg or Lys does the hydrogen bonding with the guanine; 3: Cys confers substrate specificity for GTP; 7: Asp, Asn or Ala binds to the dimer interphase (GTP/cGMP); 14: Arg or Lys stabilizes the transition state from GTP to cGMP and the 16: Glu implied in Mg^{2+}/Mn^{2+}-binding is not included in the search motif and is not always conserved] of the catalytic centre. The underlined amino acids in positions 4 and 9 are the third branched aliphatic amino acids that were not appearing in the alignment. (**B**) Representation of the domain organisation of AtWAKL10 containing a signal peptide (SP), linker to the cell wall, a transmembrane domain (TM), and a GC centre embedded in the kinase domain. The two black diamonds demarcate part of the kinase domain bearing the GC domain that was cloned into pCRT7/NT-TOPO vector for expression of the recombinant AtWAKL10. (**C**) Predicted amino acid sequence of AtWAKL10. The blue region represents the transmembrane domain that separates the extracellular domain from the intracellular domain. Sequences demarcated by the two diamond arrows represent the section that was expressed as a His-tagged AtWAKL10 fusion protein in the pCRT7/NT-TOPO expression vector. The expressed recombinant AtWAKL10 contains the GC domain (green) which is also imbedded into a kinase domain (Ludidi and Gehring, 2003).

Further analysis of the AtWAKL10 showed that its domain organization shared sequence homology with natriuretic peptide receptors (Fig. 5.2) (Ludidi and Gehring, 2003). These receptors have an extracellular ligand-binding domain and an intracellular guanylate cyclase/kinase domain (Maack, 1992).

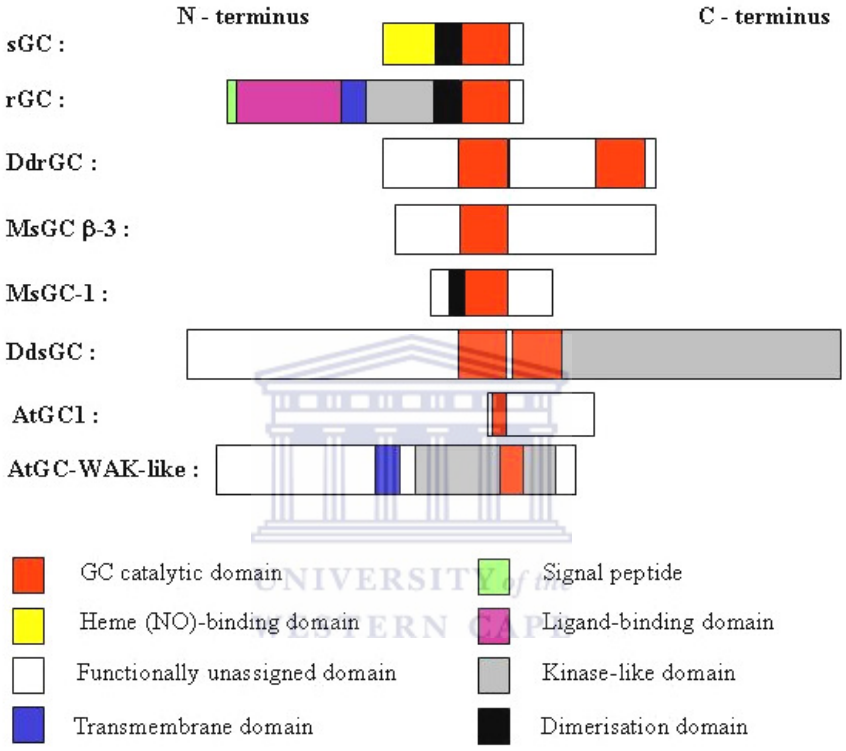

Figure 5.2: Comparison of domain organizations among different types of guanylate cyclases. Besides carrying features that allows it to physically link the extracellular matrix to the plasma membrane and modulating the diverse signaling pathways in plants, recombinant AtWAK10 also possesses a GC domain that makes it considered as a guanylate cyclase (Figure modified after Ludidi and Gehring, 2003).

Although WAKL10 does not contain the N-terminal glycine-rich domain of most annotated GCs, it seems possible that with its resemblance in domain organization to natriuretic peptide receptors (Maack, 1992; Ludidi and Gehring, 2003), it might also have functional homologies with them. These receptors operate through the functions of their GC domains (Garbers, 1991a, b; Koller and Goeddel, 1992; Garbers and Lowe, 1994) that are capable of generating cGMP from GTP. Therefore, in order to

determine whether AtWAKL10 was in fact a GC, amino acids 432 to 700 (containing the GC domain) were cloned and expressed in a prokaryotic system followed by the assessment of its *in vivo* GC activity. The expression system yielded a recombinant His-tagged fusion protein of the correct predicted molecular mass of 32 kDa (Fig. 5.3 A) while the activity assays revealed significantly higher levels of cGMP (2.36-fold) in induced cultures (2600 fmol cGMP/g fresh cell weight) than in uninduced cultures (1100 fmol cGMP/g fresh cell weight) (Fig. 5.2B) thereby indicating a functional GC activity for the recombinant AtWAKL10.

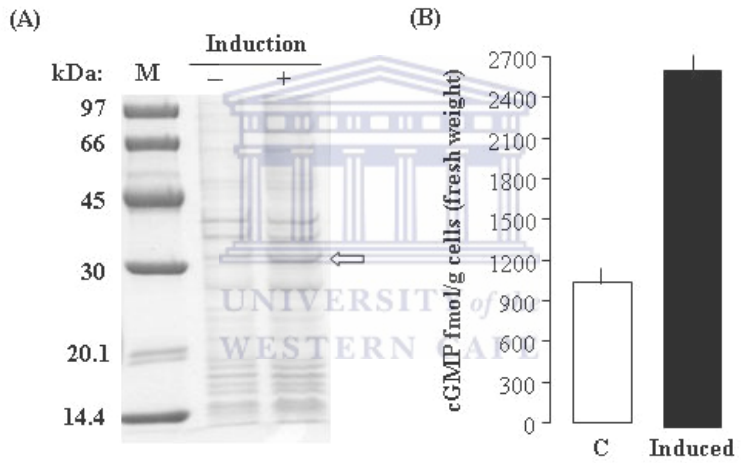

Figure 5.3: Expression of AtWAKL10 as a His-tagged recombinant fusion protein in *E. coli* and determination of its *in vivo* GC activity. (**A**) SDS PAGE of uninduced (-) and induced (+) *E. coli* BL 21 Star pLys S cell cultures (Invitrogen) transformed with the pCRT7/NT-TOPO-AtWAKL10 construct. The arrow marks the expressed recombinant AtWAKL10 and (M) is the low molecular weight marker. (**B**) Cyclic GMP levels generated with the uninduced (control) and induced cell cultures as determined by enzymeimmunoassay Biotrak (EIA) system (Amersham Biosciences, Little Chalfont, UK). The values represent the means of three experiments, with standard error bars and as analyzed by ANOVA.

After getting an indication that there was *in vivo* GC activity in recombinant AtWAKL10, its *in vitro* GC activity was also assessed. In order to determine the *in vitro* GC activity of the recombinant AtWAKL10, the expressed recombinant fusion protein was first extracted from the bacterial cells, purified on an Ni-NTA affinity system (Qiagen) under denaturing conditions and refolded with an FPLC-linked linear

gradient system as has been previously described (see sections 2.2.4-2.2.5 of Chapter 2) (QIAexpressionist, 2003) before being tested for the GC activity. Fig. 5.4A below shows an SDS-PAGE of the purified and refolded recombinant AtWAKL10 while Fig. 5.4B shows its associated *in vitro* GC activity as was determined by an enzymeimmunoassay Biotrak (EIA) system (Amersham Biosciences, Little Chalfont, UK). Over the experimental time period of 20 minutes, the purified recombinant AtWAKL10 showed a higher GC activity of up to 170 fmol cGMP/µg protein with Mg^{2+} as its cofactor than with Mn^{2+} where the GC activity was only of up to 60 fmol cGMP/µg protein (Fig. 5.4B).

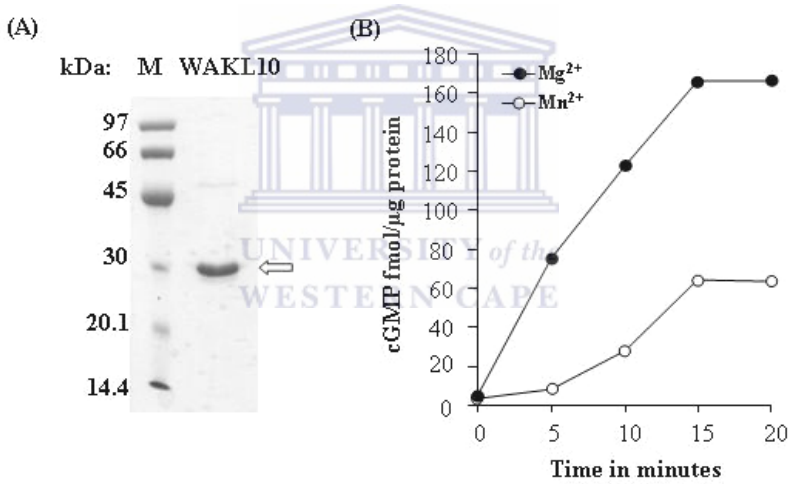

Figure 5.4: Determination of the *in vitro* GC activity of the recombinant AtWAKL10. (**A**) SDS-PAGE of the purified and refolded recombinant AtWAKL10, where (M) represents the low molecular weight marker while the arrow is marking the recombinant protein. (**B**) Cyclic GMP levels generated with 1 µg of the purified recombinant AtWAKL10 in a reaction system containing 50 mM Tris-HCl; pH 8.0, 1 mM GTP, 2 mM IBMX, and in the presents of either 5 mM Mg^{2+} or 5 mM Mn^{2+} as determined by enzymeimmunoassay Biotrak (EIA) system (Amersham Biosciences, Little Chalfont, UK). The values represent the means of three experiments, with standard error bars and as analyzed by ANOVA.

In order to validate the enzymeimmunoassay-based results obtained from both the *in vivo* and *in vitro* assays above, a further analysis of the *in vitro* samples was undertaken using mass spectrometry. As is shown in Fig. 5.5 below, this second method could also confirm the presence of cGMP in the samples thereby verifying a GC function for the recombinant AtWAKL10.

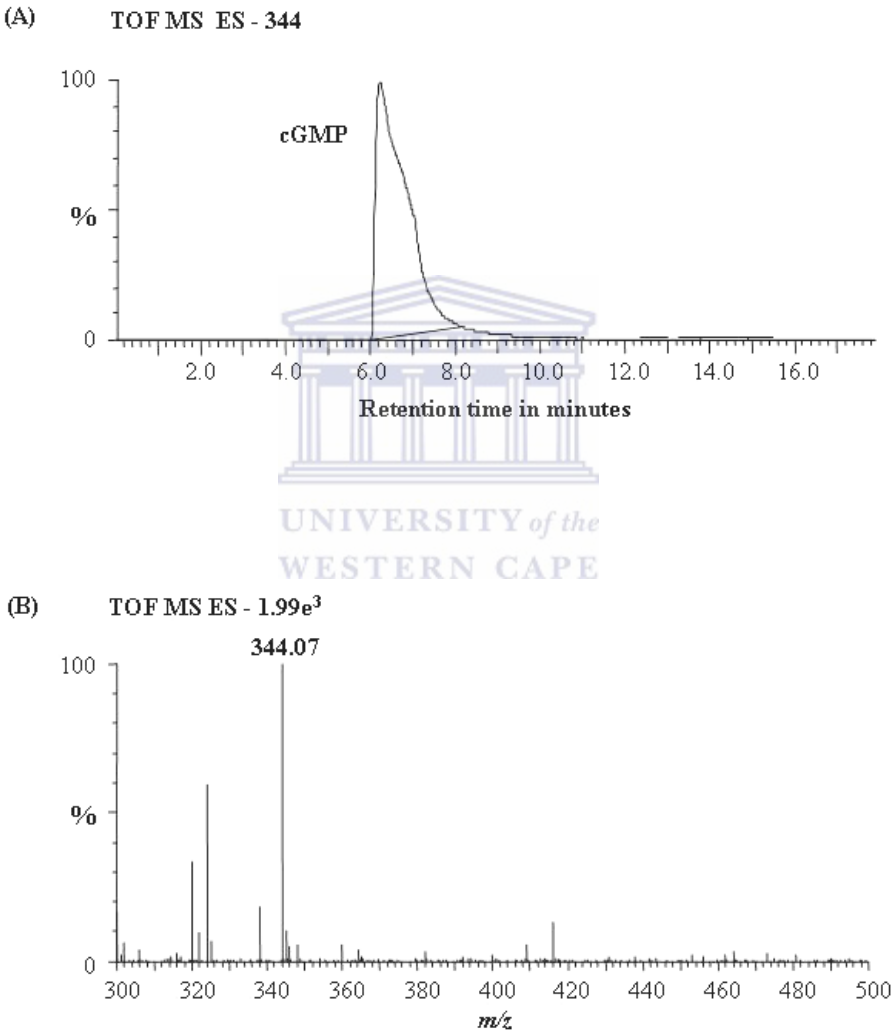

Figure 5.5: Determination of the *in vitro* GC activity of recombinant AtWAKL10 by mass spectrometry. The cGMP was generated from a reaction system containing 50 mM Tris-HCl; pH 8.0, 1 µg recombinant AtWAKL10, 1 mM GTP, 2 mM IBMX, and 5 mM Mg^{2+} after an incubation period of 20 minutes at room temperature. (**A**) An extracted mass chromatogram of the *m/z* 344 $[M-1]^{-1}$ ion of cGMP and (**B**) the resultant mass of the chromatogram peak as was generated by a Waters API Q-TOF Ultima mass spectrometer (Waters Microsep, Johannesburg, RSA).

Since the GC domain of the recombinant AtWAKL10 is imbedded into its kinase domain, it was therefore sought to find out if presence of ATP (a substrate for the kinase domain) could have any effects on the enzymatic activity of its GC domain. The GC assays were therefore carried out in the presence of an equimolar concentration of ATP to GTP, and as is shown in Fig. 5.6 below, the presence of ATP in a GC reaction had an inhibitory effect on the GC activity of the recombinant AtWAKL10. After 20 minutes of the experimental time period, the GC activity of the recombinant AtWAKL10 was reduced from 170 fmol cGMP/µg protein to 40 fmol cGMP/µg protein with Mg^{2+} as the cofactor for enzymatic activity and from 65 fmol cGMP/µg protein to 30 fmol cGMP/µg protein with Mn^{2+} as the cofactor.

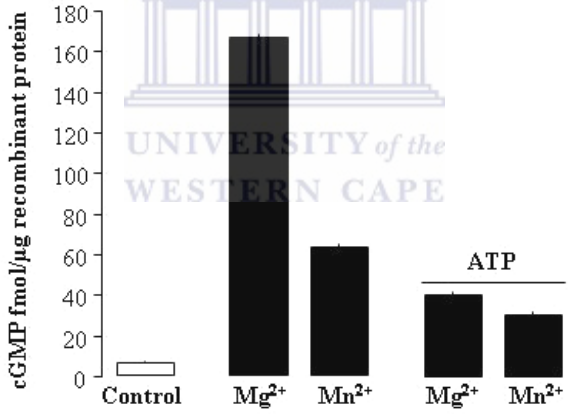

Figure 5.6: Effects of ATP on the GC activity of recombinant AtWAKL10. 1 mM ATP was added to reaction systems containing 50 mM Tris-HCl; pH 8.0, 1 µg recombinant AtWAKL10, 1 mM GTP, 2 mM IBMX, and 5 mM Mg^{2+} or 5 mM Mn^{2+} followed by an incubation at room temperature for 20 minutes. Alongside this experiment, other reaction systems containing 50 mM Tris-HCl; pH 8.0, 1 µg recombinant AtWAKL10, 1 mM GTP, 2 mM IBMX, and 5 mM Mg^{2+} or 5 mM Mn^{2+} were also set. A reaction control system containing 50 mM Tris-HCl pH 8.0, 1 mM GTP, 2 mM IBMX, and 5 mM Mg^{2+} and 5 mM Mn^{2+} only was also set. Cyclic GMP levels generated by each of the reaction systems were then measured by enzymeimmunoassay Biotrak (EIA) system (Amersham Biosciences, Little Chalfont, UK). The values represent the means of three experiments, with standard error bars and as analyzed by ANOVA.

After determining the GC activity for the recombinant AtWAKL10, its kinase activity was also assessed using an *in vitro* Omnia™ Ser/Thr-Recombinant system (BioSource) as is shown in Fig. 5.7 below. Fig. 5.7A shows the optimum calibration curve for the kinase activity that was obtained over 8 minutes with 0.1 ng recombinant AtWAKL10. Fig. 5.7B shows the levels of kinase activities obtained with the 0.1 ng recombinant AtWAKL10 and controls over a 60-minute reaction time, where the level of protein activity was 2.67-fold (4800 RFUs) more than in controls (1800 RFUs). Fig. 5.7C represents the reaction kinetics that were associated with the kinase activity of the 0.1 ng recombinant AtWAKL10 described in Panel B, where the recombinant protein had a V_{max} value of approximately 2269.74 nmoles/min/mg protein and a K_m value of around 2.66 µM. The results therefore showed that besides possessing a functional GC domain, the recombinant AtWAKL10 also had a functional kinase domain thus making it a bifunctional molecule.

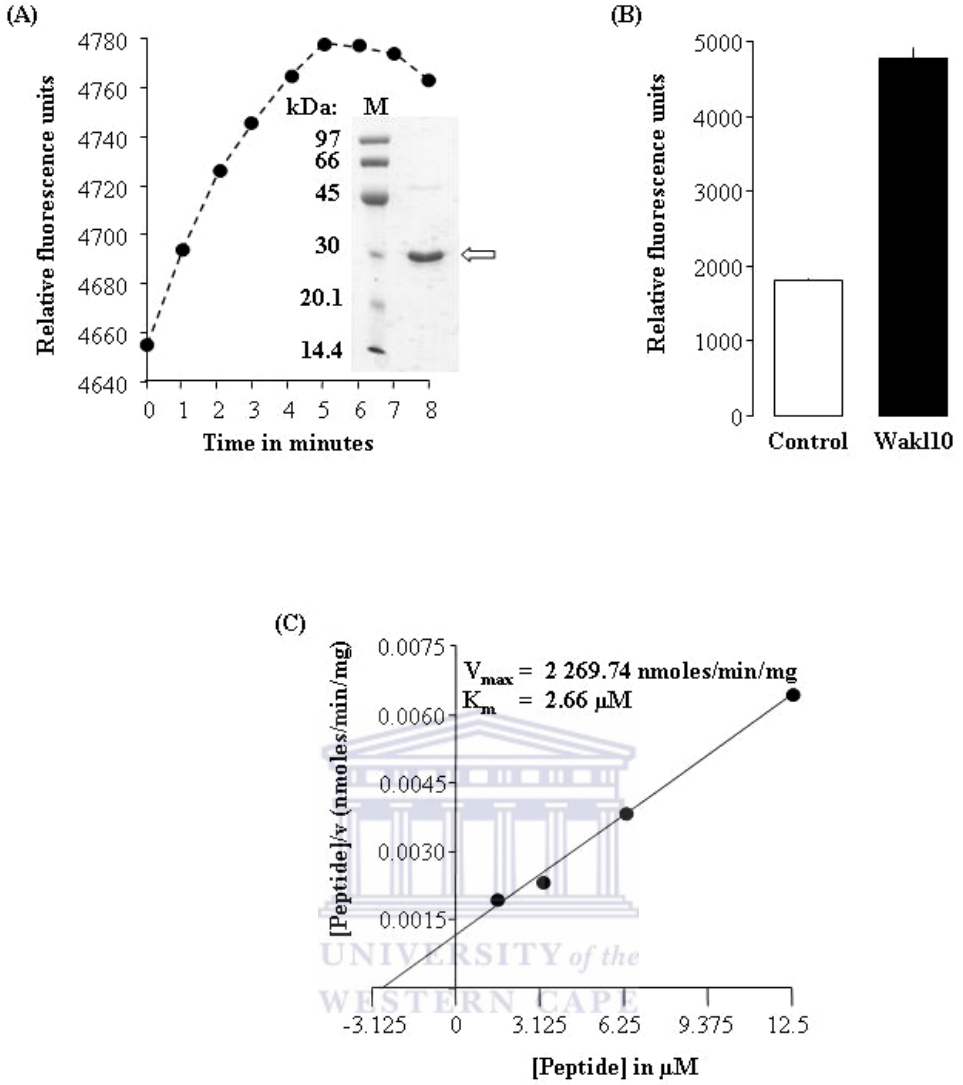

Figure 5.7: Determination of the kinase activity of recombinant AtWAKL10. (**A**) A calibration curve produced by 0.1 ng recombinant AtWAKL10 in a reaction system containing 1x reaction buffer, 1 mM ATP, 0.2 mM DTT, and 25 µM Ser/Thr-peptide. Insert: SDS-PAGE of the purified recombinant AtWAKL10 that was used in the assays, where (M) is the low molecular weight marker while the arrow is marking the recombinant protein. (**B**) Peptide phosphorylation levels generated with no protein (control) and with 0.1 ng recombinant AtWAKL10 as was determined by an Omnia™ Ser/Thr-Recombinant system (BioSource). (**C**) A Hanes plot for the determination of the reaction kinetics of the recombinant AtWAKL10. Initial velocities for a variety of Ser/Thr-peptide concentrations (1.5625, 3.125, 6.25, and 12.5 µM) were determined followed by sketching of the plot. Kinetic constants (K_m and V_{max}) for the recombinant AtWAKL10 were then derived from this plot. K_m was determined as the negative value of the x-intercept ($x = -K_m$, when $y = 0$) of the linear fit of the data, while V_{max} was calculated from the y-intercept ($y = K_m/V_{max}$, when $x = 0$) of the same linear fit. The values represent the means of three experiments, with standard error bars and as analyzed by ANOVA.

For the same reason that the GC domain of the recombinant AtWAKL10 is imbedded into its kinase domain yet both domains are enzymatically functional, it was also sought to find out if the presence of GTP (a substrate for the GC domain) could have any effects on the enzymatic activity of the kinase domain. Furthermore, GTP itself was also tested to check if it was a possible substrate for the kinase domain. Therefore, the kinase assays were carried out in the presence of an equimolar concentration of GTP to ATP, and as is shown in Fig. 5.6 below, the presence of GTP in a kinase reaction had no effect on the kinase activity of the recombinant AtWAKL10. In addition, GTP was found to be a co-substrate (with ATP) for the kinase domain of the recombinant AtWAKL10.

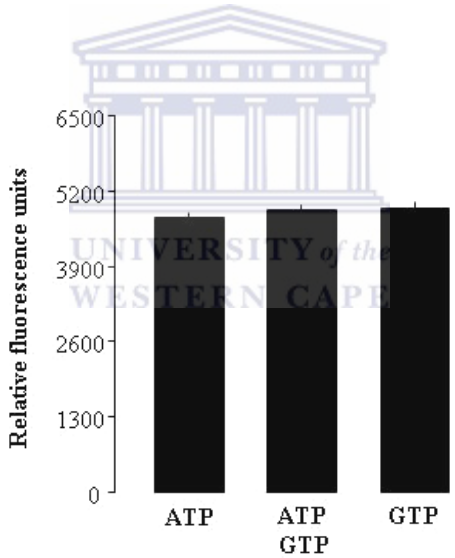

Figure 5.8: The effect of GTP on the kinase activity of recombinant AtWAKL10 and its availability as a possible substrate. The effect of GTP on the kinase activity was determined by adding 1 mM GTP into a reaction system containing 1x reaction buffer, 0.1 ng recombinant AtWAKL10, 1 mM ATP, 0.2 mM DTT, and 25 µM Ser/Thr-peptide followed by measurement of its peptide phosphorylation levels with an Omnia™ Ser/Thr-Recombinant system (BioSource). To test if GTP was a possible substrate for the kinase domain, a reaction system containing 1x reaction buffer, 0.1 ng recombinant AtWAKL10, 1 mM GTP, 0.2 mM DTT, and 25 µM Ser/Thr-peptide was prepared and its peptide phosphorylation levels also determined by the Omnia™ Ser/Thr-Recombinant system (BioSource). Alongside these two assays, another reaction system containing 1x reaction buffer, 0.1 ng recombinant AtWAKL10, 1 mM ATP, 0.2 mM DTT, and 25 µM Ser/Thr-peptide was also set as a control. The values represent the means of three experiments, with standard error bars and as analyzed by ANOVA.

As an end-product of the GC domain activity, cGMP was tested to determine if it had any effects on the enzymatic activity of the kinase domain as is shown in Fig. 5.9 below. Fig 5.9A shows that the presence of 1.0 µM cGMP in a 60-minute kinase reaction resulted in an increase of the kinase activity from 4875 RFUs to 6250 RFUs when ATP was a substrate and from 4975 RFUs to 5750 RFUs when GTP was a substrate. Fig 5.9B indicates that the effect of cGMP on the kinase activity of the recombinant AtWAKL10 was concentration-dependent (between 0.1 to 1.0 µM cGMP concentrations).

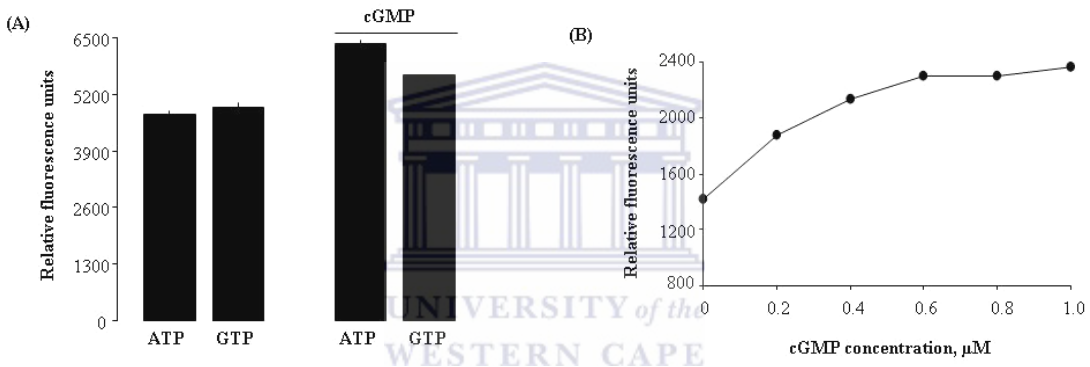

Figure 5.9: The effects of cGMP on the kinase activity of recombinant AtWAKL10. (**A**) Cyclic GMP effect on the kinase activity: Reaction systems containing 1x reaction buffer, 0.1 ng recombinant AtWAKL10, 1 mM ATP/GTP, 0.2 mM DTT, and 25 µM Ser/Thr-peptide with or without 1 µM cGMP were set followed by measurement of their peptide phosphorylation levels with an Omnia™ Ser/Thr-Recombinant system (BioSource). (**B**) Dose-response effects of the cGMP: concentrations ranging from 0-1 µM were assayed in reaction systems containing 1x reaction buffer, 0.1 ng recombinant AtWAKL10, 1 mM ATP, 0.2 mM DTT, and 12.5 µM Ser/Thr-peptide followed by measurement of the peptide phosphorylation levels with an Omnia™ Ser/Thr-Recombinant system (BioSource). The values represent the means of three experiments, with standard error bars and as analyzed by ANOVA.

In order to further elucidate the functional roles of AtWAKL10 in plants, a bioinformatic approach that uses Genevestigator (www.genevestigator.ethz.ch) as a tool was used to inspect and infer the functional roles of *AtWAKL10* in *Arabidopsis thaliana* in response to various biotic stimuli. Fig. 5.10 below shows the microarray expression profiling data for *AtWAKL10* that was recorded over a period of 24 hours in response to salicylic acid (SA) and its functional synthetic analogue benzothiadiazole S-methylester (BHT). The expression responses of *AtWAKL10* to chemical induction were also assessed in two different *Arabidopsis* mutants, *wrky18* and *npr1* where *wrky18* mutant is SA/BHT-induceable (Ulker and Somssich, 2004) while *npr1* mutant is SA/BHT-non-inducible (Cao *et al*., 1994). The *AtWAKL10* was found to be up-regulated in response to SA or BHT in the wild type and *wrky18* mutant (positive control) but not in *npr1* mutant (negative control) thus suggesting a role for AtWAKL10 in plant defense mechanisms.

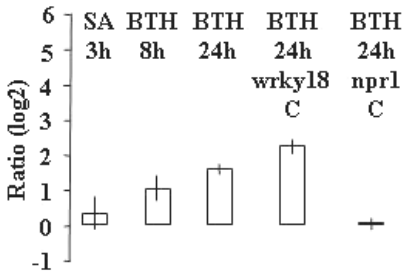

Figure 5.10: Induction of *AtWAKL10* in response to salicylic acid (SA) and its functional synthetic analogue benzothiadiazole S-methylester (BHT). The gene was induceable in response to both SA and BHT. Mutant *wrky18* is SA/BHT-inducible (Ulker and Somssich, 2004) and was used as a positive control while mutant *npr1* is SA/BHT-non-inducible (Cao *et al*., 1994) and was used as a negative control.

The expression profiling data for *AtWAKL10* in response to infection with two strains of the hemibiotrophic bacterial pathogen *Pseudomonas syringae* was also assessed over a period of 24 hours (Fig. 5.11). The response to both the virulent and avirulent strains clearly showed an up-regulation of the gene, although its up-regulatory response to the avirulent strain was significantly more pronounced than to the virulent strain.

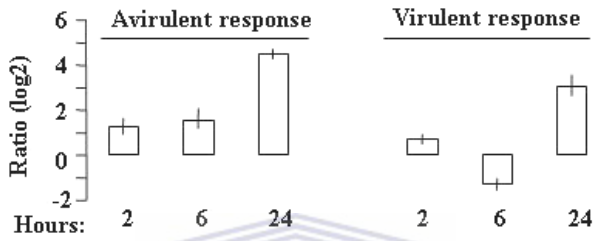

Figure 5.11: Induction of *AtWAKL10* expression in response to *Pseudomonas syringae* infection. The pathogen induced a significant expression response of *AtWAKL10* which was more pronounced with its avirulent than its virulent strain.

Besides its up-regulation response to the *Pseudomonas syringae*, *AtWAKL10* expression was also shown to be strongly induced by several biotrophic pathogenic moulds (*Erysiphe orontii*, *Erysiphe cichoracearum*, and *Phytophthora infestans*) as well as by the necrotrophic pathogenic mould *Botrytis cinerea* (Fig. 5.12). Biotrophs depend on living host tissue for survival and are capable of inducing SA-dependent defense mechanisms (Ward *et al*., 1991; Glazebrook, 2004) while necrotrophs promote host cell death at early stages of infection and are capable of inducing jasmonic acid (JA) and ethylene (ET)-dependent defense mechanisms (Penninckx *et al*., 1998; Glazebrook, 2004).

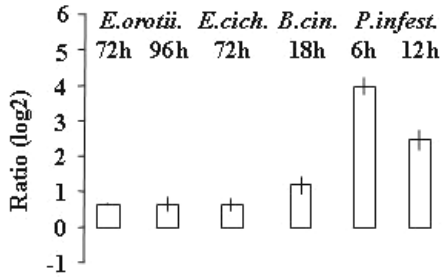

Figure 5.12: Expression profiles of *AtWAKL10* in response to plant infection with various fungal pathogens. The gene was strongly induced by both the biotrophic and necrotrophic pathogenic moulds. *E. orontii* is a virulent obligate biotrophic fungal pathogen, *E. cichoracearum* is a biotrophic parasitic fungus and *P. infestans* is a biotrophic pathogenic fungus and their infection induces an SA-dependent defense mechanism in plants (Ward *et al*., 1991; Glazebrook, 2004). *B. cinerea* is a necrotrophic fungal pathogen whose infection induces the JA/ET-dependent defense mechanisms in plants (Penninckx *et al*., 1998; Glazebrook, 2004).

Further insights into the functional roles of *AtWAKL10* were gained through an assessment of its transcriptional profiles in various SAR-related Arabidopsis mutants that were accessible through the "mutant surveyor" function of the Genevestigator as is shown in Fig. 5.13 below. Consistent with its role in pathogen defense mechanisms, *AtWAKL10* was strongly expressed in all mutants capable of inducing either the SA-dependent or the JA/ET-dependent pathogen resistance gene expression (Kieber *et al*., 1993; Bowling *et al*., 1994; Cao *et al*., 1994; Bowling *et al*., 1997; Felix *et al*., 1999; Kunze *et al*., 2004). Furthermore, its expression was also markedly reduced in a mutant that was defective of the pathogen resistance mechanisms (Xie *et al*., 1998).

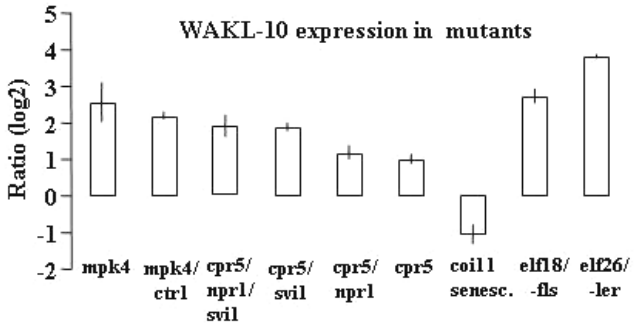

Figure 5.13: Expression profiles of *AtWAKL10* in different SAR-related Arabidopsis mutants. The expression levels were assessed in single, double and triple mutants, and *AtWAKL10* was found to be strongly expressed in all mutants capable of inducing either the SA-dependent or the JA/ET-dependent pathogen resistance gene expression. Mutant *mpk4* lacks the JA signalling regulation system and as such leading to enhanced SA accumulation and its signalling in pathogen-infected plants. Mutant *ctr1* grows as if ET is always present (Kieber *et al*., 1993). Mutant *cpr5* contains a high level of SA and it constitutively expresses the PR genes to show enhanced resistance to pathogens (Bowling *et al*., 1994; Bowling *et al*., 1997). Mutant *npr1* is SA-non-inducible (Cao *et al*., 1994) although its characteristic was overshadowed by other SA-dependent mutations in its double or triple mutant forms. Mutant *svi1* carries the provirus *SL-Kh virus integration-1* gene. Mutant *coi11 senesc* is defective in JA signalling (promotes JA senescence) and is therefore susceptible to pathogenesis (Xie *et al*., 1998). Mutants *elf18* and *elf26* contain the bacterial proteins (elongation factors 12 and 26 respectively) that can induce an oxidative burst and biosynthesis of ET to trigger resistance to subsequent infection with pathogenic bacteria (Kunze *et al*., 2004). Mutant *fls* can not sense bacterial flagellins (proteins that are commonly associated with the triggering of innate immune responses in plants) (Felix *et al*., 1999) although its effect was masked by *elf18* in the double mutant *elf18/-fls*. Mutant *Ler* is a mutant form of the Landsberg ecotype.

5.4 Discussion

When Ludidi and Gehring (2003) identified the first higher plant protein with *in vitro* guanylate cyclase (GC) activity in *Arabidopsis thaliana* (AtGC1) by querying the Arabidopsis genome using a search motif based on conserved and functionally assigned amino acids in the catalytic centre of annotated GCs, six other potential candidates were also identified, and among them was a wall associated kinase-like protein (AtWAKL10) that has a domain organization resembling that of vertebrate natriuretic peptide (NP) receptors (Fig. 5.1) (Maack, 1992; Ludidi and Gehring, 2003). Vertebrate NP receptors contain an extracellular ligand-binding domain and an intracellular GC/kinase domain (He *et al*., 1999) and signal through the activity of their GC domain (Garbers, 1991a, b; Koller and Goeddel, 1992; Garbers and Lowe, 1994) that is capable of generating intracellular cGMP from GTP. Although AtWAKL10 does not contain the N-terminal glycine-rich motif commonly found in most annotated GCs (Fig. 5.2), its resemblance to vertebrate NP receptors could suggest a functional homology with receptor molecules and it might even propose that such a receptor molecule may recognize PNPs as ligands. Therefore, in an attempt to elucidate the functional properties of AtWAKL10, a biologically active recombinant AtWAKL10 was prepared (Fig. 5.4A) and shown to function *in vitro* as a GC (Figs 5.4B and 5.5) and a kinase (Fig. 5.7) making it a bi-functional signaling molecule. Furthermore, a bioinformatic analysis of the AtWAKL10 suggests a role in pathogen responses and defense mechanisms (Figs 5.10 – 5.13).

GCs are enzymes capable of converting guanosine 5′-triphosphate (GTP) to the second messenger molecule, guanosine 3′,5′-cyclic monophosphate (cGMP) (Schaap, 2005) while kinases are enzymes that can add a phosphate group to other molecules

(phosphorylation) or to themselves (autophosphorylation) (Shiu and Bleecker, 2001b). In plants, cGMP as a second messenger has been implicated in the mediation of several cellular and physiological processes such as responses to drought and salinity (Maathuis and Sanders, 2001; Donaldson *et al*., 2004), expression of pathogenesis-related proteins (Durner *et al*., 1998) and phytochrome A-mediated anthocyanin biosynthesis (Bowler *et al*., 1994). Furthermore, protein phosphorylation has also been implicated in several regulatory mechanisms known to control protein activities and cellular signalling including pathogenesis and defence-related signalling (He *et al*., 1998). In this study, the recombinant AtWAKL10 displayed both the GC and kinase functions *in vitro*, and this bi-functionality of the recombinant AtWAKL10 appears to be a characteristic feature associated with several plant GCs since AtGC1 was also shown to possess a GC activity (Ludidi and Gehring, 2003) and a protease activity (Ndiko Ludidi, personal communication) while AtBRI1 was shown to possess a GC activity (Kwezi *et al*., 2007) and a kinase activity (Lusisizwe Kwezi, personal communication).

The fact that the GC domain of the recombinant AtWAKL10 is embedded in the cytosolic kinase domain and that both domains display *in vitro* activities prompted an interest in trying to understand if there was any inter-dependence in biological functions between the two domains and if so, whether such a property had any physiological significance in plants. When ATP (the kinase substrate) was added at equimolar concentrations to GTP in a GC reaction, the GC catalytic activity was reduced (Fig. 5.6). This observation was rationalized to reflect a competition between GTP and ATP for the substrate binding site on the catalytic domain of the recombinant AtWAKL10, where ATP was only able to bind but not hydrolysed by the

enzyme to produce cGMP, thus slowing GTP hydrolysis. This inhibitory effect of ATP on GTP hydrolysis was previously confirmed in rat intestines where the GC activity of a particulate guanylyl cyclase was inhibited by the presence of ATP (Parkinson *et al*., 1994). When equimolar concentrations of GTP (the GC substrate) to ATP were also added to a kinase reaction, no significant changes of the kinase activity were observed (Fig. 5.8). In addition, when ATP was substituted with GTP in a kinase reaction, a similar level of activity to that displayed during ATP hydrolysis was observed (Fig. 5.8) leading the conclusion that like ATP, GTP can also be a possible substrate for the kinase of the recombinant AtWAKL10. When low concentrations (0.2 – 1.0 µM) of cGMP (a product of the GC domain) were added to a kinase reaction in which ATP or GTP was the sole substrate, the kinase activity was significantly promoted (Fig. 5.9A) and such an effect was concentration-dependent with respect to cGMP (Fig. 5.9B). This outcome was consistent with previous findings where cGMP was shown to promote autophosphorylation in a soluble protein kinase that was purified from *Pharbitis nil* seedlings where such a promotion was also concentration-dependent with a maximal activity level reached at 1.0 µM cGMP concentration (Szmidt-Jaworska *et al*., 2003). In summary, these reported findings gave an indication for the presence of an interactive functional relationship between the GC and kinase domains of AtWAKL10 that may have physiological importance in plant signaling and transduction pathways.

The resemblance in domain organization between recombinant AtWAKL10 and veterbrate NP receptors (Maack, 1992; Ludidi and Gehring, 2003) together with the observed *in vitro* GC and kinase activities of the recombinant AtWAKL10 may suggest that AtWAKL10 functions as a receptor for AtPNP-A. This would be

consistent with the finding that AtPNP-A application to plant cells also triggers cGMP transients (Pharmawati *et al*., 1998a; Pharmawati *et al*., 2001; Ludidi and Gehring, 2003). The idea that AtWAKL10 could be a possible receptor for AtPNP-A can lead to a model of action where AtPNP-A is expected to bind, as a ligand, to AtWAKL10, as its receptor, resulting in the generation of intracellular cGMP and the cGMP would then act as a second messenger molecule that would then drive a variety of cellular and physiological processes in plants.

In an attempt to elucidate the biological roles of AtWAKL10, a number of bioinformatics tools were applied in a sequential protocol (Meier *et al*., 2008b). Using this approach, it was shown that *AtWAKL10* expression could be significantly induced when Arabidopsis plants were treated with salicylic acid (SA) or its functional synthetic analogue benzothiadiazole S-methylester (BHT) (Fig. 5.10). Endogenous SA is often produced in pathogen infected tissues and later in distal uninfected tissues resulting in subsequent induction of a selected group of pathogenesis-related (*PR*) genes (Weigel *et al*., 2005). Several studies have previously shown a strong correlation between the increased levels of SA with both the expression of such SA-inducible *PR* genes and plant disease resistance (Malamy *et al*., 1990; Metraux *et al*., 1990; Uknes *et al*., 1993). The expression of *AtWAKL10* due to SA or BHT treatments therefore strongly suggests that the *AtWAKL10* may be necessary for responses to pathogens and it is conceivable that AtWAKL10 acts as a pathogen-related (PR) protein. Furthermore, the expression levels of the *AtWAKL10* in response to BHT treatment were found to be relatively higher in *wrky18* mutants than in wild types (Fig. 5.10) thus indicating that the *wrky18* transcription factor (TF) (Ulker and Somssich, 2004) is its positive regulator in plant defense systems.

AtWAKL10 expression was also shown to be up-regulated when Arabidopsis plants were infected with either the avirulent or virulent strains of the hemibiotrophic pathogenic bacteria *Pseudomonas syringae.* Notably, the responses were more pronounced after infection with the avirulent strain than with the virulent strain (Fig. 5.11). In resistance (*R*) gene-mediated resistances, the direct or indirect recognition of pathogen-specific elicitors (avirulence proteins) by the plant *R* gene product can lead to rapid activation of a hypersensitive response (HR) that confers specific and effective resistance against pathogens (Matthews, 1991; Dangl and Jones, 2001). This pathogen-induced HR can be associated with the activation of SA-regulated defense mechanisms in the surrounding or even distal parts of the plants, leading to the development of a systemic acquired resistance (SAR), a long-lasting systemic immunity that protects the entire plant from subsequent invasion of a broad range of pathogens (Chester, 1933; Ross, 1961). Therefore, the observed high and differential expression levels of the *AtWAKL10* in Arabidopsis in response to the avirulent strain of *Pseudomonas syringae* suggests a role of the AtWAKL10 in both the *R* gene-mediated resistance and SAR systems of the plant. The functional role of AtWAKL10 may be similar to that of WAK1 which mediates signaling between the extracellular matrix (ECM) and the cytoplasm and was previously shown to be up-regulated following an infection of Arabidopsis plants with an avirulent strain of *Pseudomonas syringae* (He *et al*., 1998; Maleck *et al*., 2000a).

An increased expression profile of the *AtWAKL10* was also observed when the Arabidopsis plants were challenged with the biotrophic pathogenic moulds *Erysiphe orontii*, *Erysiphe cichoracearum*, and *Phytophthora infestans* as well as with the

necrotrophic pathogenic mould *Botrytis cinerea* (Fig. 5.12). Biotrophs depend on living host tissue for survival and are capable of inducing SA-dependent defense mechanisms while necrotrophs promote host cell death at early stages of infection and can induce jasmonate (JA)/ethylene (ET)-dependent defense mechanisms (Thomma *et al*., 1998; Glazebrook, 2004). The association of AtWAKL10 protein with these fungal pathogens further strengthened its role as a defense-related protein in plants.

When the expression profiles of the *AtWAKL10* were assessed in several Arabidopsis mutants, it was also observed that the gene was strongly expressed in all mutants that were capable of eliciting either the SA- or JA/ET-dependent defense responses while on the other hand, its expression was markedly down-regulated in a mutant that was defective of the defense mechanisms (Fig. 5.12) (Kieber *et al*., 1993; Cao *et al*., 1994; Bowling *et al*., 1997; Felix *et al*., 1999; Kunze *et al*., 2004). Again, this observation is consistent with a role of AtWAKL10 in plant pathogen defense mechanisms.

The fact that AtWAKL10, a molecule suspected to be an AtPNP-A receptor, appears to have a role in plant pathogen responses and defense mechanisms is interesting since AtPNP-A has also been previously inferred, through bioinformatics, to have a role in plant pathogen responses and defense mechanisms (Meier *et al*., 2008b). AtPNP-A expressions were up-regulated by SA, BHT, *WRKY70*, a number of SA-mediated SAR-inducing conditions as well as in *cpr5* and *mpk4* Arabidopsis mutants, the latter mutants having elevated SA acid levels (Meier *et al*., 2008b). This therefore suggests that both AtWAKL10 and AtPNP-A expressions may be independently induced by a number of similar biotic and abiotic stimuli and in addition, that the two proteins participate in related and/or common physiological functions.

General Conclusion and Outlook

Since climate change will continue to occur and extreme stresses are likely to increase, we can expect increasing difficulties in growing crops in many parts of the world (White *et al*., 2004; Vinocur and Altman, 2005). Food security is therefore heavily dependent on the development of crop plants with increased resistance to both biotic and abiotic stresses such as pathogen infections and droughts respectively. The urgent need to use rational approaches to develop crop plants with increased stress tolerance has led to an impressive body of work in the areas of plant genetics, plant physiology, plant biochemistry and plant molecular biology, and a realization that only an integrated and systems-based approach can possibly deliver effective biotechnological solutions (Denby and Gehring, 2005).

Since proteins that systemically affect homeostasis in plants are a target candidate group for biotechnology, one such candidate molecule was prepared in this study from *Arabidopsis thaliana* in form a recombinant plant natriuretic peptide (AtPNP-A) (Chapter 2) and its mode of action was partially elucidated. The recombinant AtPNP-A was demonstrated to have important regulatory roles in cellular processes such as photosynthesis, respiration, transpiration as well as net water uptake and retention capacities of a soft South African perennial forest sage *Plectranthus ecklonii* (Chapter 3). Conditions where photosynthesis is down-regulated while respiration is up-regulated have previously been reported, and they occur during plant infections by virulent strains of *Pseudomonas syringae* (Bonfig *et al*., 2006), during leaf wounding (Ehness *et al*., 1997) as well as when plants are exposed to excessive light energy that may result in damages of their photosynthetic apparatus due to the inevitable generation of light-induced reactive intermediates and by-products (Niyogi, 2000).

The involvement of recombinant AtPNP-A in the simultaneous down-regulation of photosynthesis and up-regulation of respiration may suggest participation in such conditions thus implying an important role in plant growth and cellular homeostasis. Bioinformatic analyses of the transcriptional regulation of *AtPNP-A* in *Arabidopsis thaliana*, has indicated that *AtPNP-A* expression is significantly correlated with that of genes involved in the systemic acquired resistance (SAR), defence response pathways, and in response to various abiotic (*e.g.*, osmotic stress and K^+ starvation) and biotic (*e.g.*, pathogen infections) stimuli (Meier *et al.*, 2008b). This therefore supports the idea of AtPNP-A having a role in plant growth and cellular homeostasis as a stress-induced signalling molecule.

Recombinant AtPNP-A was also shown to induce respiratory and net water transport response signals in *Plectranthus ecklonii* whose signalling was demonstrated to be phloem-mediated (Chapter 4). These findings indicated a systemic mode of action for AtPNP-A in plants that appears to be closely associated with the phloem tissue. The association of plant natriuretic peptides (PNPs) with the phloem tissue has previously been reported. Firstly, *in situ* immunoreactivity and immunofluorescence assays of *Hedera helix* and *Solanum tuberosum* with anti-human atrial natriuretic peptide antibodies and anti-potato natriuretic peptide antibodies respectively have shown the association of PNPs with the phloem tissues of both plants (Maryani *et al.*, 2003). Secondly, PNPs have recently been identified in differentiating phloem tissues of leaves and inflorescence stems of *Arabidopsis thaliana* using a microarray analyses approach that was based on a predicted increase in vascular-related gene expression in response to an auxin transport inhibitor-induced vascular overgrowth (Wenzel *et al.*, 2008).

In a quest to further understand the physiological roles of recombinant AtPNP-A in plants, another recombinant *Arabidopsis thaliana* molecule termed wall associated kinase-like 10 (AtWAKL10) and suspected to be a possible AtPNP-A receptor was expressed and its functional properties partially characterized (Chapter 5). AtWAKL10 is structurally related to vertebrate atrial natriuretic peptide (ANP) receptors in that they both have an extracellular N-terminal ligand-binding domain, a single trans-membrane region, and an intracellular C-terminal guanylate cyclase (GC)/kinase domain (Maack, 1992; Ludidi and Gehring, 2003). In vertebrates, ANP receptors operate through the function of their GC domains (Garbers, 1991b, a; Koller and Goeddel, 1992; Garbers and Lowe, 1994) that are capable of generating intracellular cyclic guanosine monophosphate (cGMP), which in turn functions as a second messenger for the regulation of different signal transduction pathways and functions. The resemblance in domain organization between AtWAKL10 and ANP receptors (Maack, 1992; Ludidi and Gehring, 2003) may suggest a functional homology between these two molecules and furthermore, proposing AtWAKL10 as a potential PNP receptor.

The partial characterization of recombinant AtWAKL10 showed that, like the vertebrate ANP receptors, the molecule could function *in vitro* as a GC and a kinase (bifunctional) thus further strengthening the suggestion that it can act as a PNP receptor, particularly since AtPNP-A applications to plant cells also trigger cGMP transients (Pharmawati *et al*., 1998a; Pharmawati *et al*., 2001; Ludidi and Gehring, 2003). AtWAKL10 is of the three plant proteins with *in vitro* GC activity that have so far been identified in higher plants. The other GC candidates are AtGC1 (Ludidi

and Gehring, 2003) and AtBRI1 (Kwezi *et al*., 2007). The bi-functionality of the recombinant AtWAKL10 appears to be a characteristic feature associated with higher plant GCs since AtGC1 was also shown to possess a protease activity (Ndiko Ludidi, personal communication) while AtBRI1 was also shown to possess kinase activity (Lusisizwe Kwezi, personal communication).

In defining the role of PNPs in plants, it will be necessary to elucidate their exact mode of action. One way of doing this would be to search for a PNP receptor, characterize its physiological functions and then linking such functions to those of PNPs. Since PNPs have been shown to elicit physiological responses in protoplasts (Maryani *et al*., 2001; Morse *et al*., 2004), plasmalemma vesicles (Maryani *et al*., 2000) and microsomes (Suwastika *et al*., 2000), one could search for a PNP receptor molecule in plant cell membranes. From the cell membranes, PNP receptor molecules could possibly be isolated by passing membrane proteins over a PNP affinity column followed by elution of the bound proteins. Another approach is to incubate membrane proteins with (fluorescently) labelled PNP followed by the isolation of PNP-receptor complexes using techniques such as gel retardation and/or immuno-precipitation and then characterizing the isolated receptor molecules.

References

Altschul, S.F., Madden, T.L., Schäffer, A.A., Zhang, J., Zhang, Z., Miller, W., and Lipman, D.J. (1997). Gapped BLAST and PSI-BLAST: A new generation of protein database search programs. *Nucleic Acids Research* **25,** 3389-3402.

Ames, I.H., Richman, R.A., and Weiss, J.P. (1980). Is cyclic GMP involved in the regulation of tumorigenesis in the Nicotiana genetic tumor system? *Plant Cell Physiology* **21,** 367-372.

Amtmann, A., Jelitto, T.C., and Sanders, D. (1999). K^+-Selective inward-rectifying channels and apoplastic pH in barley roots. *Plant Physiology* **120,** 331-338.

Anand-Srivastava, M.B., and Trachte, G.J. (1993). Atrial natriuretic factor receptors and signal transduction mechanisms. *Pharmacological Reviews* **45,** 455-497.

Anant, J. (2008). Histidine-tagged protein purification using recombinant DNA techniques. *Amersham Biosciences Protocols* **1,** 1-3.

Anderson, C.M., Wagner, T.A., Perret, M., He, Z.H., He, D., and Kohorn, B.D. (2001). WAKs: cell wall-associated kinases linking the cytoplasm to the extracellular matrix. *Plant Molecular Biology* **47,** 197-206.

Anderson, J.A., Huprikar, S.S., Kochian, L.V., Lucas, W.J., and Gaber, R.F. (1992). Functional expression of a probable *Arabidopsis thaliana* potassium channel in *Saccharomyces cerevisiae*. *Proceedings of the National Academy of Sciences of the United States of America* **89,** 3736-3740.

Assmann, S.M., and Shimazaki, K. (1999). The multisensory guard cell. Stomatal responses to blue light and abscisic acid. *Plant Physiology* **119,** 809-816.

Balachandran, S., Xiang, Y., Schobert, C., Thompson, G.A., and Lucas, W.J. (1997). Phloem sap proteins from *Cucurbita maxima* and *Ricinus communis* have the capacity

to traffic cell to cell through plasmodesmata. *Proceedings of the National Academy of Sciences of the United States of America* **94,** 14150-14155.

Barre, A., and Rouge, P. (2002). Homology modeling of the cellulose-binding domain of a pollen allergen from rye grass: structural basis for the cellulose recognition and associated allergenic properties. *Biochemical and Biophysical Research Communications* **296,** 1346-1351.

Barry, C.S., Blume, B., Bouzayen, M., Cooper, W., Hamilton, A.J., and Grierson, D. (1996). Differential expression of the 1-aminocyclopropane-1-carboxylate oxidase gene family of tomato. *Plant Journal* **9,** 525-535.

Bartel, B. (1997). Auxin biosynthesis. *Annual Review of Plant Physiology and Plant Molecular Biology* **48,** 51-66.

Bartel, B., and Fink, G.R. (1994). Differential regulation of an auxin-producing nitrilase gene family in *Arabidopsis thaliana*. *Proceedings of the National Academy of Sciences of the United States of America* **91,** 6649-6653.

Basra, A.S. (2000). Plant growth regulators in agriculture and horticulture, their role and commercial uses. (New York: The Haworth Press, Inc).

Berger, S., Benediktyova, Z., Matous, K., Bonfig, K., Mueller, M., Nedbal, L., and Roitsch, T. (2006). Visualization of dynamics of plant-pathogen interaction by novel combination of chlorophyll fluorescence imaging and statistical analysis: differential effects of virulent and avirulent strains of *Pseudomonas syringae* and of oxylipins on *Arabidopsis thaliana*. *Journal of Experimental Botany* **58,** 797-806.

Bergey, D.R., Howe, G.A., and Ryan, C.A. (1996). Polypeptide signaling for plant defensive genes exhibits analogies to defense signaling in animals. *Proceedings of the National Academy of Sciences of the United States of America* **93,** 12053-12058.

Bialek, K., Michalczuk, L., and Cohen, J.D. (1992). Auxin biosynthesis during seed germination in *Phaseolus vulgaris*. *Plant Physiology* **100,** 509-517.

Billington, T., Pharmawati, M., and Gehring, C.A. (1997). Isolation and immunoaffinity purification of biologically active plant natriuretic peptide. *Biochemical and Biophysical Research Communications* **235,** 722-725.

Binns, A.N. (1994). Cytokinin accumulation and action: Biochemical, genetic, and molecular approaches. *Annual Review of Plant Physiology and Plant Molecular Biology* **45,** 173-196.

Blackwell, J.R., and Horgan, R. (1994). Cytokinin biosynthesis by extracts of *Zea mays. Phytochemistry* **35,** 339-342.

Blasing, O.E., Gibon, Y., Gunther, M., Hohne, M., Morcuende, R., Osuna, D., Thimm, O., Usadel, B., Scheible, W.R., and Stitt, M. (2005). Sugars and circadian regulation make major contributions to the global regulation of diurnal gene expression in Arabidopsis. *Plant Cell* **17,** 3257-3281.

Blázquez, M.A., Ferrándiz, C., Madueńo, F., and Parcy, F. (2006). How floral meristems are built. *Plant Molecular Biology* **60,** 855-870.

Bleeker, A. B. (2001). Ethylene. *Current Biology* **11,** R952.

Bleecker, A.B., and Kende, H. (2000). Ethylene: a gaseous signal molecule in plants. *Annual Review of Cell and Developmental Biology* **16,** 1-18.

Bleecker, A.B., Estelle, M.A., Somerville, C., and Kende, H. (1988). Insensitivity to ethylene conferred by a dominant mutation in *Arabidopsis thaliana*. *Science* **241,** 1086-1089.

Bonfig, K.B., Schreiber, U., Gabler, A., Roitsch, T., and Berger, S. (2006). Infection with virulent and avirulent *Pseudomonas syringae* strains differentially affects photosynthesis and sink metabolism in Arabidopsis leaves. *Planta* **225,** 1-12.

Boudart, G., Jamet, E., Rossignol, M., Lafitte, C., Borderies, G., Jauneau, A., Esquerre-Tugaye, M.T., and Pont-Lezica, R. (2005). Cell wall proteins in apoplastic fluids of *Arabidopsis thaliana* rosettes: identification by mass spectrometry and bioinformatics. *Proteomics* **5,** 212-221.

Bowler, C., and Chua, N.H. (1994). Emerging themes of plant signal transduction. *Plant Cell* **6,** 1529-1541.

Bowler, C., Yamagata, H., Neuhaus, G., and Chua, N.H. (1994). Phytochrome signal transduction pathways are regulated by reciprocal control mechanisms. *Genes and Development* **8,** 2188-2202.

Bowler, C., Frohnmeyer, H., Schafer, E., Neuhaus, G., and Chua, N.H. (1997). Phytochrome and ultraviolet signal transduction pathways. *Acta Physiologiae Plantarum* **19,** 475-483.

Bowling, S.A., Clarke, J.D., Liu, Y., Klessig, D.F., and Dong, X. (1997). The cpr5 mutant of Arabidopsis expresses both NPR1-dependent and NPR1-independent resistance. *Plant Cell* **9,** 1573-1584.

Bowling, S.A., Guo, A., Cao, H., Gordon, A.S., Klessig, D.F., and Dong, X. (1994). A mutation in Arabidopsis that leads to constitutive expression of systemic acquired resistance. *Plant Cell* **6,** 1845-1857.

Bradford, M.M. (1976). A rapid and sensitive method for the quantitation of microgram quantities of protein utilizing the principle of protein-dye binding. *Analytical Biochemistry* **72,** 248-254.

Briskin, D.P., and Gawienowski, M.C. (1996). Role of the plasma membrane H^+-ATPase in K^+ transport. *Plant Physiology* **111,** 1199-1207.

Bynum, M.R., and Smith, W.K. (2001). Floral movements in response to thunderstorms improve reproductive effort in the alpine species *Gentiana algida* (Gentianaceae). *American Journal of Botany* **88,** 1088-1095.

Cao, H., Bowling, S.A., Gordon, A.S., and Dong, X. (1994). Characterization of an Arabidopsis mutant that is non-responsive to inducers of systemic acquired resistance. *Plant Cell* **6,** 1583-1592.

Casson, S.A., Chilley, P.M., Topping, J.F., Evans, M., Souter, M.A., and Lindsey, K. (2002). The *POLARIS* gene of Arabidopsis encodes a predicted peptide required for correct root growth and leaf vascular patterning. *Plant Cell* **14,** 1705-1721.

Castillo R., Mizuguchi K., Dhanaraj V., Albert A., Blundell T., and Murzin A. (1999). A six-stranded double-psi beta barrel is shared by several protein superfamilies. *Structure and Fold Description* **15,** 227-236.

Ceccardi, T.L., Barthe, G.A., and Derrick, K.S. (1998). A novel protein associated with citrus blight has sequence similarities to expansin. *Plant Molecular Biology* **38,** 775-783.

Chang, C., and Shockey, J.A. (1999). The ethylene-response pathway:signal perception to gene regulation. *Current Opinion in Plant Biology* **2,** 352-358.

Chen, C.M., and Ertl, J.R. (1994). Cytokinin biosynthetic enzymes in plants and slime mold. In Cytokinins: Chemistry, activity, and function, D.W.S. Mok and M.C. Mok, eds (Boca Raton, FL: CRC Press), pp. 81-85.

Chester, K.S. (1933). The problem of acquired physiological immunity in plants. *Quarterly Review of Biology* **8,** 275-324.

Chinkers, M., Garbers, D.L., Chang, M.S., Lowe, D.G., Goeddel, D.V., and Schulz, S. (1989). A membrane form of guanylate cyclase is an atrial natriuretic peptide receptor. *Nature* **388,** 78-83.

Clark, S.E., Williams, R.W., and Meyerowitz, E.M. (1997). The CLAVATA1 gene encodes a putative receptor kinase that controls shoot and floral meristem size in Arabidopsis. *Cell* **89,** 575-585.

Cosgrove, D.J. (2000). Loosening of plant cell walls by expansins. *Nature* **407,** 321-326.

Cosgrove, D.J., Bedinger, P.A., and Durachko, D.M. (1997). Group I allergens of grass pollen as cell wall loosening agents. *Proceedings of the National Academy of Sciences of the United States of America* **94,** 6559-6564.

Cousson, A. (2004). Pharmacological evidence for a putative mediation of cyclic GMP and cytosolic Ca^{2+} within auxin-induced *de novo* root formation in the monocot plant *Commelina communis* L. *Plant Science* **166,** 1117-1124.

Cousson, A., and Vavasseur, A. (1998). Putative involvement of cytosolic Ca^{2+} and GTP-binding proteins in cyclic-GMP-mediated induction of stomatal opening by auxin in *Commelina communis* L. *Planta* **206,** 308-314.

Creelman, R.A., and Mullet, J.E. (1991). Abscisic acid accumulates at positive turgor potential in excised soybean seedling growing zones. *Plant Physiology* **95,** 1209-1213.

Cronshaw, J. (1981). Phloem structure and function. *Annual Review of Plant Physiology* **32,** 465-484.

Dangl, J.L., and Jones, J.D. (2001). Plant pathogens and integrated defence responses to infection. *Nature* **411,** 826-833.

Davies, P. (1995). The plant hormones: their nature, occurrence and function. In: Plant hormones - Physiology, biochemistry and molecular biology, pp 1-12. Davies P.J. (Ed.) Kluwer, Dordrecht.

Davies, W., and Jones, H. (1991). Abscisic acid: physiology and biochemistry. (Oxford: BIOS Scientific).

De Bernardez Clark, E., Hevehan, D., Szela, S., and Maachupalli-Reddy, J. (1998). Oxidative renaturation of hen egg-white lysozyme. Folding versus aggregation. *Biotechnology Progress* **14,** 47-54.

deBold, A., Borenstein, B., Veress, A., and Sonnenberg, H. (1981). A rapid and potent natriuretic response to intravenous injection of atrial myocardial extract in rats. *Life Sciences* **28,** 89-94.

Demidchik, V., and Tester, M. (2002). Sodium fluxes through non-selective cation channels in the plasma membrane of protoplasts from Arabidopsis roots. *Plant Physiology* **128,** 379-387.

Demidchik, V., Davenport, R.J., and Tester, M. (2002). Nonselective cation channels in plants. *Annual Review of Plant Biology* **53,** 67-107.

Denby, K., and Gehring, C. (2005). Engineering drought and salinity tolerance in plants: lessons from genome-wide expression profiling in Arabidopsis. *Trends in Biotechnology* **23,** 547.

Donaldson, L., Ludidi, N., Knight, M.R., Gehring, C., and Denby, K. (2004). Salt and osmotic stress cause rapid increases in *Arabidopsis thaliana* cGMP levels. *FEBS Letters* **569,** 317-320.

Durner, J., Wendehenne, D., and Klessig, D. (1998). Defense gene induction in tobacco by nitric oxide, cyclic GMP, and cyclic ADP-Ribose. *Proceedings of the National Academy of Sciences of the United States of America* **95,** 10328-10333.

Ehness, R., Ecker, M., Godt, D.E., and Roitsch, T. (1997). Glucose and stress independently regulate source and sink metabolism and defense mechanisms via signal transduction pathways involving protein phosphorylation. *Plant Cell* **9,** 1825-1841.

Ejiri, S.I., and Honda, H. (1985). Effect of cyclic AMP and cyclic GMP on the autophosphorylation of elongation factor 1 from wheat embryos. *Biochemical and Biophysical Research Communications* **128,** 53-60.

Essah, P.A., Davenport, R., and Tester, M. (2003). Sodium influx and accumulation in Arabidopsis. *Plant Physiology* **133,** 307-318.

Fang, Y., and Hirsch, A.M. (1998). Studying early nodulin gene ENOD40 expression and induction by nodulation factor and cytokinin in transgenic alfalfa. *Plant Physiology* **116,** 53-68.

Felix, G., Duran, J.D., Volko, S., and Boller, T. (1999). Plants have a sensitive perception system for the most conserved domain of bacterial flagellin. *Plant Journal* **18,** 265-276.

Feller, S.M., Gagelmann, M., and Forssmann, W.G. (1989). Urodilatin: a newly described member of the ANP family. *Trends in Pharmacological Sciences* **10,** 93-94.

Fernández-Maculet, J.C., Dong, J.G., and Yang, S.F. (1993). Activation of 1-aminocyclopropane-1-carboxylateoxidase by carbon dioxide. *Bichemical and Biophysical Research Communications* **193,** 1168-1173.

Fisher, D.B., Wu, Y., and Ku, M.S. (1992). Turnover of soluble proteins in the wheat sieve tube. *Plant Physiology* **100,** 1433-1441.

Fletcher, J.C., Brand, U., Running, M.P., Simon, R., and Meyerowitz, E.M. (1999). Signaling of cell fate decisions by *CLAVATA3* in Arabidopsis shoot meristems. *Science* **283,** 1911-1914.

Forbes, J.C., and Watson, R.D. (1992). Plants in agriculture. (Cambridge University Press).

Fridborg, I., Kuusk, S., Robertson, M., and Sundberg, E. (2001). The Arabidopsis protein SHI represses gibberellin responses in Arabidopsis and barley. *Plant Physiology* **127,** 937-948.

Garbers, D., and Lowe, D. (1994). Guanylate cyclase receptors. *Journal of Biological Chemistry* **269,** 30741-30744.

Garbers, D.L. (1991a). Guanylyl cyclase-linked receptors. *Pharmacology and Therapeutics* **50,** 337-345.

Garbers, D.L. (1991b). The guanylyl cyclase-receptor family. *Canadian Journal of Physiology and Pharmacology* **69,** 1618-1621.

Garcia-Olmedo, F., Rodriguez-Palenzuela, P., Molina, A., Alamillo, J.M., López-Solanilla, E., Berrocal-Lobo, M., and Poza-Carrión, C. (2001). Antibiotic activities of peptides, hydrogen peroxide and peryoxynitrite in plant defence. *FEBS Letters* **498,** 219-222.

Garthwaite, J., Southam, E., Boulton, C.L., Nielsen, E.B., Schmidt, K., and Mayer, B. (1995). Potent and selective inhibition of nitric oxide-sensitive guanylyl cyclase by 1H-[1,2,4]oxadiazolo[4,3-a]quinoxalin-1-one. *Molecular Pharmacology* **48,** 184-188.

Gaudin, V., Vrain, T., and Jouanin, L. (1994). Bacterial genes modifying hormonal balances in plants. *Plant Physiology and Biochemistry* **32,** 11-29.

Gehring, C.A. (1999). Natriuretic peptides - a new class of plant hormone? *Annals of Botany* **83,** 329-334.

Gehring, C.A., and Irving, H.R. (2003). Natriuretic peptides--a class of heterologous molecules in plants. *International Journal of Biochemistry and Cell Biology* **35,** 1318-1322.

Gehring, C.A., Khalid, K.M., Toop, T., and Donald, J.A. (1996). Rat natriuretic peptide binds specifically to plant membranes and induces stomatal opening. *Biochemical and Biophysics Research Communications* **228,** 739-744.

Giaquinta, R.T., and Geiger, D.R. (1973). Mechanism of inhibition of translocation by localized chilling. *Plant Physiology* **51,** 372-377.

Giovannoni, J.J. (2007). Fruit ripening mutants yield insights into ripening control. *Current Opinion in Plant Biology* **10,** 283-289.

Glazebrook, J. (2004). Contrasting mechanisms of defense against biotrophic and necrotrophic pathogens. *Annual Reviews of Phytopathology* **43,** 205-227.

Goetz, K.L. (1991). Renal natriuretic peptide (urodilatin) and atriopeptin - evolving concepts. *American Journal of Physiology* **261,** 921-932.

Gomez-Cadenas, A., Zentella, R., Walker-Simmons, M.K., and Ho, T.H. (2001). Gibberellin/abscisic acid antagonism in barley aleurone cells: site of action of the protein kinase PKABA1 in relation to gibberellin signaling molecules. *Plant Cell* **13,** 667-679.

Goodwin, T., and Mercer, E. (1983). Introduction to plant biochemistry. (Oxford: Pergamon Press Ltd).

Gottig, N., Garavaglia, B.S., Daurelio, L.D., Valentine, A., Gehring, C., Orellano, E.G., and Ottado, J. (2008). *Xanthomonas axonopodis* pv. *citri* uses a plant natriuretic peptide-like protein to modify host homeostasis. *Proceedings of the National Academy of Sciences of the United States of America* **105,** 18631-18636.

Gould, N., Minchin, P.E.H., and Thorpe, M.R. (2004). Direct measurements of sieve element hydrostatic pressure reveal strong regulation after pathway blockage. *Functional Plant Biology* **31,** 987-993.

Graebe, J.E. (1988). Gibberellin biosynthesis and control. *Annual Review in Plant Physiology* **38,** 419-465.

Green, T.R., and Ryan, C.A. (1972). Wound-induced proteinase inhibitor in plant leaves: a possible defense mechanism against insects. *Science* **175,** 776-777.

Grusak, M.A., Minchin, P.E.H. (1989). Cold-inhibited phloem translocation in sugar beet. Analysis of the cooling-induced repartitioning hypothesis. *Journal of Experimental Botany* **40,** 215-223.

Hamilton, A.J., Lycett, G.W., and Grierson, D. (1990). Antisense gene that inhibits synthesis of the hormone ethylene in transgenic plants. *Nature* **346,** 284-287.

Hannah, M.A., Iqbal, M.J., and Sanders, F.E. (2001). Adaptation to long-term cold-girdling in genotypes of common bean (*Phaseolus vulgaris* L.). *Journal of Experimental Botany* **52,** 1123-1127.

Hasunuma, K., Funadera, K., Furukawa, K., and Miyamoto-Shinohara, Y. (1988). Rhythmic oscillation of cyclic 3′,5′-AMP and -GMP concentration and stimulation of flowering by cyclic 3′,5′-GMP in *Lemna paucicostata*. *Photochemical Photobiology* **48,** 89-92.

He, Z.H., Fujiki, M., and Kohorn, B.D. (1996). A cell wall-associated, receptor-like protein kinase. *Journal of Biological Chemistry* **271,** 19789-19793.

He, Z.H., He, D., and Kohorn, B.D. (1998). Requirement for the induced expression of a cell wall associated receptor kinase for survival during the pathogen response. *Plant Journal* **14,** 55-63.

He, Z.H., Cheeseman, I., He, D., and Kohorn, B.D. (1999). A cluster of five cell wall-associated receptor kinase genes, *Wak1-5*, are expressed in specific organs of Arabidopsis. *Plant Molecular Biology* **39,** 1189-1196.

Hedden, P., and Kamiya, Y. (1997). Gibberellin biosynthesis: Enzymes, genes and their regulation. *Annual Review of Plant Physiology and Plant Molecular Biology* **48,** 431-460.

Hetherington, A.M. (2001). Guard cell signaling. *Cell* **107,** 711-714.

Hirsch, A.M., and Fang, Y. (1994). Plant hormones and nodulation: what's the connection? *Plant Molecular Biology* **26,** 5-9.

Hisamatsu, M., Mishima, T., Teranishi, K., and Yamada, T. (1997). The correlation between adhesion of schizophyllan to yeast glucan and its effect on regeneration of yeast protoplast. *Carbohydrate Research* **298,** 117-121.

Hoffmann-Benning, S., and Kende, H. (1992). On the role of abscisic acid and gibberellin in the regulation of growth in rice. *Plant Physiology* **99,** 1156-1161.

Holzinger, A., Phillips, K.S., and Weaver, T.E. (1996). Single-step purification/solubilization of recombinant proteins: application to surfactant protein B. *BioTechniques* **20,** 804-806, 808.

Hoshi, T. (1995). Regulation of voltage dependence of the Kat1 channel by intracellular factors. *Journal of General Physiology* **105,** 309-328.

John, P., Zhang, K., Dong, C., Diedrich, L., and Wightman, F. (1993). p34cdc2 related proteins in control of cell cycle progression, the switch between division and differentiation in tissue development, and stimulation of division by auxin and cytokinin. *Australian Journal of Plant Physiology* **45,** 503-526.

Johri, M., and Mitra, D. (2001). Action of plant hormones. *Current Science* **80,** 199-205.

Kende, H. (1993). Ethylene biosynthesis. *Annual Review of Plant Physiology and Plant Molecular Biology* **44,** 283-307.

Kende, H., and Zeevaart, J. (1997). The five "classical" plant hormones. *Plant Cell* **9,** 1197-1210.

Kieber, J.J., Rothenberg, M., Roman, G., Feldmann, K.A., and Ecker, J.R. (1993). CTR1, a negative regulator of the ethylene response pathway in Arabidopsis, encodes a member of the raf family of protein kinases. *Cell* **72,** 427-441.

Kinoshita, T., Nishimura, M., and Shimazaki, K. (1995). Cytosolic concentration of Ca^{2+} regulates the plasma membrane H^+-ATPase in guard cells of fava bean. *Plant Cell* **7,** 1333-1342.

Kionka, C., and Amrhein, N. (1984). The enzymatic malonylation of 1-aminocyclopropane-l-carboxylic acid in homogenates of mung-bean hypocotyls. *Planta* **162,** 226-235.

Klee, H.J., and Romano, C.P. (1994). The roles of phytohormones in development as studied in transgenic plants. Critical Reviews in Plant Sciences **13,** 311-324.

Klessig, D.F., Durner, J., Noad, R., Navarre, D.A., Wendehenne, D., Kumar, D., Zhou, J.M., Shah, J., Zhang, S., Kachroo, P., Trifa, Y., Pontier, D., Lam, E., and Silva, H. (2000). Nitric oxide and salicylic acid signaling in plant defense. *Proceedings of the National Academy of Sciences of the United States of America* **97,** 8849-8855.

Knoblauch, M., and van Bel, A.J.E. (1998). Sieve tubes in action. *Plant, Cell and Environment* **10,** 35-50.

Ko, C.H., and Gaber, R.F. (1991). TRK1 and TRK2 encode structurally related K^+ transporters in *Saccharomyces cerevisiae*. *Molecular and Cellular Biology* **11,** 4266-4273.

Kobayashi, M., Spray, C.R., Phinney, B.O., Gaskin, P., and MacMillan, J. (1996). Gibberellin metabolism in maize. The step-wise conversion of gibberellin A_{12}-aldehyde to gibberellin A_{20}. *Plant Physiology* **110,** 413-418.

Kohler, C., and Makarevich, G. (2006). Epigenetic mechanisms governing seed development in plants. *EMBO Reports* **7,** 1223-1227.

Kohorn, B.D. (1999). Shuffling the deck: plant signalling plays a club. *Trends in Cell Biology* **9,** 381-383.

Kohorn, B.D. (2000). Plasma membrane cell wall contacts. *Plant Physiology* **124,** 31-38.

Kohorn, B.D. (2001). WAKs; cell wall associated kinases. *Current Opinion in Cell Biology* **13,** 529-533.

Koller, K.J., and Goeddel, D.V. (1992). Molecular biology of the natriuretic peptides and their receptors. *Circulation* **86,** 1081-1088.

Komor, E. (2000). Source physiology and assimilate transport: the interaction of sucrose metabolism, starch storage and phloem export in source leaves and the effects on sugar status in phloem. *Australian Journal of Plant Physiology* **27,** 497-505.

Kone, B.C. (2001). Molecular biology of natriuretic peptides and nitric oxide synthases. *Cardiovascular Research* **51,** 429-441.

Kourie, J.I., and Rive, M.J. (1999). Role of natriuretic peptides in ion transport mechanisms. *Medicinal Research Reviews* **19,** 75-94.

Kraulis, P.J. (1991). Similarity of protein G and ubiquitin. *Science* **254,** 581-582.

Kunze, G., Zipfel, C., Robatzek, S., Niehaus, K., Boller, T., and Felix, G. (2004). The N terminus of bacterial elongation factor Tu elicits innate immunity in Arabidopsis plants. *Plant Cell* **16,** 3496-3507.

Kwezi, L., Meier, S., Mungur, L., Ruzvidzo, O., Irving, H., and Gehring, C. (2007). The *Arabidopsis thaliana* brassinosteroid receptor (AtBRI1) contains a domain that functions as a guanylyl cyclase *in vitro*. *PLoS ONE* **2,** e449.

Lally, D., Ingmire, P., Tong, H.Y., and He, Z.H. (2001). Antisense expression of a cell wall-associated protein kinase, WAK4, inhibits cell elongation and alters morphology. *Plant Cell* **13,** 1317-1331.

Lalonde, S., Tegeder, M., Throne-Holst, M., Frommer, W.B., and Patrick, J.W. (2003). Phloem loading and unloading of sugars and amino acids. *Plant, Cell and Environment* **26,** 37-56.

Lang, A., and Minchin, P.E.H. (1986). Phylogenetic distribution and mechanism of translocation inhibition by chilling. *Journal of Experimental Botany* **37,** 389-398.

LCi User Guide, (2000). LCi Photosynthetic system. (Hertfordshire: ADC Bioscientific).

LC*pro*+. (2005). Getting started with LCpro. (Hertfordshire: ADC Bioscientific).

Leng, Q., Mercier, R., Yao, W., and Berkowitz, G. (1999). Cloning and first functional characterisation of a plant cyclic nucleotide-gated cation channel. *Plant Physiology* **121,** 753-761.

Li, M., Poliakov, A., Danielson, U.H., Su, Z., and Janson, J.C. (2003). Refolding of a recombinant full-length non-structural (NS3) protein from hepatitis C virus by chromatographic procedures. *Biotechnology* **25,** 1729-1734.

Li, M., Su, Z.G., and Janson, J.C. (2004). *In vitro* protein refolding by chromatographic procedures. *Protein Expression and Purification* **33,** 1-10.

Li, Y., and Walton, D.C. (1990). Violaxanthin is an abscisic acid precursor in water-stressed dark-grown bean leaves. *Plant Physiology* **92,** 551-559.

Liang, X., Abel, S., Keller, J.A., Shen, N.F., and Theologis, A. (1992). The 1-aminocyclopropane-1-carboxylate synthase gene family of *Arabidopsis thaliana*. *Proceedings of the National Academy of Sciences of the United States of America* **89,** 11046-11050.

Lilie, H., Schwarz, E., and Rudolph, R. (1998). Advances in refolding of proteins produced in E. coli. *Current Opinion in Biotechnology* **9,** 497-501.

Linder, M., and Teeri, T.T. (1997). The roles and function of cellulose-binding domains. *Journal of Biotechnology* **57,** 15-28.

Lindsey, K., Casson, S., and Chilley, P. (2002). Peptides: new signalling molecules in plants. *Trends in Plant Science* **7,** 78-83.

Lindwall, G., Chau, M., Gardner, S.R., and Kohlstaedt, L.A. (2000). A sparse matrix approach to the solubilization of overexpressed proteins. *Protein Engineering* **13,** 67-71.

Lough, T.J., and Lucas, W.J. (2006). Integrative plant biology: role of phloem long-distance macromolecular trafficking. *Annual Review of Plant Biology* **57,** 203-232.

Lucas, K., Pitari, G., Kazerounian, S., Ruiz-Stewart, I., Park, J., Schulz, S., Chepenik, K., and Waldman, S. (2000). Guanylyl cyclases and signaling by cyclic GMP. *Pharmacological Review* **52,** 375-414.

Ludidi, N., and Gehring, C. (2003). Identification of a novel protein with guanylyl cyclase activity in *Arabidopsis thaliana*. *Journal of Biological Chemistry* **278,** 6490-6494.

Ludidi, N., Morse, M., Sayed, M., Wherrett, T., Shabala, S., and Gehring, C. (2004). A recombinant plant natriuretic peptide causes rapid and spatially differentiated K^+, Na^+ and H^+ flux changes in *Arabidopsis thaliana* roots. *Plant and Cell Physiology* **45,** 1093-1098.

Ludidi, N.N., Heazlewood, J.L., Seoighe, C., Irving, H.R., and Gehring, C.A. (2002). Expansin-like molecules: novel functions derived from common domains. *Journal of Molecular Evolution* **54,** 587-594.

Maack, T. (1992). Receptors of atrial natriuretic factor. *Annual Review of Physiology* **54,** 11-27.

Maathuis, F.J., and Sanders, D. (2001). Sodium uptake in Arabidopsis roots is regulated by cyclic nucleotides. *Plant Physiology* **127,** 1617-1625.

MacMillan, J., Ward, D.A., Phillips, A.L., Sanchez-Beltran, M.J., Gaskin, P., Lange, T., and Hedden, P. (1997). Gibberellin biosynthesis from gibberellin A12-aldehyde in endosperm and embryos of *Marah macrocarpus*. *Plant Physiology* **113,** 1369-1377.

Malamy, J., Carr, J.P., Klessig, D.F., and Raskin, I. (1990). Salicylic acid: a likely endogenous signal in the resistance response of tobacco to viral infection. *Science* **250,** 1002-1004.

Maleck, K., Levine, A., Eulgem, T., Morgan, A., Schmid, J., Lawton, K.A., Dangl, J.L., and Dietrich, R.A. (2000a). The transcriptome of *Arabidopsis thaliana* during systemic acquired resistance. *Nature Genetics* **26,** 403-410.

Maleck, K., Levine, A., Eulgem, T., Morgan, A., Schmidl, J., Lawton, K., Dangl, J., and Dietrich, R. (2000b). An Arabidopsis promoter element shared among genes co-regulated during systemic acquired disease resistance. *Nature Genetics* **26,** 403-410.

Marentes, E., and Grusak, M.A. (1998). Mass determination of low-molecular-weight proteins in phloem sap using matrix-assisted laser desorption/ionization time-of-flight mass spectrometry. *Journal of Experimental Botany* **49,** 903-911.

Martin, D.N., Proebsting, W.M., Parks, T.D., Dougherty, W.G., Lange, T., Lewis, M.J., Gaskin, P., and Hedden, P. (1996). Feed-back regulation of gibberellin biosynthesis and gene expression in *Pisum sativum* L. *Planta* **200,** 159-166.

Martin, R.C., Mok, M.C., and Mok, D.W.S. (1993). Cytolocalization of zeatin O-xylosyltransferase in Phaseolus. *Proceedings of the National Academy of Sciences of the United States of America* **90,** 953-957.

Maryani, M.M., Shabala, S.N., and Gehring, C.A. (2000). Plant natriuretic peptide immunoreactants modulate plasma-membrane H^+ gradients in *Solanum tuberosum* L. leaf tissue vesicles. *Archives of Biochemistry and Biophysics* **376,** 456-458.

Maryani, M.M., Bradley, G., Cahill, D.M., and Gehring, C.A. (2001). Natriuretic peptides and immunoreactants modify osmoticum-dependent volume changes in *Solanum tuberosum* L. mesophyll cell protoplasts. *Plant Science* **161,** 443-452.

Maryani, M.M., Morse, M.V., Bradley, G., Irving, H.R., Cahill, D.M., and Gehring, C.A. (2003). *In situ* localization associates biologically active plant natriuretic peptide immuno-analogues with conductive tissue and stomata. *Journal of Experimental Botany* **54,** 1553-1564.

Mathews, C., Holde, K., and Ahern, K. (1999). Biochemistry. (San Francisco: Benjamin/Cumming).

Matsubayashi, Y., and Sakagami, Y. (1996). Phytosulfokine, sulfated peptides that induce the proliferation of single mesophyll cells of *Asparagus officinales* L. *Proceedings of the National Academy of Sciences of the United States of America* **93,** 7623-7627.

Matsubayashi, Y., Yang, H., and Sakagami, Y. (2001). Peptide signals and their receptors in higher plants. *Trends in Plant Science* **6,** 573-577.

Matthews, R.E.F. (1991). Plant virology (San Diego: Academic Press).

McGurl, B., and Ryan, C.A. (1992). The organization of the prosystemin gene. *Plant Molecular Biology* **20,** 405-409.

Meier, S., and Gehring, C. (2008). A guide to the integrated application of on-line data mining tools for the inference of gene functions at the systems level. *Biotechnology* **11**, 1375-1387.

Meier, S., Irving, H., and Gehring, C. (2008a). Plant natriuretic peptides - emerging roles in fluid and salt balance. In: Cardiac Hormones, pp 1-17. Vesely D.L. (Trivandrum, Kerala, India: Transworld Research Network).

Meier, S., Bastian, R., Donaldson, L., Murray, S., Bajic, V., and Gehring, C. (2008b). Co-expression and promoter content analyses assign a role in biotic and abiotic stress responses to plant natriuretic peptides. *BMC Plant Biology* **8,** 24.

Metraux, J.P., Signer, H., Ryals, J., Ward, E., Wyss-Benz, M., Gaudin, J., Raschdorf, K., Schmid, E., Blum, W., and Inverardi, B. (1990). Increase in salicylic acid at the onset of systemic acquired resistance in Cucumber. *Science* **250,** 1004-1006.

Meyerowitz, E.M. (1997). Control of cell division patterns in developing shoots and flowers of *Arabidopsis thaliana*. *Cold Spring Harbor Symposia on Quantitative Biology* **62,** 369-375.

Minchin, P.E.H., and Thorpe, M.R. (1984). Apoplastic phloem unloading in the stem of bean. *Journal of Experimental Botany* **35,** 538-550.

Mockler, T.C., Michael, T.P., Priest, H.D., Shen, R., Sullivan, C.M., Givan, S.A., McEntee, C., Kay, S.A., and Chory, J. (2007). The DIURNAL project: DIURNAL and circadian expression profiling, model-based pattern matching, and promoter analysis. *Cold Spring Harbor Symposia on Quantitative Biology* **72,** 353-363.

Morse, M., Pironcheva, G., and Gehring, C. (2004). AtPNP-A is a systemically mobile natriuretic peptide immunoanalogue with a role in Arabidopsis thaliana cell volume regulation. *FEBS Letters* **556,** 99-103.

Mortimer, P., Pérez-Fernández, M.A., and Valentine, A.J. (2008). The role of arbuscular mycorrhizal colonization in the carbon and nutrient economy of the

tripartite symbiosis with nodulated *Phaseolus vulgaris*. *Soil Biology and Biochemistry* **40,** 1019-1027.

Mortimer, P., Swart, J.C., Valentine, A.J., Jacobs, G., and Cramer, M.D. (2003). Does irrigation influence the growth, yield and water use efficiency of the protea hybrid 'Sylvia' (*Protea susannae* X *Protea eximia*)? *South African Journal of Botany* **69,** 1-9.

Motyka, V., Faiss, M., Strnad, M., Kamínek, M., and Schmülling, T. (1996). Changes in cytokinin content and cytokinin oxidase activity in response to derepression of *ipt* gene transcription in transgenic tobacco calli and plants. *Plant Physiology* **112,** 1035-1043.

Mukhopadhyay, A. (1997). Inclusion bodies and purification of proteins in biologically active forms. *Advances in Biochemical Engineering/Biotechnology* **56,** 61-109.

Mulsch, A., Busse, R., Liebau, S., and Forstermann, U. (1988). LY 83583 interferes with the release of endothelium-derived relaxing factor and inhibits soluble guanylate cyclase. *Journal of Pharmacology and Experimental Therapeutics* **247,** 283-288.

Namiki, S., Hirose, K., and Lino, M. (2001). Mapping of heme-binding domains in soluble guanylyl cyclase beta 1 subunit. *Bichemical and Biophysical Research Communications* **288,** 798-804.

Nankervis, S., Powell, M. D., McLeod, J., and Toop, T. (2007). Identification and expression of natriuretic peptide receptor type-A and -B mRNA in freshwater and seawater rainbow trouts. *Journal of Comparative Physiology B* **177**, 259-267.

Neuhaus, G., Bowler, C., Hiratsuka, K., Yamagata, H., and Chua, N.H. (1997). Phytochrome-regulated repression of gene expression requires calcium and cGMP. *EMBO Journal* **16,** 2554-2564.

Newton, R., and Smith, C. (2004). Cyclic nucleotides. *Phytochemistry* **65,** 2423-2437.

Nicol, F., His, I., Jauneau, A., Vernhettes, S., Canut, H., and Hofte, H. (1998). A plasma membrane-bound putative endo-1,4-beta-D-glucanase is required for normal wall assembly and cell elongation in Arabidopsis. *EMBO Journal* **17,** 5563-5576.

Niyogi, K.K. (2000). Safety valves for photosynthesis. *Current Opinion in Plant Biology* **3,** 455-460.

Norman, S.M., Maier, V.P., and Pon, D.L. (1990). Abscisic acid accumulation and carotenoid and chlorophyll content in relation to water stress and leaf age of different types of citrus. *Journal of Agricultural and Food Chemistry* **38,** 1326-1334.

Normanly, J., Slovin, J.P., and Cohen, J.D. (1995). Rethinking auxin biosynthesis and metabolism. *Plant Physiology* **107,** 323-329.

Novagen. (1998). Protein Refolding Kit, pp. 1-9.

Olesen, S.P., Drejer, J., Axelsson, O., Moldt, P., Bang, L., Nielsen-Kudsk, J.E., Busse, R., and Mulsch, A. (1998). Characterization of NS 2028 as a specific inhibitor of soluble guanylyl cyclase. *British Journal of Pharmacology* **123,** 299-309.

Olson, D.C., White, J.A., Edelman, L., Harkins, R.N., and Kende, H. (1991). Differential expression of two genes for l-aminocyclopropane-1-carboxylate synthase in tomato fruits. *Proceedings of the National Academy of Sciences of the United States of America* **88,** 5340-5344.

Oparka, K.J. (1990). What is phloem unloading? *Plant Physiology* **94,** 393-396.

Oparka, K.J., and Turgeon, R. (1999). Sieve elements and companion cells-traffic control centers of the phloem. *Plant Cell* **11,** 739-750.

Oxley, D., and Bacic, A. (1999). Structure of the glycosylphosphatidylinositol anchor of an arabinogalactan protein from *Pyrus communis* suspension-cultured cells.

Proceedings of the National Academy of Sciences of the United States of America **96,** 14246-14251.

Parkinson, S.J., Carrithers, S.L., and Waldman, S.A. (1994). Opposing adenine nucleotide-dependent pathways regulate guanylyl cyclase C in rat intestine. *Journal of Biological Chemistry* **269,** 22683-22690.

Parry, A.D., Neill, S.J., and Horgan, R. (1990). Measurement of xanthoxin in higher plant tissues using ^{13}C labeled interna1 standards. *Phytochemistry* **29,** 1033-1039.

Parry, A.D., Griffiths, A., and Horgan, R. (1992). Abscisic acid biosynthesis in roots. The effects of water-stress in wild-type and abscisic-acid-deficient *(notabilis)* plants of *Lycopersicon esculentum* Mill. *Planta* **187,** 192-197.

Patrick, J.W. (1997). Phloem unloading: sieve element unloading and post-sieve element transport. *Annual Review of Plant Physiology and Plant Molecular Biology* **48,** 191-222.

Pear, J.R., Kawagoe, Y., Schreckengost, W.E., Delmer, D.P., and Stalker, D.M. (1996). Higher plants contain homologs of the bacterial cell A genes encoding the catalytic subunit of cellulose synthase. *Proceedings of the National Academy of Sciences of the United States of America* **93,** 12637-12642.

Pearce, G., Strydom, D., Johnson, S., and Ryan, C.A. (1991). A polypeptide from tomato leaves induces wound-inducible proteinase inhibitor proteins. *Science* **253,** 895-898.

Pearce, G., Moura, D.S., Stratmann, J., and Ryan, C.A. (2001). RALF, a 5-kDa ubiquitous polypeptide in plants, arrests growth and development. *Proceedings of the National Academy of Sciences of the United States of America* **98,** 12843-12847.

Peiser, G.D., Wang, T.T., Hoffman, N.E., Yang, S.F., Liu, H.W., and Walsh, C.T. (1984). Formation of cyanide from carbon 1 of 1-aminocyclopropane-1-carboxylic

acid during its conversion to ethylene. *Proceedings of the National Academy of Sciences of the United States of America* **81,** 3059-3063.

Penninckx, I.A., Thomma, B.P., Buchala, A., Metraux, J.P., and Broekaert, W.F. (1998). Concomitant activation of jasmonate and ethylene response pathways is required for induction of a plant defensin gene in Arabidopsis. *Plant Cell* **10,** 2103-2113.

Penson, S.P., Schuurink, R.C., Fath, A., Gubler, F., Jacobsen, J.V., and Jones, R.L. (1996). cGMP is required for gibberellic acid-induced gene expression in barley aleurone. *Plant Cell* **8,** 2325-2333.

Petersen, M.l.C., Hejgaard, J., Thompson, G.A., and Schulz, A. (2005). Cucurbit phloem serpins are graft-transmissible and appear to be resistant to turnover in the sieve element-companion cell complex. *Journal of Experimental Botany* **56,** 3111-3120.

Peuke, A.D., Windt, C., and Van As, H. (2006). Effects of cold-girdling on flows in the transport phloem in *Ricinus communis*: is mass flow inhibited? *Plant, Cell and Environment* **29,** 15-25.

Pharmawati, M., Gehring, C.A., and Irving, H.R. (1998a). An immunoaffinity purified plant natriuretic peptide analogue modulates cGMP level in the *Zea mays* root stele. *Plant Science* **137,** 107-115.

Pharmawati, M., Billington, T., and Gehring, C.A. (1998b). Stomatal guard cell responses to kinetin and natriuretic peptides are cGMP-dependent. *Cellular and Molecular Life Sciences* **54,** 272-276.

Pharmawati, M., Shabala, S.N., Newman, I.A., and Gehring, C.A. (1999). Natriuretic peptides and cGMP modulate K^+, Na^+ and H^+ fluxes in *Zea mays* roots. *Molecular Cell Biological Research Communications* **2,** 53-57.

Pharmawati, M., Maryani, M.M., Nikolakopoulos, T., Gehring, C.A., and Irving, H.R. (2001). Cyclic GMP modulates stomatal opening induced by natriuretic peptides and immunoreactive analogues. *Plant Physiology and Biochemistry* **39,** 385-394.

Pickard, W.P., and Minchin, P.E.H. (1990). The transient inhibition of phloem translocation in *Phaseolus vulgaris* by abrupt temperature drops, vibration, and electric shock. *Journal of Experimental Botany* **41,** 1361-1369.

Powell, M. D., McWilliam, H., McLeod, J., Nankervis, S., Butler, R., and Toop, T. (2008). Expression of natriuretic peptide receptor mRNA and functional response to atrial natriuretic peptide and C-type natriuretic peptide in rainbow trout (*Oncorhynchus mykiss*) head kidney leucocytes. *Fish and Shellfish Immunology* **24,** 373-378.

Rafudeen, S., Gxaba, G., Makgoke, G., Bradley, G., Pironcheva, G., Raitt, L., Irving, H., and Gehring, C. (2003). A role for plant natriuretic peptide immuno-analogues in NaCl- and drought-stress responses. *Physiologia Plantarum* **119,** 554-562.

Rao, D.L., Giller, K.E., Yeo, A.R., and Flowers, T.J. (2002). The effects of salinity and sodicity upon nodulation and nitrogen fixation in chickpea (*Cicer arietinum*). *Annals of Botany* **89,** 563-570.

Rekoslavskaya, N.I., and Bandurski, R.S. (1994). Indole as a precursor of indole-3-acetic acid in *Zea mays*. *Phytochemistry* **35,** 905-909.

Robels, P., and Pelaz, S. (2005). Flower and fruit development in *Arabidopsis thaliana*. *International Journal of Developmental Biology* **49,** 633-643.

Rock, C.D., and Zeevaart, J.A.D. (1991). The *aba* mutant of Arabidopsis thaliana is impaired in epoxy-carotenoid biosynthesis. *Proceedings of the National Academy of Sciences of the United States of America* **88,** 7496-7499.

Rohring, H., Schmindt, J., Miklashevichs, E., Schell, J., and John, M. (2002). Soybean ENOD 40 encodes two peptieds that bind sucrose synthase. *Proceedings of the National Academy of Sciences of the United States of America* **99,** 1915-1920.

Roitsch, T., and Gonzalez, M.C. (2004). Function and regulation of plant invertases: sweet sensations. *Trends in Plant Science* **9,** 606-613.

Rojo, E., Sharma, V.K., Kovaleva, V., Raikhel, N.V., and Fletcher, J.C. (2002). CLV3 is localized to the extracellular space, where it activates the Arabidopsis CLAVATA stem cell signaling pathway. *Plant Cell* **14,** 969-977.

Ross, A.F. (1961). Systemic acquired resistance induced by localized virus infections in plants. *Virology* **14,** 340-358.

Rudolph, R., and Lilie, H. (1996). *In vitro* folding of inclusion body proteins. *FASEB Journal* **10,** 49-56.

Ryals, J.A., Neuenschwander, U.H., Willits, M.G., Molina, A., Steiner, H.Y., and Hunt, M.D. (1996). Systemic acquired resistance. *Plant Cell* **8,** 1809-1819.

Sanders, I.O., Smith, AR., and Hall, M.A. (1989). Ethylene metabolism in *Pisum sativum* L. *Planta* **179,** 104-114.

Schaap, P. (2005). Guanylyl cyclases across the tree of life. *Frontiers in Bioscience* **10,** 1485-1498.

Scheer, J.M., and Ryan, C.A. (1999). A 160-kD systemin receptor on the surface of lycopersicon peruvianum suspension-cultured cells. *Plant Cell* **11,** 1525-1536.

Schobert, C., Baker, L., Szederkenyi, J., Grossmann, P., and Komor, E. (1998). Identification of immunologically related proteins in sieve-tube exudate collected from monocotyledonous and dicotyledonous plants. *Planta* **206,** 245-252.

Schobert, C., Gottschalk, M., Kovar, D.R., Staiger, C.J., Yoo, B.C., and Lucas, W.J. (2000). Characterization of *Ricinus communis* phloem profilin, RcPRO1. *Plant Molecular Biology* **42,** 719-730.

Schofer, C.R., Nasrallah, M.E., and Nasrallah, J.B. (1999). The male determinant of self-incompatibility in Brassica. *Science* **286,** 1697-1700.

Schrammel, A., Behrends, S., Schmidt, K., Koesling, D., and Mayer, B. (1996). Characterization of 1H-[1,2,4]oxadiazolo[4,3-a]quinoxalin-1-one as a heme-site inhibitor of nitric oxide-sensitive guanylyl cyclase. *Molecular Pharmacology* **50,** 1-5.

Schwartz, S.H., Léon-Kloosterziel, K.M., Koornneef, M., and Zeevaart, J.A.D. (1997). Biochemical characterization of the *aba2* and *aba3* mutants in *Arabidopsis thaliana. Plant Physiology* **114,** 161-166.

Shimazaki, K., Goh, G.H., and Kinoshita, T. (1999). Involvement of intracellular Ca^{2+} in blue light-dependent proton pumping in guard cell protoplasts from *Vicia faba*. *Physiologia Plantarum* **105,** 554-561.

Shiu, S.H., and Bleecker, A.B. (2001a). Receptor-like kinases from Arabidopsis form a monophyletic gene family related to animal receptor kinases. *Proceedings of the National Academy of Sciences of the United States of America* **98,** 10763-10768.

Shiu, S.H., and Bleecker, A.B. (2001b). Plant receptor-like kinase gene family: diversity, function, and signaling. *Science STKE* **2001,** RE22.

Shiu, S.H., and Bleecker, A.B. (2003). Expansion of the receptor-like kinase/Pelle gene family and receptor-like proteins in Arabidopsis. *Plant Physiology* **132,** 530-543.

Sindhu, R.K., and Walton, D.C. (1988). Xanthoxin metabolism in cell-free preparations from wild type and wilty mutants of tomato. *Plant Physiology* **88,** 178-182.

Sinha, A.K., Hofmann, M.G., Romer, U., Kockenberger, W., Elling, L., and Roitsch, T. (2002). Metabolizable and non-metabolizable sugars activate different signal transduction pathways in tomato. *Plant Physiology* **128,** 1480-1489.

Stempfer, G., Holl-Neugebauer, B., and Rudolph, R. (1996). Improved refolding of an immobilized fusion protein. *Nature Biotechnology* **14,** 329-334.

Sudoh, T., Kangawa, K., Minamino, N., and Matsuo, H. (1988). A new natriuretic peptide in porcine brain. *Nature* **332,** 78-81.

Sudoh, T., Minamino, N., Kangawa, K., and Matsuo, H. (1990). C-type natriuretic peptide (CNP): a new member of natriuretic peptide family identified in porcine brain. *Biochemical and Biophysical Research Communications* **168,** 863-870.

Suwastika, I.N., and Gehring, C.A. (1998). Natriuretic peptide hormones promote radial water movements from the xylem of Tradescantia shoots. *Cellular and Molecular Life Sciences* **54,** 1161-1167.

Suwastika, I.N., and Gehring, C.A. (1999). The plasma-membrane H^+-ATPase from Tradescantia stem and leaf tissue is modulated in vitro by cGMP. *Archives of Biochemistry and Biophysics* **367,** 137-139.

Suwastika, I.N., Toop, T., Irving, H.R., and Gehring, C.A. (2000). *In situ* and *in vitro* binding of natriuretic peptide hormones in *Tradescantia multiflora*. *Plant Biology* **2,** 1-3.

Suzuki, Y., Yamane, H., Spray, C.R., Gaskin, P., MacMillan, J., and Phinney, B.O. (1992). Metabolism of *ent*-kaurene to gibberellin A_{12}-aldehyde in young shoots of normal maize. *Plant Physiology* **98,** 602-610.

Svetek, J., Yadav, M.P., and Nothnagel, E.A. (1999). Presence of a glycosylphosphatidylinositol lipid anchor on rose arabinogalactan proteins. *Journal of Biological Chemistry* **274,** 14724-14733.

Sze, H., Li, X., and Palmgren, M.G. (1999). Energization of plant cell membranes by H^+-pumping ATPases. Regulation and biosynthesis. *Plant Cell* **11,** 677-690.

Szerszen, J.B., Szczyglowski, K., and Bandurski, R.S. (1994). *iaglu*, a gene from *Zea mays* involved in conjugation of growth hormone indole-3-acetic acid. *Science* **265,** 1699-1701.

Szmidt-Jaworska, A., Jaworski, K., Tretyn, A., and Kopcewicz, J. (2003). Biochemical evidence for a cGMP-regulated protein kinase in *Pharbitis nil*. *Phytochemistry* **63,** 635-642.

Takayama, S., and Sakagami, Y. (2002). Peptide signalling in plants. *Current Opinion in Plant Biology* **5,** 382-387.

Taylor, I.B. (1991). Genetics of ABA synthesis. In Abscisic acid: Physiology and biochemistry, W.J. Davies and H.G. Jones, eds (Oxford, UK: BlOS Scientific), pp. 23-37.

The QIAexpressionist. (2003). A handbook for high-level expression and purification of 6xHis-tagged proteins. (QIAGEN Inc).

Thomma, B.P., Eggermont, K., Penninckx, I.A., Mauch-Mani, B., Vogelsang, R., Cammue, B.P., and Broekaert, W.F. (1998). Separate jasmonate-dependent and salicylate-dependent defense-response pathways in Arabidopsis are essential for resistance to distinct microbial pathogens. *Proceedings of the National Academy of Sciences of the United States of America* **95,** 15107-15111.

Thompson, J.D., Gibson, T.J., Plewniak, F., Jeanmougin, F., and Higgins, D.G. (1997). The Clustal X windows interface: flexible strategies for multiple sequence alignment aided by quality analysis tools. *Nucleic Acids Research* **24,** 4876-4882.

Trebitsh, T., Staub, J.E., and O'Neill, S.D. (1997). Identification of a 1-aminocyclopropane-1-carboxylic acid synthase gene linked to the Female (F) locus that enhances female sex expression in cucumber. *Plant Physiology* **113,** 987-995.

Trotochaud, A.E., Hao, T., Wu, G., Yang, Z., and Clark, S.E. (1999). The CLAVATA1 receptor-like kinase requires CLAVATA3 for its assembly into a signaling complex that includes KAPP and a Rho-related protein. *Plant Cell* **11,** 393-406.

Tsai, F.Y., and Coruzzi, G.M. (1990). Dark-induced and organ-specific expression of two asparagine synthetase genes in *Pisum sativum*. *EMBO Journal* **9,** 323-332.

Turgeon, R., and Wolf, S. (2009). Phloem Transport: Cellular Pathways and Molecular Trafficking. *Annual Review of Plant Biology* **60,** 207-21.

Tyerman, S.D., and Skerrett, I.M. (1999). Root ion channels and salinity. *Scientia Horticulturae* **78,** 175-235.

Uknes, S., Winter, A., Delaney, T., Vernooij, B., Morse, A., Friedrich, L., Nye, G., Potter, S., Ward, E., and Ryals, J. (1993). Biological induction of systemic acquired resistance in Arabidopsis. *Molecular Plant-Microbe Interactions* **6,** 692-698.

Ulker, B., and Somssich, I.E. (2004). WRKY transcription factors: from DNA binding towards biological function. *Current Opinion in Plant Biology* **7,** 491-498.

Umetsu, M., Tsumoto, K., Hara, M., Ashish, K., Goda, S., Adschiri, T., and Kumagai, I. (2003). How additives influence the refolding of immunoglobulin-folded proteins in a stepwise dialysis system. Spectroscopic evidence for highly efficient refolding of a single-chain Fv fragment. *Journal of Biological Chemistry* **278,** 8979-8987.

Valentine, A.J., and Kleinert, A. (2007). Respiratory responses of arbuscular mycorrhizal roots to short-term alleviation of P deficiency. *Mycorrhiza* **17,** 137-143.

Valentine, A.J., Osborne, B.A., and Mitchell, D.T. (2002). Form of inorganic nitrogen influences mycchorizal colonization and photosynthesis of cucumber. *Scientia Horticulturae* **92,** 229-239.

Valentine, A.J., Mortimer, P., Lintnaar, M., and Borgo, R. (2006). Drought responses of arbuscular mycorrhizal grapevines. *Symbiosis* **41,** 127-133.

van Bel, A.J.E. (1993). The transport phloem. Specifics of its functioning. *Progress in Botany* **54,** 134-150.

van Bel, A.J.E. (2003a). The phloem, a miracle of ingenuity. *Plant, Cell and Environment* **26,** 125-149.

van Bel, A.J.E. (2003b). Transport phloem: low profile, high impact. *Plant Physiology* **131,** 1509-1510.

van de Sande, K., Pawlowski, K., Czaja, I., Wieneke, U., Schell, J., Schmidt, J., Walden, R., Matvienko, M., Wellink, J., van Kammen, A., Franssen, H., and Bisseling, T. (1996). Modification of phytohormone response by a peptide encoded by *ENOD40* of legumes and a non-legumes. *Science* **273,** 370-373.

van Jaarsveld, E. (2001). *Plectranthus ecklonii* Benth. (Kirstenbosch: South African National Biodiversity Institute).

Verica, J.A., and He, Z.H. (2002). The cell wall-associated kinase (WAK) and WAK-like kinase gene family. *Plant Physiology* **129,** 455-459.

Ververidis, P., and John, P. (1991). Complete recovery *in vitro* of ethylene-forming enzyme activity. *Phytochemistry* **30,** 725-727.

Vesely, D., and Giordano, A. (1991). Atrial natriuretic peptide hormonal system in plants. *Biochemical and Biophysical Research Communications* **179,** 695-700.

Vesely, D.L., Gower, W.R., and Giordano, A.T. (1993). Atrial natriuretic peptides are present throughout the plant kingdom and enhance solute flow in plants. *American Journal of Physiology* **265,** E465-E477.

Vincentelli, R., Canaan, S., Campanacci, V., Valencia, C., Maurin, D., Frassinetti, F., Scappucini-Calvo, L., Bourne, Y., Cambillau, C., and Bignon, C. (2004). High-throughput automated refolding screening of inclusion bodies. *Protein Science* **13,** 2782-2792.

Vinocur, B., and Altman, A. (2005). Recent advances in engineering plant tolerance to abiotic stress: achievements and limitations *Current Opinion in Biotechnology* **16,** 123-132.

Vogler, H., and Kuhlemeier, C. (2003). Simple hormoes but complex signalling. *Current Opinion in Plant Biology* **6,** 51-56.

Volotovski, I.D., Sokolovsky, S.G., Molchan, O.V., and Knight, M.R. (1998). Second messengers mediate increases in cytosolic calcium in tobacco protoplasts. *Plant Physiology* **117,** 1023-1030.

Von Caemmerer, S., and Farquhar, G.D. (1981). Some relationships between the biochemistry of photosynthesis and the gas exchange of leaves. *Planta* **153,** 376-387.

Wagner, T.A., and Kohorn, B.D. (2001). Wall-associated kinases are expressed throughout plant development and are required for cell expansion. *Plant Cell* **13,** 303-318.

Walton, D. (1980). Biochemistry and physiology of abscisic acid. *Annual Review in Plant Physiology* **31,** 453-489.

Walz, C., Giavalisco, P., Schad, M., Juenger, M., Klose, J., and Kehr, J. (2004). Proteomics of curcurbit phloem exudate reveals a network of defence proteins. *Phytochemistry* **65,** 1795-1804.

Wang, Y., Gehring, C., Cahill, D., and Irving, H. (2007). Plant natriuretic peptide active site determination and effects on cGMP and cell volume regulation. *Functional Plant Biology* **34,** 645-653.

Ward, E.R., Uknes, S.J., Williams, S.C., Dincher, S.S., Wiederhold, D.L., Alexander, D.C., Ahl-Goy, P., Metraux, J.P., and Ryals, J.A. (1991). Coordinate gene activity in response to agents that induce systemic acquired resistance. *Plant Cell* **3,** 1085-1094.

Watanabe, N., Evans, J.R., and Chow, S. (1994). Changes in the photosynthetic properties of Australian wheat cultivars over the last century. *Australian Journal of Plant Physiology* **21,** 169-183.

Webb, J.A. (1967). Translocation of sugars in *Cucurbita melopepo*. Effects of temperature change. *Plant Physiology* **42,** 881-885.

Weigel, R.R., Pfitzner, U.M., and Gatz, C. (2005). Interaction of NIMIN1 with NPR1 modulates PR gene expression in Arabidopsis. *Plant Cell* **17,** 1279-1291.

Wenzel, C.L., Hester, Q., and Mattsson, J. (2008). Identification of genes expressed in vascular tissues using NPA-induced vascular overgrowth in Arabidopsis. *Plant and Cell Physiology* **49,** 457-468.

White, J.W., McMaster, G.S., and Edmeades, G.O. (2004). Genomics and crop response to global change: what have we learned? *Field Crops Research* **90,** 165-169.

Wingfield, P.T., Stahl, S.J., Williams, R.W., and Steven, A.C. (1995). Hepatitis core antigen produced in *Escherichia coli*: subunit composition, conformational analysis, and *in vitro* capsid assembly. *Biochemistry* **34,** 4919-4932.

Wright, A.D., Sampson, M.B., Neuffer, M.G., Michalczuk, L., Slovin, J.P., and Cohen, J.D. (1991). Indole-3-acetic acid biosynthesis in the mutant *maize orange* pericarp tryptophan auxotroph. *Science* **254,** 998-1000.

Wu, Y., Hiratsuka, K., Neuhaus, G., and Chua, N.H. (1996). Calcium and cGMP target distinct phytochrome-responsive elements. *Plant Journal* **10,** 1149-1154.

Xie, D.X., Feys, B.F., James, S., Nieto-Rostro, M., and Turner, J.G. (1998). COI1: an Arabidopsis gene required for jasmonate-regulated defense and fertility. *Science* **280,** 1091-1094.

Yang, S., and Hoffmann, N. (1984). Ethylene biosynthesis and its regulation in higher plants. *Annual Review in Plant Physiology* **35,** 155-189.

Yip, W. K., Moore, T., and Yang, S.F. (1992). Differential accumulation of transcripts for four tomato 1-aminocyclopropane-1-carboxylate synthase homologs under various conditions. *Proceedings of the National Academy of Sciences of the United States of America* **89,** 2475-2479.

Zagotta, W.N., and Siegelbaum, S.A. (1996). Structure and function of cyclic nucleotide-gated channels. *Annual Review of Neuroscience* **19,** 235-263.

Zeevaart, J.A.D., and Creelman, R. (1988). Metabolism and physiology of abscisic acid. *Annual Review of Plant Physiology and Plant Molecular Biology* **39,** 439-473.

Zeevaart, J.A.D., Rock, C.D., Fantauzzo, F., Heath, T.G., and Gage, D.A. (1991). Metabolism of abscisic acid and its physiological implications. In Abscisic acid: Physiology and biochemistry W.J. Davies and H.G. Jones, eds (Oxford, UK: BlOS Scientific), pp. 39-52.

Zentella, R., Yamauchi, D., and Ho, T.H. (2002). Molecular dissection of the gibberellin/abscisic acid signaling pathways by transiently expressed RNA interference in barley aleurone cells. *Plant Cell* **14,** 2289-2301.

Zimmermann, P., Hirsch-Hoffmann, M., Hennig, L., and Gruissem, W. (2004). Genevestigator. Arabidopsis microarray database and analysis toolbox. *Plant Physiology* **136,** 2621-2632.